

International Atomic Energy Agency

INDC(CCP)-18/L

---

**INDC**

**INTERNATIONAL NUCLEAR DATA COMMITTEE**

---

USSR State Committee on the Utilization of Atomic Energy

Bulletin of the Nuclear Data Centre

Issue 7

(Supplement 1)

PROMPT EMISSION ACCOMPANYING NUCLEAR FISSION

A.E. Saveliev

(English translation)

December 1971

---

IAEA NUCLEAR DATA SECTION, KÄRNTNER RING 11, A-1010 VIENNA



USSR State Committee on the Utilization of Atomic Energy

Bulletin of the Nuclear Data Centre

Issue 7

(Supplement 1)

PROMPT EMISSION ACCOMPANYING NUCLEAR FISSION

A.E. Saveliev

Atomizdat, 1971



## CONTENTS

	<u>Page</u>
Foreword	iii
Introduction	1
<u>Chapter I.</u>	
<u>The current theory of the decay of compound nuclei</u>	6
1. The Hauser-Feshbach method and its generalization to cover multiparticle nuclear reactions.	6
2. Calculation of cross-sections for the elastic and inelastic scattering of neutrons with $\epsilon_n = 0.3-6$ MeV by atomic nuclei.	16
3. The inelastic interaction of neutrons with nuclei accompanied by the emission of protons and alpha particles.	23
4. The cascade theory of neutron and gamma photon emission by compound nuclei.	28
<u>Chapter II.</u>	
<u>Prompt fission neutron spectra</u>	31
<u>Induced <math>^{235}\text{U}</math> fission</u>	
1. A short historical review of calculations of the spectra of prompt fission neutrons.	31
2. A method of neutron spectrum calculation in the "centre of fragment mass" system.	37
3. Neutron spectrum conversion to the laboratory system of co-ordinates. A qualitative investigation of the spectrum of fission neutrons.	41
4. Discussion of calculation of the spectra of neutrons emitted in $^{235}\text{U}$ fission.	45

	<u>Page</u>
<u>Chapter III.</u>	
<u>Prompt fission neutron spectra</u>	46
<u>Spontaneous <math>^{252}\text{Cf}</math> fission</u>	
1. A kinematic analysis of the spectra of prompt neutrons emitted in spontaneous $^{252}\text{Cf}$ fission.	46
2. Calculations of the spectra of prompt neutrons emitted in spontaneous $^{252}\text{Cf}$ fission. Basic formulas and assumptions.	49
3. Calculations of $^{252}\text{Cf}$ neutron spectra and discussion of the results.	55
4. The hypothesis of "isothermal" neutron emission from fission fragments.	60
<u>Chapter IV.</u>	
<u>Prompt gamma photons emitted in nuclear fission</u>	65
1. Method and results of calculating the spectra of gamma photons accompanying $^{235}\text{U}$ and $^{252}\text{Cf}$ fission.	65
2. Influence of the angular momenta of fission fragments on gamma photon spectra.	70
<u>Conclusions</u>	73
<u>References</u>	79

## FOREWORD

The present work is on the one hand a review, for it touches to some extent on all basic work dealing with the theoretical study of the spectra of prompt neutrons and gamma photons produced in nuclear fission; on the other hand, it is also an independent study, not only because it contains quite a lot of hitherto unpublished material, but also because an attempt is made to interpret all available theoretical material - both from the point of view of further theoretical and experimental work on the spectra of neutrons and gamma photons produced in fission, and from that of further study of the nuclear fragmentation process.

The first chapter, in which the current theory of the decay of compound nuclei is set forth, may seem rather strange: it does not touch directly on questions connected with the properties of the prompt emission accompanying fission. The first chapter has two purposes: one is to establish the fact that the statistical theory may claim to be a fairly good (and not only in the qualitative sense) description of fission neutron and gamma spectra; the other is to expound the statistical theory in a manner acceptable for the further study of neutron and gamma spectra.

For the sake of conciseness, we have omitted from the first chapter a great deal of graphic material illustrating the applicability of the statistical theory of nuclear reactions to elastic and inelastic neutron scattering in intermediate and heavy nuclei. However, this material is described sufficiently for the subsequent parts of the present work not to be affected.





## INTRODUCTION

Nuclear fission is a very complex process characterized by many degrees of freedom. There is at present no unified theory for explaining this process. Certain aspects or stages can be explained by various limited models. Consequently, there is a perfectly natural desire to combine the various models, to seek connections between them and to generalize them with a view to explaining more and more of the facts relating to fission.

It is because the fission process is characterized by many degrees of freedom that the statistical parts of the various theories are the most suitable for describing it. If by "statistical model" we mean not only the theory of nuclear reactions based on N. Bohr's ideas about the compound nucleus and the elaboration of this theory by Hauser and Feshbach [1], but also the Fermi gas theory with its quasi-classical consequences and the shell correction method, it may be said that the statistical model in this broad sense explains more facts relating to nuclear fission than any other model. It follows that, for a future unified theory of fission, the "statistical model" will be the most interesting limiting case. It is also clear that from this point of view it is worth examining in detail and on the basis of the statistical model the individual phenomena which accompany fission and seeking connections between the various phenomena within the framework of the same model.

We shall review briefly the main facts explained by the statistical model, discuss the connection between this and other models, and determine the place occupied by the statistical description of prompt neutron and gamma spectra within the overall fission picture.

It should first be pointed out that the traditional liquid drop model is the quasi-classical limiting case of the Fermi gas model [2]. Even the dynamics of the liquid drop model can probably be obtained as a limiting case of the Fermi gas theory if one introduces interactions (pair formation). This question has not yet been discussed in the literature; however, it is of great interest and awaits a solution.

Consideration of a Fermi gas in some self-consistent potential field, computation of its energy as the sum of the energies of the individual particles and subtraction from it of the corresponding quasi-classical

(smoothed) sum lead to the shell correction method [3-5]. This method lends itself to nuclear mass computations [6]. The fission barrier obtained with the use of the shell correction method has a complex structure (double-humped, triple-humped etc.) which leads to the appearance of fine structure in the fission cross-section when the excitation energy of the fissionable nucleus is in the sub-barrier range [7].

The generalized nuclear model, which considers the motion of individual nucleons in the field of a liquid "core", may also be regarded as one form of the theory of a Fermi gas located in an external field [8-10].

The connection between the statistical model and other nuclear models (for example, the model of Nilsson [11]) in the sense just discussed is obvious.

The shell correction method can also be used for finding the distribution of fission fragments by mass, charge and kinetic energy [12].

The Fermi gas theory gives the nuclear level density as a function of the excitation energy and angular momentum of the nucleus [13-15]. This relationship is widely used in the theory of nuclear reactions and especially in fission theory.

The level densities of fission fragments play a fundamental part in the studies of nuclear fission conducted by Fong [16,17], Newton [18] and Cameron [20]. These authors have been fairly successful in describing fission fragment mass and kinetic energy yields.

The concept "level density of a compound nucleus" is central to the study of questions connected with the competition between fission and neutron emission [20]. As D. Huizenga and R. Vandenbosch have shown, the statistical theory of the ratio  $\Gamma_n/\Gamma_f$  in which this concept is used provides a good description of the relevant experimental data.

Calculations performed in the present work show that the level density is also the principal quantity when describing the spectra of prompt neutrons and gamma photons produced in fission.

Another aspect of the statistical theory, based on N. Bohr's concept of the "compound nucleus" and most fully developed by Hauser and Feshbach [1], enables one to break down the description of the fission process into two stages: the formation of the compound fissionable nucleus and its subsequent decay. Experience has shown that this breakdown is fully justified if the levels of the fissionable nucleus already overlap. In this case, the

fission cross-section has the form

$$\sigma_{\alpha,f}^{\gamma} = \frac{\pi}{k_{\alpha}^2} \frac{2J+1}{(2\sigma_{\alpha}+1)(2I_{\alpha}+1)} \cdot T_{\ell_{\alpha}}^{\gamma K} W_{j_1 j_2 \ell_1 \ell_2}^{\gamma K}(E_0; E_1, E_2, t_1, t_2, \theta) \quad (1, B)$$

Here  $J$  is the total angular momentum of the system consisting of an incident particle ( $\alpha$ ) and a target nucleus;  $\sigma_{\alpha}, \ell_{\alpha}$  and  $J_{\alpha}$  are respectively the spin of the incident particle, its orbital moment and its total angular momentum;  $I_{\alpha}$  is the spin of the target nucleus;  $K$  is the projection of the total angular momentum  $J$  onto the symmetry axis of the system;  $j_1, j_2, \ell_1, \ell_2$  are the total angular momenta and orbital moments of the fission fragments;  $E_0$  is the excitation energy of the fissionable nucleus;  $E_1, E_2, t_1, t_2$  are the excitation energies and kinetic energies of the fission fragments;  $\theta$  is the angle between the direction in which the fission fragments fly off and the direction of the particle (or gamma photon) inducing fission.  $T_{\alpha}$  is the permeability coefficient, usually calculated on the basis of the optical model. The function  $W$  is the probability of decay of the compound nucleus into a configuration characterized by the enumerated quantum numbers. Lastly,  $k_{\alpha}$  is the wave number of the incident particle.

Relation (1,B) obviously presupposes that the formation of the compound nucleus and its decay are independent processes. At the same time, the usual laws of conservation of energy, angular momentum and parity must, of course, be satisfied. This situation obtains if the compound nucleus is a mixture of a large number of states.  $T$  and  $W$  are characteristics of the process averaged over the states of the compound nucleus.

A formula of the type (1,B) is the starting point for analysing the angular distributions of fission fragments [21].

When considering the emission of neutrons and gamma photons from fission fragments, it is also possible to break down the fission fragment decay process into stages or cascades. At the same time, the density of the states of the intermediate nuclei-fragments is so great that it becomes necessary to adopt the level density function. As will be seen, in the description of the process here, the two aspects of the theory which we discussed above merge.

In the present work, a study is made of the spectra of prompt neutrons and photons produced in fission with a view to showing that the statistical model is also a good one for describing the decay of fission fragments.

Another aim of the present work was to ascertain the thermodynamic characteristics of fission nuclei-fragments.

It is also clear that only by studying the spectra of neutrons and gamma photons can one obtain answers to questions concerning the deformation of fission fragments, their momenta, the rate of conversion of the deformation energy of a fission fragment into excitation energy, the influence of Coulomb acceleration of fission fragments on the shape of the neutron spectrum in the laboratory system of co-ordinates, and so on. All these and similar questions are discussed in the present work.

The study is divided into four chapters.

The first chapter deals with the current theory concerning the decay of compound nuclei. In it the theory of Hauser and Feshbach [1] is generalized for the case of multiparticle nuclear reactions; calculations are performed with a view to showing that the statistical model provides a good description of the cross-sections for the interaction between neutrons and ordinary nuclei and that on this basis it can be applied in its limiting form to fission fragments. From the form of the cross-sections for multiparticle nuclear reactions it is easy to derive the formulas of the cascade theory of neutron and gamma photon evaporation. The possibility of correlation of the emitted particles is also discussed.

In the second chapter, on the basis of the cascade theory of evaporation derived in the first chapter we calculate the spectra of  $^{235}\text{U}$  fission neutrons at  $0^\circ$ ,  $45^\circ$  and  $90^\circ$  to the direction in which the fission fragments fly off. The effects associated with fission fragment motion are analysed and the discrepancy between calculated spectra and experimental data is discussed.

The third chapter contains a kinematic analysis of the spectra of the prompt neutrons produced in spontaneous  $^{252}\text{Cf}$  fission. The calculated neutron spectra are compared with the experimental data and good agreement is found. By comparing the calculated and experimental data one is able to determine the dependence of level density on fission fragment mass number. We discuss the idea of "isothermal" emission of neutrons from fission fragments.

The results of the gamma photon spectrum calculations are presented in the fourth chapter. We discuss the question of the total energy removed by gamma photons from the fission fragments. In addition, we consider the competition between neutron and gamma photon emission and its influence on the total amount of energy removed by gamma emission. Attention is also paid to the role which the energy gap in the excitation spectrum of fission fragments plays in the description of gamma spectra.

Lastly, in the section entitled "Conclusions" there is a general discussion of the results. On the basis of these discussions various recommendations are made to experimentalists regarding the further study of the spectra of neutrons and gamma photons produced in fission. A programme is also proposed for further calculations which it is felt would be useful.

Chapter I. THE CURRENT THEORY OF THE DECAY OF COMPOUND NUCLEI

1. The Hauser-Feshbach method and its generalization to cover multi-particle nuclear reactions

Niels Bohr's concept of the compound nucleus found its fullest expression in the formalism developed by Hauser and Feshbach [1]. As already mentioned, Bohr's concept enables one to regard the formation and decay of a compound nucleus as independent processes. Being a mixture of a large number of states, a compound nucleus does not "remember" anything concerning its formation except the most general integrals of motion - energy, angular momentum and parity - so that one can immediately write a cross-section formula of the type (1.B). The requirements imposed upon the compound nucleus decay probability  $W$  by the detailed-balance relations for direct and inverse reactions and normalization (unitarity) make it possible to express the probability of decay of a compound nucleus in terms of the penetrability of the nuclear surface  $T$ .

In the representation of the total angular momentum  $J$  of a system consisting of a neutron plus a target nucleus and with the nucleon spin-orbit interaction taken into account, the differential cross-section obtained in the above manner for the inelastic scattering of - for example - neutrons by a nucleus is [22].

$$\begin{aligned} \sigma_{n,n'}(\epsilon_n, \epsilon_{n'}, \theta) &= \frac{g_i}{4k_n^2(2I_0+1)2} \sum_{J_n, \ell_n, J} T_{\ell_n J_n}^J(\epsilon_n) (2J+1)^2 \times \\ &\times \frac{\sum_{J_n', \ell_n', J_n'} T_{\ell_n' J_n'}^J(\epsilon_{n'})}{\sum_{q, J_q, \ell_q} T_{\ell_q J_q}^J(\epsilon_q)} \cdot \sum_{e(4\pi n n')} (-1)^{I_0 - I'} Z(\ell_n, J_n, \ell_n', J_n'; \frac{1}{2} \ell) \times \\ &\times Z(\ell_n, J_n, \ell_n', J_n'; \frac{1}{2} \ell) W(J, J_n, J, J_n'; I, \ell) W(J, J_n, J, J_n'; I_0, \ell) P_\ell(\cos \theta), \end{aligned}$$

where  $W$  and  $Z$  represent the Racah and Blatt-Biedenharn coefficients respectively;  $\epsilon_n$  and  $\epsilon_{n'}$  are the energies of the incident and emergent neutrons;  $I_0$  and  $I'$  are the spins of the ground state of the target nucleus and the residual nucleus;  $J_n, J_n', \ell_n, \ell_n'$  are the total angular momenta and

the orbital moments of the incident and emergent neutrons;  $\vartheta$  is the angle at which the scattered neutron emerges relative to the direction of the incident beam.

It follows from expression (1.I) that the angular distribution is symmetric relative to  $\vartheta = 90^\circ$ . The symmetry of the angular distribution stems from the assumption that the phases of the states of the compound system are random [23].

Integrating expression (1.I) with respect to the angle, we obtain the corresponding total cross-section:

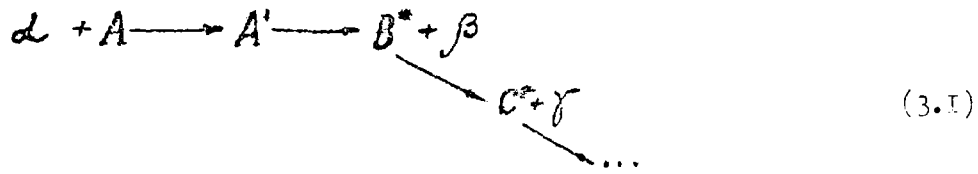
$$\sigma_{n,n'} = \frac{g}{k^2} \sum_n \frac{2J+1}{2(2I_0+1)} \frac{T_{en}^J(\epsilon_n) \sum_{n', \ell, n'} T_{en', \ell}^J(\epsilon_{n'})}{\sum_{q, J_q, \ell_q} T_{eq, J_q}^J(\epsilon_q)} \quad (2.I)$$

As can be seen, the statistical method of Hauser and Feshbach has the advantage that it expresses the two-particle reaction cross-section averaged over the states of the compound nucleus in terms of the "penetrability of the nuclear surface", which is well known from the optical model. Another important advantage of this method is that the discreteness of the spectrum of the excited states of the final nucleus is taken into account automatically.

It is natural to try generalizing the Hauser-Feshbach method to cover multi-particle nuclear reactions while retaining the above-mentioned advantages [26] and, for the sake of simplicity, we consider in the remainder of this section only total cross-sections for multi-particle nuclear reactions.

For a multi-particle nuclear reaction passing through the stage of compound nucleus formation, it may be assumed that - exactly as in the two-particle case - the nuclear reaction breaks down into several clearly defined stages: formation of the compound nucleus, decay of the compound nucleus into a stable particle and an excited residual nucleus, decay of this excited nucleus with the emission of a new stable particle, etc. None of the intermediate nuclei "remember" anything concerning their formation, except characteristics following from the laws of energy, angular momentum and parity conservation.

This picture of the way the reaction proceeds immediately offers the possibility of writing the cross-section for a process of the kind



in the form

$$\sigma_{\alpha, \beta \gamma \dots}^{\sigma} = \frac{g}{k_{\alpha}^2} \frac{2J+1}{(2I_{\alpha}+1)(2I_{\alpha'}+1)} \cdot T_{\alpha \alpha'}^{\sigma}(E_{\alpha}) \times \\ \times W_{J_{\beta} l_{\beta} I_{\beta}}^{\sigma}(E_0; E_{\beta}, E_{\beta}) W_{J_{\gamma} l_{\gamma} I_{\gamma}}^{I_{\beta}}(E_{\beta}; E_{\gamma}, E_{\gamma}) \dots \quad (4.I)$$

Here  $W_{J_{\beta} l_{\beta} I_{\beta}}^{\sigma}(E_0; E_{\beta}, E_{\beta})$  is the probability of decay of a compound nucleus with excitation energy  $E_0$  leading to the formation of a residual nucleus with momentum  $I_{\beta}$  and excitation energy  $E_{\beta}$  and of a particle with kinetic energy  $E_{\beta}$ , total angular momentum  $J_{\beta}$  and orbital moment  $l_{\beta}$ ;  $W^{I_{\beta}}$  is the probability of decay of the intermediate nucleus after emission of a beta particle, etc.

The task of completely determining the cross-section (4.I) obviously reduces to a determination of the probabilities of decay of the intermediate nuclei  $W$ .

Assuming that all the intermediate nuclei have sufficiently long life-times, one can write a system of detailed-balance relations for successive decay events in the form

$$T_{\alpha \alpha'}^{\sigma}(E_{\alpha}) W_{J_{\beta} l_{\beta} I_{\beta}}^{\sigma}(E_0; E_{\beta}, E_{\beta}) = T_{\beta \beta'}^{\sigma}(E_{\beta}) W_{\alpha \alpha'}^{\sigma}(E_0; 0, E_{\alpha}), \\ T_{\beta \beta'}^{I_{\beta}}(E_{\beta}) W_{\gamma \gamma' l_{\gamma} I_{\gamma}}^{I_{\beta}}(E_{\beta}; E_{\gamma}, E_{\gamma}) = T_{\gamma \gamma'}^{I_{\beta}}(E_{\gamma}) W_{\beta \beta'}^{I_{\beta}}(E_{\beta}; E_{\gamma}, E_{\gamma}). \quad (5.I)$$

The number of equations in the system (5.I) is determined by energy considerations:

$$E_0 = E_{\alpha} + Q_{\alpha}, \quad E_0 = E_{\beta} + Q_{\beta} + E_{\beta}, \quad E_{\beta} = E_{\gamma} + Q_{\gamma} + E_{\gamma}, \dots \\ 0 \leq E - \sum_{\gamma=1}^{\gamma_{max}} Q_{\gamma} \leq Q_{\gamma_{max}+1} \quad (6.I)$$



where  $v_{\max}$  determines the number of equations for a given value of  $E_0$ . In the relations (6.I),  $Q_\nu$  represents the particle separation energies.

To the system (5.I) one must also add the corresponding normalization conditions:

$$\begin{aligned} \sum_{\beta, E_\beta=0}^{E_0-Q_\beta} \sum_{J_\beta, l_\beta, I_\beta} W_{J_\beta, l_\beta, I_\beta}^{J'}(E_0; E_\beta, \mathcal{E}_\beta) &= 1, \\ \sum_{\gamma, E_\gamma=0}^{E_\beta-Q_\gamma} \sum_{J_\gamma, l_\gamma, I_\gamma} W_{J_\gamma, l_\gamma, I_\gamma}^{I_\beta}(E_\beta; E_\gamma, \mathcal{E}_\gamma) &= 1, \end{aligned} \quad (7.I)$$

All the equations in the system (5.I), except the first, represent conditions for the equilibrium of the emerging nucleus and the imaginary  $\beta, \nu \dots$  particle "pair".

The relations (5.I) and (7.I) are quite sufficient for determining all the decay probabilities  $W$  of the intermediate nuclei. Solution of the system (5.I)-(7.I) gives

$$W_{J_\beta, l_\beta, I_\beta}^{J'}(E_0; E_\beta, \mathcal{E}_\beta) = \frac{T_{J_\beta, l_\beta}^{J'}(\mathcal{E}_\beta)}{\sum_{\beta', E_{\beta'}=0}^{E_0-Q_{\beta'}} \sum_{J_{\beta'}, l_{\beta'}, I_{\beta'}} T_{J_{\beta'}, l_{\beta'}}^{J'}(\mathcal{E}_{\beta'})}, \quad (8.I)$$

$$W_{J_\gamma, l_\gamma, I_\gamma}^{I_\beta}(E_\beta; E_\gamma, \mathcal{E}_\gamma) = \frac{T_{J_\gamma, l_\gamma}^{I_\beta}(\mathcal{E}_\gamma)}{\sum_{\gamma', E_{\gamma'}=0}^{E_\beta-Q_{\gamma'}} \sum_{J_{\gamma'}, l_{\gamma'}, I_{\gamma'}} T_{J_{\gamma'}, l_{\gamma'}}^{I_\beta}(\mathcal{E}_{\gamma'})},$$

In the relations (7.I) and (8.I), when one summates over the quantum numbers  $J_\nu, l_\nu, I_\nu$ , the following conditions must be satisfied:

$$\overline{J} = \overline{J}_\beta + \overline{I}_\beta = \overline{J}_\alpha + \overline{I}_\alpha, \quad \overline{J}_\alpha = \overline{l}_\alpha + \overline{I}_\alpha, \dots \quad (9.I)$$

$$(-1)^{l_\alpha} g_\alpha = (-1)^{l_\beta} g_\beta, \quad g_\beta = (-1)^{l_\gamma} g_\gamma, \dots,$$

where  $\pi$  is the parity of the states of the corresponding nuclei.

The cross-section (4.I) is now completely defined by the formulas (8.I).

As one would expect, in the two-particle reaction case the usual Hauser-Feshbach expression (2.I) follows from expressions (4.I) and (8.I).

Accordingly, the cross-section for a three-particle reaction will be

$$\sigma_{\alpha,\beta\gamma} = \frac{g}{k^2} \sum_{j,l,\ell_u} \frac{2j+1}{(2j+1)(2l_u+1)} \cdot T_{j,\ell_u}^j(E_u)^\pi$$

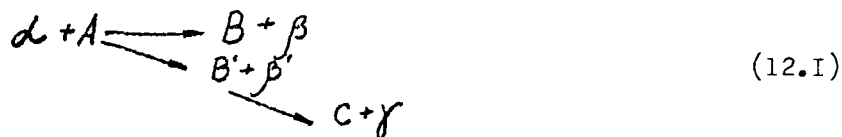
$$\frac{\sum_{j,\ell_\beta} T_{j,\ell_\beta}^j(E_\beta)}{\sum_{\substack{E_\beta=Q_\beta \\ \beta', E_{\beta'}=0}} T_{j,\ell_{\beta'}}^j(E_{\beta'})} \cdot \frac{\sum_{j,\ell_\gamma} T_{j,\ell_\gamma}^{j\beta}(E_\gamma)}{\sum_{\substack{E_\gamma=Q_\gamma \\ \gamma', E_{\gamma'}=0}} \sum_{j',\ell_{\gamma'}} T_{j',\ell_{\gamma'}}^{j\beta}(E_{\gamma'})} \quad (10.I)$$

etc.

It should be borne in mind that formula (2.I) is valid for  $E_\beta < Q_\gamma$  ( $\beta = n'$ ) if it is used in calculating the cross-section for a process in the final state of which there is a specific nucleus (with a fixed number of protons and neutrons). If the radiation width for  $E_\beta \geq Q_\gamma$  is neglected, there will necessarily be emission of a gamma particle from the nucleus, i.e. a three-particle reaction will occur. If, on the other hand, we are interested in the cross-section for the appearance of a particle regardless of what kind of nucleus will result in the final state, then we have to write

$$\sum_{\alpha,\beta}^\sigma = \sum_{E_{\beta'}=0}^{Q_\gamma} \sum_{j,\ell_{\beta'},j',\ell_{\beta'}} \sigma_{\alpha,\beta'}^\sigma + \sum_{E_{\beta'}=Q_\gamma}^{E_n-Q_\gamma} \sum_{j,\ell_{\beta'},j',\ell_{\beta'}} \sum_{E_{\gamma'}=0}^{Q_\beta} \sum_{j',\ell_{\gamma'}} \sigma_{\alpha,\beta\gamma}^\sigma + \dots \quad (11.I)$$

For a process of the kind



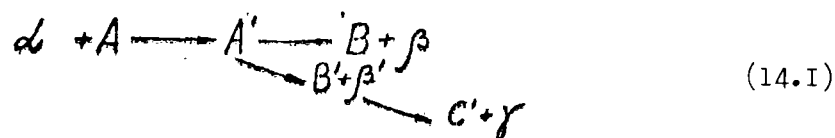
the relations (4.I), (7.I) and (11.I) give

$$\sum_{\alpha, \beta}^{\sigma} = \sum_{E_{\beta}=0}^{E_0-Q_{\beta}} \sum_{\gamma_{\beta} E_{\beta} l_{\beta}} \sigma_{\alpha, \beta}^{\sigma} \quad (13.I)$$

This means that, if only two- and three-particle processes occur and we are not interested in the final nuclei, the cross-section for the occurrence of a beta particle may also be obtained from the usual Hauser-Feshbach expression (2.I) for the two-particle reaction cross-section provided that one summates in accordance with expression (13.I).

All the results obtained above presuppose the absence of interference between levels of the intermediate compound nuclei; it was also assumed that there was no correlation between successively emitted particles. We shall now consider the problem more rigorously, but also more formally. Our purpose is to obtain cross-section expressions containing coefficients of the correlation between the emerging particles and coefficients which take into account the interference among levels of the intermediate compound nuclei.

For the sake of simplicity, we shall consider only two- and three-particle processes of the type



The very appearance of the process points to the existence of intermediate compound nuclei. However, we shall assume that their duration - although longer than the nuclear lifetime - is short enough for one to speak of a correlation between cascades.

We shall also assume that the decay scheme (14.I) does not contain direct processes.

Let  $P_{\alpha\beta}$  represent the two-particle scattering matrix and  $S_{\alpha, \beta\gamma}$  a scattering matrix which takes into account the three-particle channel of process (14.I).

It is henceforth convenient to assume that [24]

$$S_{\alpha, \beta\gamma} = P_{\alpha\beta} \cdot Q_{\beta\gamma}^{\alpha} \quad (15.I)$$

The matrix  $Q_{\beta\gamma}^{\alpha}$  cannot be defined as the usual two-particle scattering matrix as none of its indices except  $\gamma$  corresponds any more to particle pairs removed to infinity.

Taking into account expression (15.I), one can write the cross-sections for two- and three-particle processes in the form

$$\tilde{\sigma}_{\alpha\beta}^{\gamma} = \frac{g_1}{k_{\alpha}^2} \frac{2\gamma+1}{(2\sigma_{\alpha}+1)(2l_{\alpha}+1)} \cdot |P_{\alpha\beta}|^2, \quad E_{\beta} < Q_{\gamma}, \quad (16.I)$$

$$\tilde{\sigma}_{\alpha,\beta\gamma}^{\gamma} = \frac{g_1}{k_{\alpha}^2} \frac{2\gamma+1}{(2\sigma_{\alpha}+1)(2l_{\alpha}+1)} |P_{\alpha\beta}|^2 \cdot |Q_{\beta\gamma}^{\alpha}|^2, \quad E_{\beta} \geq Q_{\gamma} \quad (17.I)$$

Cross-sections (16.I) and (17.I) are, broadly speaking, strongly fluctuating functions of the energy of the incident particle. For comparison with the expressions derived above, it is necessary to average them over the states of the intermediate compound nuclei.

The corresponding cross-sections are

$$\overline{\sigma}_{\alpha,\beta}^{\gamma} = \overline{\tilde{\sigma}_{\alpha,\beta}^{\gamma}} = \frac{g_1}{k_{\alpha}^2} \frac{2\gamma+1}{(2\sigma_{\alpha}+1)(2l_{\alpha}+1)} \cdot \overline{|P_{\alpha\beta}|^2}, \quad E_{\beta} < Q_{\gamma}, \quad (18.I)$$

$$\overline{\sigma}_{\alpha,\beta\gamma}^{\gamma} = \langle \tilde{\sigma}_{\alpha,\beta\gamma}^{\gamma} \rangle = \frac{g_1}{k_{\alpha}^2} \frac{2\gamma+1}{(2\sigma_{\alpha}+1)(2l_{\alpha}+1)} \langle |P_{\alpha\beta}|^2 \cdot |Q_{\beta\gamma}^{\alpha}|^2 \rangle, \quad E_{\beta} \geq Q_{\gamma} \quad (19.I)$$

In formulas (18.I) and (19.I), averaging only over the compound nucleus A' is denoted by a prime above the corresponding quantity; averaging over the two compound nuclei A' and B' is denoted by  $\langle \rangle$ .

We now introduce the following definitions:

$$P_{\alpha,\beta}^{\gamma} = \frac{t_{\alpha}^{\gamma} \cdot t_{\beta}^{\gamma} \cdot \gamma_{\alpha\beta}}{\xi} \quad (20.I)$$

$$Q_{\beta\gamma}^{\alpha} = \frac{t_{\gamma}^{I\beta} \cdot S_{\beta\gamma}^{\alpha}}{q}, \quad (21.I)$$

$$|t_{\alpha}^{\gamma}|^2 = T_{\alpha}^{\gamma} \quad (22.I)$$

$$\frac{\rho^{\alpha}}{T_{\beta\gamma}} = \frac{\langle |P_{\alpha\beta}|^2 \cdot |Q_{\beta\gamma}^{\alpha}|^2 \rangle}{\langle |P_{\alpha\beta}|^2 \rangle \cdot \langle |Q_{\beta\gamma}^{\alpha}|^2 \rangle}. \quad (23.I)$$

In definitions (20.I)-(23.I) it is assumed that the dependence of the functions  $t_{\alpha}$  on the energy of the incident and emergent particles is so weak that they can be removed from beneath the averaging sign.

Use of the definitions (20.I)-(23.I) gives

$$\bar{\sigma}_{\alpha,\beta}^{\gamma} = \frac{g_{\beta}}{K_{\alpha}^2} \cdot \frac{2\gamma+1}{(2\sigma_{\alpha}+1)(2l_{\alpha}+1)} \cdot \frac{T_{\alpha}^{\gamma} T_{\beta}^{\gamma}}{\xi^2} \cdot C_{\alpha\beta}, \quad (24.I)$$

$$\bar{\sigma}_{\alpha,\beta\gamma}^{\gamma} = \frac{g_{\beta}}{K_{\alpha}^2} \frac{(2\gamma+1) t_{\beta\gamma}^{\alpha}}{(2\sigma_{\alpha}+1)(2l_{\alpha}+1)} \cdot \frac{T_{\alpha}^{\gamma} T_{\beta}^{\gamma}}{\xi^2} \cdot C'_{\alpha\beta} \cdot \frac{T_{\gamma}^{I\beta}}{\langle q^2 \rangle} \cdot d_{\beta\gamma}^{\alpha} \quad (25.I)$$

where

$$C_{\alpha\beta} = \overline{\left( |r_{\alpha\beta}|^2 \cdot \frac{\xi^2}{\xi^2} \right)}, \quad (26.I)$$

$$C'_{\alpha\beta} = \left\langle |r_{\alpha\beta}|^2 \frac{\xi^2}{\xi^2} \right\rangle \quad (26.Ia)$$

$$d_{\beta\gamma}^{\alpha} = \left\langle |S_{\beta\gamma}^{\alpha}|^2 \frac{\langle q^2 \rangle}{q^2} \right\rangle \quad (27.I)$$

From the form of formulas (24.I) and (25.I) it is clear that the quantities

$$\frac{T_{\beta}^{\gamma}}{\xi^2} C_{\alpha\beta} \quad \text{u} \quad f_{\beta\gamma}^{\alpha} \frac{T_{\beta}^{\gamma}}{\xi^2} C'_{\alpha\beta} \frac{T_{\gamma}^{\beta}}{\langle q^2 \rangle} d_{\beta\gamma}^{\alpha}$$

can be interpreted as the probabilities of decay of the compound nucleus A' with the ejection of one and two particles respectively. Moreover, if one assumes that there occur no processes except those indicated in decay scheme (14.I), it is possible to write

$$\sum_{\beta, E_{\beta} < Q_{\gamma}} \frac{T_{\beta}^{\gamma}}{\xi^2} C_{\alpha\beta} + \sum_{\substack{\beta, \gamma, \\ E_{\beta} \geq Q_{\gamma} \\ E_{\gamma} < Q_{\delta}}} f_{\beta\gamma}^{\alpha} C'_{\alpha\beta} d_{\beta\gamma}^{\alpha} \frac{T_{\beta}^{\gamma}}{\xi^2} \frac{T_{\gamma}^{\beta}}{\langle q^2 \rangle} = 1 \quad (28.I)$$

It follows from expression (28.I) that

$$\overline{\xi^2} = \sum_{\beta, E_{\beta} < Q_{\gamma}} T_{\beta}^{\gamma} C_{\alpha\beta} + \sum_{\substack{\beta, \gamma, \\ E_{\beta} \geq Q_{\gamma}}} f_{\beta\gamma}^{\alpha} C'_{\alpha\beta} d_{\beta\gamma}^{\alpha} \frac{T_{\beta}^{\gamma}}{\langle q^2 \rangle} \frac{T_{\gamma}^{\beta}}{\langle q^2 \rangle} \quad (29.I)$$

By analogy with expression (28.I), we can write for the decay of the nucleus B'

$$\sum_{\gamma, E_{\gamma} < Q_{\delta}} d_{\beta\gamma}^{\alpha} \frac{T_{\gamma}^{\beta}}{\langle q^2 \rangle} = 1, \quad (30.I)$$

$$\text{i.e. } \langle q^2 \rangle = \sum_{\gamma, E_{\gamma} < Q_{\delta}} d_{\beta\gamma}^{\alpha} T_{\gamma}^{\beta} \quad (31.I)$$

In the absence of correlation between cascades

$$f_{\beta', \gamma'}^{\alpha} = 1$$

and expression (29.I) is transformed with the help of expression (30.I) into

$$\overline{S^2} = \sum_{\beta, E_{\beta}} T_{\beta}^{\gamma} C_{\alpha, \beta} \quad (32.I)$$

Lastly, if there is no interference among levels in the compound nuclei A' and B', i.e.

$$C_{\alpha, \beta} = d_{\beta \gamma}^{\alpha} = 1$$

then it follows from formulas (31.I) and (32.I) that

$$G_{\alpha, \beta}^{\gamma} = \frac{g_{\beta}}{k_{\alpha}^2} \cdot \frac{2\gamma+1}{(2\sigma_{\alpha}+1)(2l_{\alpha}+1)} \cdot \frac{T_{\alpha}^{\gamma} T_{\beta}^{\gamma}}{\sum_{\beta', E_{\beta'} < Q_{\beta}} T_{\beta'}^{\gamma}}, \quad E_{\beta} < Q_{\gamma}, \quad (33.I)$$

$$G_{\alpha, \beta \gamma}^{\gamma} = \frac{g_{\beta}}{k_{\alpha}^2} \cdot \frac{2\gamma+1}{(2\sigma_{\alpha}+1)(2l_{\alpha}+1)} \cdot T_{\alpha}^{\gamma} \cdot \frac{T_{\beta}^{\gamma}}{\sum_{\beta', E_{\beta'} < Q_{\beta}} T_{\beta'}^{\gamma}} \cdot \frac{T_{\beta}^{\beta}}{\sum_{\beta', E_{\beta'} < Q_{\beta}} T_{\beta'}^{\beta}}, \quad E_{\beta} > Q_{\beta} \quad (34.I)$$

Expressions (33.I) and (34.I) coincide with expression (4.I) in the case of two- and three-particle reactions respectively if one substitutes into expression (4.I) the values of  $W_{\beta}^J$  and  $W_{\gamma}^{I\beta}$  given by expressions (8.I) and then makes a number of trivial conversions.

The coefficients reflecting interference among levels in the intermediate nuclei A' and B' can be estimated by a method similar to that of Moldauer [25].

The coefficients of the correlation between cascades  $f_{\beta \gamma}^{\alpha}$  can be obtained from a rigorous examination of the three-particle nuclear reaction. Here, however, we would merely point out that the formulas obtained can be used for the qualitative analysis of experimental data from the point of view of the correlation between cascades.

When  $f_{\beta,\gamma}^{\alpha} \neq 1$  and the energy of the incident particle is higher than the three-particle reaction threshold, the cross-section for the two-particle reaction has the form

$$\sigma_{\alpha\beta}^{\gamma} = \frac{g}{k_{\alpha}^2} \frac{2\gamma+1}{(2\alpha+1)(2\beta+1)} \frac{T_{\alpha}^{\gamma} \cdot T_{\beta}^{\gamma} \cdot C_{\alpha\beta}}{\sum_{\beta', \gamma', E_{\beta'} < Q_{\gamma}} T_{\beta'}^{\gamma} C_{\alpha\beta'}^{\gamma} + \sum_{\beta', \gamma'} f_{\beta', \gamma'}^{\alpha} C_{\alpha\beta'}^{\gamma} d_{\beta', \gamma'}^{\alpha} \frac{T_{\beta'}^{\gamma} T_{\gamma'}^{\beta}}{(Q^2)}} \quad (35.I)$$

It is characteristic that the denominator of expression (35.I) contains the sum of the products of the penetrability coefficients. This fact distinguishes formula (35.I) qualitatively from expression (33.I) in the case where  $f_{\beta\gamma}^{\alpha} = C_{\alpha\beta} = d_{\beta\gamma}^{\alpha} = 1$ . It cannot be otherwise, for in the absence of correlation between cascades the dependence of the cross-section for the first cascade on the characteristics of the second ( $T_{\gamma'}^{\beta}$  and  $d_{\beta', \gamma'}^{\alpha}$ ) will naturally vanish. In formula (35.I), the three-particle reaction emerges as a reaction channel competing with the two-particle channel. In the absence of correlation between cascades, the concept of competition between channels loses its meaning.

2. Calculation of cross-sections for the elastic and inelastic scattering of neutrons with  $\epsilon_n = 0.3-6$  MeV by atomic nuclei

The method set forth in the preceding section will, after appropriate adaptation (see section 4), be used in describing the spectra of prompt neutrons and gamma photons produced in fission. However, the fission fragments to which this method will be applied have a negligible lifetime, and (unlike the case of stable nuclei) it is difficult experimentally to investigate their interaction with neutrons. It is therefore natural to apply the method to stable nuclei, for with them it is easy to see that it works in the energy range in which the spectrum of prompt fission nuclei lies. There remains, of course, the question of applying this method to fission fragments, in view of the fact that they are heavily overloaded with neutrons; this question will be discussed elsewhere (see below).

In the present section, we analyse by means of the statistical method experimental data on differential cross-sections for the elastic and inelastic scattering of neutrons with  $\epsilon_n = 0.3-6$  MeV by atomic nuclei with  $A = 23-238$  [28, 29].



Since the publication of the work of Hauser and Feshbach [1] many calculations have been performed of cross-sections for the inelastic scattering of neutrons using the method discussed. However, the situation cannot be regarded as satisfactory, for the question of the limits of the Hauser-Feshbach method and the conditions for applying it has still not been answered. There are two reasons for this: firstly, calculations performed so far have not been sufficiently systematic (no one has investigated the variations in the model parameters from nucleus to nucleus and over a sufficiently wide range of incident neutron energies); secondly, the literature contains very little experimental data on the inelastic scattering of neutrons by nuclei.

The most systematic calculations of inelastic scattering cross-sections using the Hauser-Feshbach method have been performed by Auerbach and Moore [27]. They have shown that the calculated cross-sections for inelastic neutron scattering by  $^{27}\text{Al}$  and  $^{56}\text{Fe}$  nuclei at incident neutron energies from the threshold to 4 MeV and by  $^{238}\text{U}$ ,  $^{232}\text{Th}$ ,  $^{209}\text{Bi}$ ,  $^{208}\text{Pb}$ ,  $^{197}\text{Au}$ ,  $^{184}\text{W}$  and  $^{181}\text{Ta}$  nuclei at neutron energies from 0.1 MeV to 3 MeV are in good agreement with the experimental data. The penetrability coefficients  $T_{\ell\alpha}^J$  were calculated using the optical model with a spherical local potential of the Woods-Saxon type, with surface absorption, having the shape of a Gaussian curve. Comparison of the calculated and experimental cross-sections showed that nuclear deformation within the limits of the experimental errors could be ignored. For the nuclei enumerated above, it may therefore be said that inelastic neutron scattering at the energies indicated involves mainly the stage of compound nucleus formation.

When spin-orbit interaction is taken into account, the cross-section for elastic and inelastic scattering involving a compound nucleus is given by formula (1.I).

The penetrability coefficients  $T_{\ell\alpha}^J$  were calculated using the optical model with the potential [30] corrected for the isotopic dependence of the real part:

$$\begin{aligned}
 V(r) = & (V_0 - V_1 \frac{K-Z}{A}) [1 + \exp(\frac{r-R}{a})]^{-1} + \\
 & + iV_2 \exp[-(\frac{r-R}{b})^2] - V_3 \frac{1}{r} (\frac{\hbar}{\mu_{\text{sc}} c})^2 \times \\
 & \times \frac{d}{dr} [1 + \exp(\frac{r-R}{a})]^{-1} (\vec{\sigma} \vec{\ell}), \quad R = r_0 A^{1/3}
 \end{aligned}
 \tag{36.I}$$

As soon as the potential has the form (36.I), the problem reduces to one of selecting the parameters which determine it in such a way as to achieve agreement between the calculated cross-sections and the experimental data. As a first approximation, it is natural to take for the parameters of the potential (36.I) those which enable one to describe correctly the elastic scattering of neutrons by nuclei. For nuclei heavier than Ca and not close to those having magic numbers (of neutrons), elastic neutron scattering is adequately described by the usual optical model. For nuclei lighter than Ca and close to those having magic numbers (of neutrons), a considerable contribution to the total elastic scattering cross-section is bound to be made by scattering involving a compound nucleus. This contribution must be described by formula (1.I) when  $\epsilon_n = \epsilon_{n'}$ .

Calculations of differential cross-sections for the elastic scattering of neutrons with  $\epsilon_n = 2-6$  MeV for many nuclei which are heavier than Na, but for which one can neglect the contribution of elastic scattering involving a compound nucleus, give the values of the parameters of the potential (36.I) brought together in Table I. The standard set [30] was used as the geometric parameters of the model ( $r_0, a, b$ ).

Table I

$$r_0 = 1,25 \text{ F}; \quad a = 0,65 \text{ F}; \quad b = 0,98 \text{ F}; \quad V_3 = 6 \text{ MeV}$$

$\epsilon_n, \text{ MeV}$	MeV		
	$V_{10}$	$V_{11}$	$V_2$
2,0	53,5	38	5,0
2,5	52,5	30	5,6
3,2	51,5	22	6,0
4,0	50,0	17	7,0
5,0	48,5	10	8,0
6,0	47,0	6	9,2

As the graphic material takes up a great deal of space (comparison of calculated and experimental cross-sections for many nuclei), it is not presented here. We give only a description of the material, which is to be found in Refs [28, 29].

In Annex I to Ref. [28], Averyanov et al. present experimental (points) and calculated (curves) values of differential cross-sections for elastic neutron scattering. The agreement between calculated and experimental values of the differential cross-sections for all nuclei where there is negligible elastic scattering involving a compound nucleus is satisfactory (cf. nuclei where there is only one continuous curve).

The parameters obtained in this way are later used in describing elastic scattering involving a compound nucleus in the case of nuclei and energies where these parameters cannot be neglected. It is found that these parameters lead with no modification to correct values for a differential cross-section of this type; the broken curves showing the potential elastic scattering of neutrons in the figures presented in Annex I to Ref. [28] become a total elastic scattering cross-section (denoted by a continuous curve) when supplemented by the cross-section for elastic scattering involving a compound nucleus.

It should be noted that, in order to calculate elastic and inelastic scattering cross-sections, one has to know the system of levels, spins and parities of the target nucleus. The systems of levels for the nuclei in question were taken mainly from Ref. [31]. For those nuclei where either individual levels, or the spins and parities, or just the parities of some levels are not known, in calculations of the cross-sections for elastic scattering involving a compound nucleus it was necessary to supplement the missing information by introducing approximate, possible values of levels and their spins and parities. An error in such information will not have a large effect on the calculated cross-section for elastic scattering involving a compound nucleus. When the information concerning the levels of the target nucleus proved to be very scarce, it became necessary to limit the calculations to the potential cross-section for elastic neutron scattering (for example, by Pr and Te nuclei).

As the parameters of the optical potential (36.I) which were obtained describe correctly the contribution of inelastic neutron scattering involving a compound nucleus, it may be hoped that the same parameters can also be used for describing inelastic neutron scattering if the latter involves the formation of a compound nucleus. Indeed, calculations of differential cross-sections for inelastic scattering at incident neutron energies in the range 2-5 MeV satisfactorily reproduce the experimental values of the corresponding cross-sections in the case of  $^{23}\text{Na}$ ,  $^{27}\text{Al}$ ,  $^{28}\text{Si}$ ,  $^{31}\text{P}$ ,  $^{32}\text{S}$ ,  $^{48}\text{Ti}$ ,  $^{51}\text{V}$  and  $^{56}\text{Fe}$ . A comparison of the calculated and experimental cross-sections for inelastic scattering to different target nucleus levels or level groups is made in Annex II to Ref. [28].

Comparison of the calculated cross-sections for inelastic neutron scattering obtained with the parameters presented in Table I with the corresponding experimental data for  $^{39}\text{K}$ ,  $^{89}\text{Y}$ , and  $^{206}\text{Pb}$  (with a magic or near-magic number of neutrons) does not lead to satisfactory agreement. For the nuclei just indicated, neutron absorption must be reduced substantially: ( $^{39}\text{K} \rightarrow V_2 = 3.8 \text{ MeV}$ ,  $^{89}\text{Y} \rightarrow V_2 = 1.4 \text{ MeV}$ ,  $^{206}\text{Pb} \rightarrow V_2 = 3.2 \text{ MeV}$ ). Calculated cross-sections with a lower value of  $V_2$  are compared with the corresponding experimental cross-sections for inelastic neutron scattering by  $^{39}\text{K}$ ,  $^{89}\text{Y}$  and  $^{206}\text{Pb}$  nuclei in the figures contained in Annex III to Ref. [28]. The elastic neutron scattering cross-sections calculated with a lower value of  $V_2$  remain in satisfactory agreement with the experimental data.

A bibliography of the works from which the experimental data were taken is not given here because of its size (see Ref. [28]).

Calculations similar to those just described, but for incident neutron energies  $\epsilon_n = 0.3\text{-}1.5 \text{ MeV}$  and for  $A = 23\text{-}238$ , were performed in Ref. [29]. The optical potential parameters chosen from the condition for agreement between the theoretical and experimental data on elastic and inelastic scattering are presented in Tables II and III. Graphic material or bibliography is not given, for the same reasons as before.

The calculations performed in Refs [28, 29] of differential cross-sections for elastic and inelastic neutron scattering and comparison with experimental data show that, for nuclei heavier than Na and for incident neutron energies up to  $\sim 6 \text{ MeV}$ , scattering (excluding potential scattering) involves the formation of a compound nucleus.

Table II

(obtained from an analysis of differential cross-sections for elastic scattering)

$$a = 0,65 \text{ F}; \quad b = 0,98 \text{ F}; \quad r_0 = 1,25 \text{ F}; \quad V_3 = 6 \text{ MeV}$$

Nu- cl- eus	$\mathcal{E}_n = 0,3 \text{ MeV}$		$\mathcal{E}_n = 0,5 \text{ MeV}$		$\mathcal{E}_n = 0,8 \text{ MeV}$		$\mathcal{E}_n = 1,5 \text{ MeV}$	
	MeV		MeV		MeV		MeV	
	$V_1$	$V_2$	$V_1$	$V_2$	$V_1$	$V_2$	$V_1$	$V_2$
Na	65,0	2,0					67,0	4,6
Mg	54,5	2,0						
Al	56,0	2,0					59,0	4,6
Si	55,0	2,0	57,0	2,5	56,0	3,5	59,0	4,6
P							56,0	4,6
K							52,6	4,6
Ca							54,0	4,6
Ti			45,0	5,0				
Cr	45,0	5,0	45,0	5,0	47,0	5,0		
Fe	44,0	5,0	45,0	5,0				
Co					56,0	3,5	49,0	4,6
Ni	56,0	2,0						
Cu							49,0	4,6
Zn	53,3	2,0	54,8	2,5	56,8	3,5	48,0	4,6
Y							48,0	4,6
Zr	54,8	2,0			54,2	3,5	48,0	4,6
Nb							48,0	4,6
Cd	49,0	2,0	50,3	2,5	49,4	3,5		
Sn	47,4	2,0	48,5	2,5	47,5	3,5		
Te	47,0	2,0						
Ba			45,3	2,5	44,3	3,5		
Au							46,0	4,6
Hg	47,5	2,0	46,0	2,5	46,0	3,5		
Pb	46,5	2,0	45,0	2,5	45,0	3,5	45,0	4,6
Bi	46,5	2,0	45,0	2,5	45,0	3,5		
Th							41,0	4,6
U	41,8	2,0	41,0	2,5	40,0	3,5		

Table III

(obtained from an analysis of differential cross-sections for inelastic scattering)

$$a = 0,65 \text{ F}; \quad b = 0,98 \text{ F}; \quad r_0 = 1,25 \text{ F}; \quad V_3 = 6 \text{ MeV}$$

Nucleus	M e V		
	$\epsilon_n$	$V_1$	$V_2$
<sup>23</sup> Na	0,98	66,0	4,0
<sup>51</sup> V	1,50	67,0	4,6
<sup>95</sup> Mo	1,61	49,8	4,7
<sup>95</sup> Mo	0,78	59,0	3,5
<sup>107</sup> Ag	1,10	50,0	4,1
<sup>181</sup> Ta	0,71	42,5	3,2
<sup>184</sup> W	0,50	42,9	2,5
<sup>232</sup> Th	0,56	41,7	2,7
<sup>238</sup> U	0,55	40,8	2,7

In Tables II and III

$$V_1 = V_{10} - V_{11} \frac{N-Z}{A} \quad (37.1)$$

In Refs [28, 29], only the discrete excitation spectrum of the residual nucleus was used in the neutron cross-section calculations. However, when calculating fission neutron spectra one has to deal with the continuous spectrum of excited states of the final nuclei-fragments, for - firstly - the degree of excitation of the states is fairly high and - secondly - the discrete levels of the nuclei-fragments are not known from experimental data, and this makes it necessary to use the level density function at all excitation energies.

In the following section we give examples of neutron cross-section calculations using the level density function.

3. The inelastic interaction of neutrons with nuclei accompanied by the emission of protons and alpha particles

The purpose of this section is to verify that the statistical model can be used in calculating total cross-sections for (n,p) and (n, $\alpha$ ) reactions for certain light and intermediate nuclei at incident neutron energies ranging from the threshold of the reactions in question to  $\sim 14-15$  MeV [34].

Exactly as in expression (2.I), the total cross-section for excitation of the K-level of the residual nucleus in (n,p) and (n, $\alpha$ ) reactions may be written as follows:

$$\sigma_{OK}^d = \frac{g}{k_0^2} \sum_{J_0 l_0} \frac{2J+1}{(2G_0+1)(2I_0+1)} \frac{T_{l_0 J_0}^J(E_n) T_{l_K J_K}^d(E_K)}{\sum_{d', E'_K, J'_K, l'_K} T_{l'_K J'_K}^{d'}(E'_K)} \quad (38.I)$$

Here the index d' denotes summation over all possible types of particle formed in the reaction (neutron, proton, alpha particle, etc.).

The total excitation cross-section of the residual nucleus after emission of a particle of the kind d is

$$\sigma^d = \sum_K \sigma_{OK}^d \quad (39.I)$$

where summation over K extends to all levels of the residual nucleus which can be excited in accordance with the law of conservation of energy.

However, it is obvious that formula (38.I) is not directly usable for calculating cross-sections at fairly high incident neutron energies, the reason being that in order to perform calculations on the basis of this formula it is necessary to know the position of the levels, their spins and their parities for the residual nuclei. As such information is usually not available at high residual nucleus excitation energies (of the order of the nucleon binding energy and higher), we make some changes in relation (38.I), the essence of these being explained below.

Let us assume that we know from experiment the characteristics of the levels (energy, spin, parity) up to certain values ( $E_k^0, \pi_k^0, I_k^0$ ). Let us also assume that the incident particle energy is such that the excitation of compound nucleus levels with  $E_k \geq E_k^0$  is possible. The total excitation cross-section of all levels of the residual nucleus from  $E_k = 0$  to  $E_{k_{\max}} = \epsilon_0 + Q_0 - Q_\alpha$  ( $Q_i$  being the energies for particle separation from the compound nucleus) may then be represented in the form

$$\begin{aligned} \sigma^{\alpha}(\epsilon_0) = & \frac{g_1}{K_0^2} \sum_{l_0=0}^{\infty} \sum_{l_0' = |l_0 - \sigma_0|}^{l_0 + \sigma_0} \sum_{I_0 = |I_0 - J_0|}^{I_0 + J_0} \left\{ \sum_{(I_k E_k)}^{(I_k^0 E_k^0)} \sum_{J_k = |J - I_k|}^{J+I_k} \sum_{l_k = |J_k - \sigma_k|}^{J_k + \sigma_k} \frac{2J+1}{(2\sigma_0+1)(2I_0+1)} \right\} \times \\ & \times \frac{T_{l_0 J_0}^J(\epsilon_0) T_{l_k J_k}^J(\epsilon_0 + Q_0 - E_k - Q_\alpha)}{\{J, \epsilon_0\}} + \int_{E_k^0}^{\epsilon_0 + Q_0 - Q_\alpha} \sum_{I_k} \sum_{J_k = |J - I_k|}^{J+I_k} \sum_{l_k = |J_k - \sigma_k|}^{J_k + \sigma_k} \frac{2J+1}{(2\sigma_0+1)(2I_0+1)} \times (40.I) \\ & \times \left. \frac{T_{l_0 J_0}^J(\epsilon_0) T_{l_k J_k}^J(\epsilon_0 + Q_0 - E_k - Q_\alpha) (2I_k+1) \rho_\alpha(E_k)}{\{J, \epsilon_0\}} dE_k \right\}. \end{aligned}$$

The expression in the denominator of expression (40.I)

$$\begin{aligned} \{J, \epsilon_0\} = & \sum_{d=1}^N \sum_{(E_{k_d}, I_{k_d})}^{(E_{k_d}^0, I_{k_d}^0)} \sum_{J_{k_d} = |J - I_{k_d}|}^{J+I_{k_d}} \sum_{l_{k_d} = |J_{k_d} - \sigma_d|}^{J_{k_d} + \sigma_d} \times T_{l_{k_d} J_{k_d}}^J(\epsilon_0 + Q_0 - Q_\alpha - E_{k_d})^{(4I, I)} \\ & + \sum_{d=1}^N \int_{E_{k_d}^0}^{\epsilon_0 + Q_0 - Q_\alpha} dE_{k_d} \rho_\alpha(E_{k_d}) \frac{(2J+1)(2\sigma_d+1)}{g_1} \sigma_c^{\alpha}(\epsilon_0 + Q_0 - Q_\alpha - E_{k_d}) K_{k_d}^2, \end{aligned} \quad (41.I)$$

where  $\sigma_c^{\alpha}$  is the cross-section for the formation of a compound nucleus by an emergent particle and a residual nucleus (the cross-section for the reverse process);  $\rho_\alpha$  is the level density of the residual nucleus after emission of an alpha-type particle (proton, neutron, alpha particle, etc.). The wave number of the emergent particle  $K_{k_\alpha}$  is related to the incident particle energy by the expression

$$K_{k_\alpha}^2 = \frac{2m_\alpha}{\hbar^2} (\epsilon_0 + Q_0 - Q_\alpha - E_{k_\alpha})$$

Expression (41.I) is obtained from the denominator of expression (38.I)



on the basis of the following assumptions [23]:

1. The level density of the nucleus has the form

$$\rho_{\alpha}(E_k, I_k) = (2I_k + 1) \rho_{\alpha}(E_k), \quad (42.1)$$

where  $\rho_{\alpha}(E_k)$  is no longer dependent on the spins of the nuclear levels;

2. At residual nucleus excitation energies  $E_{k_{\alpha}} \geq E_{k_{\alpha}}^0$ , the angular momenta of the nucleus  $I_{k_{\alpha}}$ , and consequently the orbital moments of the emergent particles  $l_{k_{\alpha}}$ , can assume arbitrary values (with some probability).

The second of these assumptions is the usual one for the theory of evaporation and, of course, leads to some inaccuracies in the calculations.

The first of these assumptions is also an approximation. The essence of the approximation is that the expression normally used for the level density of a nucleus excited to an energy  $E_k$  and possessing angular momentum  $I_k$  has the form [32]

$$\rho_{\alpha}(E_k, I_k) = \frac{2I_k + 1}{24\sqrt{2} a^{1/4} (E - \Delta)^{5/4} G^3} \exp \left\{ 2[Q_{\alpha}(E_k - \Delta)]^{1/2} - \frac{(I_k + 1/2)^2}{2G^2} \right\}, \quad (43.1)$$

where  $a = \frac{\pi^2}{6} g(\mu)$ ,  $g(\mu)$  is the density of the single-particle states near the Fermi surface and  $\mu$  is the chemical potential;

$$G^2 = \frac{G}{g^{1/2}} \langle m^2 \rangle [a(E - \Delta)]^{1/2}$$

$\langle m^2 \rangle$  is the mean square of the projection of the total angular momentum of individual particles (averaging is performed over single-particle states near the Fermi surface). The quantity  $\Delta$  (gap) can be represented as

$$\Delta = \begin{cases} \delta p + \delta n & - \text{ for even-even nuclei,} \\ \delta n & - \text{ for even-odd nuclei,} \\ \delta n & - \text{ for odd-even nuclei,} \\ 0 & - \text{ for odd-odd nuclei} \end{cases}$$

where the pairing energies of the protons  $\delta p$  and neutrons  $\delta n$  can be calculated in accordance with, for example, the method of Nemirovsky and Adamchuk [33]. Relation (44.I) will have the form of (42.I) if  $\sigma^2$  is a sufficiently large number. This is usually the case. If assumptions 1 and 2 are valid, the numerator of the second term of relation (40.I) assumes a form similar to the second term of the expression (41.I). All the calculations performed in this section are based on assumptions 1 and 2.

In the course of the calculations there was no attempt to choose the parameters of the problem so as to explain the experimental data on the cross-sections for the (n,p) and (n, $\alpha$ ) reactions as well as possible. On the contrary, the parameters were chosen from other data. For example, the parameters of level density  $Q_\alpha$  were taken from tables given in Ref. [35]. The energy gaps  $\Delta_\alpha$  were found from tables given in Ref. [33]. The parameters of the optical potentials for neutrons, protons and alpha particles were chosen in accordance with the data in Refs [37, 36, 30], in which cross-sections for the elastic interaction of neutrons, protons and alpha particles with nuclei were calculated. This approach enables one to draw conclusions from a comparison of the calculated and experimental cross-sections regarding the nature of the reaction mechanism (whether it involves a compound nucleus or some other phenomenon).

The permeabilities of the nuclear surface  $T_{l\alpha J_\alpha}^J$  were calculated with the help of an optical potential of the form

$$V(r) = V_c(r) - V_1 f(r) - i V_2 g(r) + V_3 \left( \frac{\hbar}{\mu r c} \right)^2 \frac{1}{r} \frac{df(r)}{dr} (\vec{\sigma} \cdot \vec{e}),$$

$$f(r) = [1 + \exp(\frac{r-R}{a})]^{-1}, \quad R = r_0 A^{1/3},$$

$$g(r) = \exp[-(\frac{r-R}{b})^2], \quad (44.I)$$

$$V_c(r) = \begin{cases} \frac{Z_1 Z_2 e^2}{2R_c} (3 - \frac{r^2}{R_c^2}) & \text{for } r \leq R_c, \\ \frac{Z_1 Z_2}{r} & \text{for } r > R_c, \end{cases} \quad R_c = r_c A^{1/3}$$

In all calculations performed in this section, account was taken of the energy dependence of the optical potential parameters both for incident and for emergent particles. The imaginary part of the potential was chosen in

the form

$$V_2^n = 4 + 0,5 \epsilon_n \quad (\text{neutrons}) \quad (45.I)$$

$$V_2^p = 3 + 0,57 \epsilon_p \quad (\text{protons}) \quad (46.I)$$

where  $\epsilon_{n,p}$  are given in MeV. Relations (45.I) and (46.I) were used for all the nuclei considered. The amplitude of the spin-orbit term  $V_3^n = 6$  MeV for neutrons in the case of all nuclei, while  $V_3^p = 8$  MeV for protons - also in the case of all nuclei.

The real part of the potential for neutrons and protons respectively was written in the form

$$\begin{aligned} V_1^n &= a^n + b^n \epsilon_n, \\ V_1^p &= a^p + b^p \epsilon_p. \end{aligned} \quad (47.I)$$

Table IV gives values of the coefficients  $a^i$  and  $b^i$  for various nuclei.

Table IV

Nucleus	$a^n$	$b^n$	Nucleus	$a^p$	$b^p$
<sup>27</sup> Al	53,4	-0,67	<sup>27</sup> Mg	58,3	-0,55
<sup>54</sup> Fe	53,4	-0,67	<sup>54</sup> Mn	57,9	-0,55
<sup>58</sup> Ni	53,6	-0,68	<sup>58</sup> Co	58,0	-0,55

In calculations of cross-sections for the reaction (n,α), the energy dependence of the alpha particle potential was chosen in the form

$$\begin{aligned} V_1^\alpha &= 109,5 - 1,34 \epsilon_\alpha, \\ V_2^\alpha &= 5,4 + 0,4 \epsilon_\alpha \\ V_3^\alpha &= 0, \end{aligned} \quad (48.I)$$

where  $\epsilon_\alpha$  is given in MeV. In all cases, surface absorption was chosen. The

geometric parameters of the potentials are the same as in Refs [36, 37, 30].

The positions of the energy levels of the nuclei, their spins and parities were taken mainly from Ref. [31].

Figs 1-4 show calculated and experimental cross-sections for the (n,p) and (n, $\alpha$ ) reactions. In all the cases presented, there is fairly good agreement between theory and experiment. The experimental data are taken from Refs [38, 39].

As can be seen from a comparison of the calculated and experimental data, one can talk of quantitative agreement. On the whole, the calculations performed so far could only be said to be in qualitative agreement with the experimental results. An extensive bibliography relating to these questions is given in Ref. [40].

It is worth noting here once more that the question of the limits of the Hauser-Feshbach method and the conditions for applying it is still open. An answer to this question may be obtained only from large-scale calculations using the statistical model and various direct nuclear reaction models. It is also necessary to carry out theoretical studies of the connection between the mechanism of a nuclear reaction and the structure of the nucleus.

However, for the purposes of this paper - which is to demonstrate the applicability of the statistical method in describing nuclear reactions in stable nuclei, with a view to extrapolating the description to the decay of compound nuclei strongly overloaded with neutrons - the calculations performed in sections 2 and 3 appear to be quite adequate.

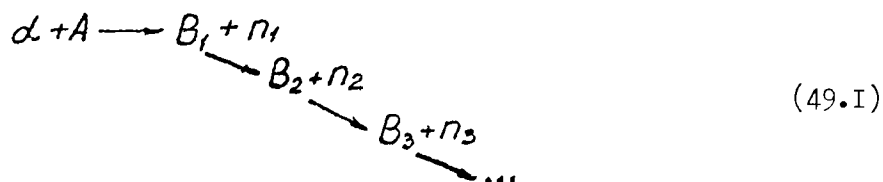
The calculations performed in the present section are also of independent value: firstly, they show that (n,p) and (n, $\alpha$ ) reactions in the nuclei under consideration on the whole involve the stage of compound nucleus formation; secondly, they make it possible to predict the cross-sections for the reactions indicated in those cases where there is some certainty that the reaction involves a compound nucleus; thirdly, they demonstrate that even in calculations using the level density function one can speak of the quantitative agreement of the theory with the experimental data.

#### 4. The cascade theory of neutron and gamma photon emission by compound nuclei

We present in this section a summary of the formulas which will be necessary in the rest of the present paper.

Let us first consider the cascade theory of neutron evaporation.

We shall assume that the neutron spectrum in which we are interested is that of neutrons occurring in the reaction



The process (49.I) may stop short at any of the cascades, beginning with the first and ending with the last, determined by relations (6.I).

The spectrum of the first neutrons is obviously determined by the following relation (see section 1):

$$\sigma_{\alpha, n_1}^{\gamma} = \frac{I}{k_{\alpha}^2} \cdot \frac{2\gamma+1}{(2\sigma_{\alpha}+1)(2I_{\alpha}+1)} T_{\alpha}^{\gamma} W_{\gamma n_1 l n_1}^{\gamma} (E_0; E_{n_1}, \epsilon_{n_1}) \quad (50.I)$$

The neutrons emitted in the second cascade are described by the formula

$$\begin{aligned} \sigma_{\alpha, n_1, n_2}^{\gamma} = & \frac{I}{k_{\alpha}^2} \cdot \frac{2\gamma+1}{(2\sigma_{\alpha}+1)(2I_{\alpha}+1)} T_{\alpha}^{\gamma} \sum_{\substack{E_{n_1}, I_{n_1} \\ \gamma_1, l_{n_1}}} W_{\gamma_1 n_1 l_{n_1} \gamma_1}^{\gamma} (E_0; E_{n_1}, \epsilon_{n_1}) * \\ & \times W_{\gamma_2 n_2 l_{n_2} \gamma_2}^{I_{n_1}} (E_{n_1}; E_{n_2}, \epsilon_{n_2}) \quad \text{etc.} \end{aligned} \quad (51.I)$$

It is obvious that the total neutron spectrum corresponding to the process (49.I) will be

$$\begin{aligned} \Sigma_{\alpha, n} = & \sum_{\gamma, l_{\alpha}, \gamma_{\alpha}} \frac{I}{k_{\alpha}^2} \frac{2\gamma+1}{(2\sigma_{\alpha}+1)(2I_{\alpha}+1)} T_{\alpha, l_{\alpha}}^{\gamma} \left\{ \sum_{\gamma_1, l_{n_1}} W_{\gamma_1 n_1 l_{n_1} \gamma_1}^{\gamma} (E_0; E_{n_1}, \epsilon_{n_1}) + \right. \\ & \left. + \sum_{\substack{E_{n_1}, I_{n_1}, \gamma_1, l_{n_1} \\ \gamma_2, l_{n_2}}} W_{\gamma_1 n_1 l_{n_1} \gamma_1}^{\gamma} (E_0; E_{n_1}, \epsilon_{n_1}) W_{\gamma_2 n_2 l_{n_2} \gamma_2}^{I_{n_1}} (E_{n_1}; E_{n_2}; \epsilon_{n_2}) + \dots \right\} \end{aligned} \quad (52.I)$$

In exactly the same way as expression (52.I), one can write the cross-section for the formation of the gamma photons occurring in the process  $(\alpha; \beta, \gamma_1, \gamma_2)$  as follows:

$$\begin{aligned} \sigma_{\gamma_1, \gamma_2, \dots}^{\gamma}(\alpha; \beta) = \sigma_{\alpha, \beta}^{\gamma}(E_{\alpha}, E_{\beta}, \epsilon_{\beta}) \left\{ \sum_{\ell_1} P_{\ell_1}^{I_{\beta}}(E_{\beta}; E_{\gamma_1}, \epsilon_{\gamma_1}) + \right. \\ \left. + \sum_{\substack{\ell_1, \ell_2 \\ \gamma_1', I_1', \epsilon_1'}} P_{\ell_1}^{I_{\beta}}(E_{\beta}; E_{\gamma_1}', \epsilon_{\gamma_1}') P_{\ell_2}^{I_{\gamma_1'}}(E_{\gamma_1}', E_{\gamma_2}, \epsilon_{\gamma_2}) + \dots \right\} \end{aligned} \quad (53.I)$$

In the relation (53.I),  $P_{\ell_1}^{I_{\beta}}(E_{\beta}; E_{\gamma_1}, \epsilon_{\gamma_1})$  is the probability of decay of a compound nucleus having excitation energy  $E_{\beta}$  and spin  $I_{\beta}$  with the emission of a gamma photon of multipole order  $\ell_1$  and energy  $\epsilon_{\gamma_1}$ ; the residual nucleus will here have an excitation energy  $E_{\gamma_1}$ .

Let us assume that the excitation spectrum  $E_{\gamma}$  of a gamma-emitting nucleus is discrete up to  $E_{\gamma} = E_{\gamma}^0$  and that at  $E_{\gamma} \geq E_{\gamma}^0$  it is characterized by the level density function  $\rho(E_{\gamma}, I_{\gamma})$ . Then

$$P_{\ell_1}^{I_{\beta}}(E_{\beta}, E_{\gamma_1}, \epsilon_{\gamma_1}) = \frac{A_{\ell_1}^{I_{\beta}}(E_{\gamma_1}, \epsilon_{\gamma_1}) \rho(E_{\gamma_1}, I_{\gamma_1})}{\sum_{\substack{S, E_S \\ \gamma_S, I_S, \epsilon_S}} \Gamma_{\gamma_S}^{I_{\beta}}(\epsilon_S) + \sum_{\substack{E_{\gamma_1}', I_{\gamma_1}', \epsilon_{\gamma_1}'}} A_{\ell_1}^{I_{\beta}}(E_{\gamma_1}', \epsilon_{\gamma_1}') + \sum_{\substack{E_{\gamma_1}^0 \\ I_{\gamma_1}^0, \epsilon_{\gamma_1}^0}} \int_{E_{\gamma_1}^0}^{E_{\beta}} A_{\ell_1}^{I_{\beta}}(E_{\gamma_1}') \rho(E_{\gamma_1}', I_{\gamma_1}') dE_{\gamma_1}'} \quad (54.I)$$

if  $E_{\gamma_1} \geq E_{\gamma}^0$  and

$$P_{\ell_1}^{I_{\beta}}(E_{\beta}, E_{\gamma_1}, \epsilon_{\gamma_1}) = \frac{A_{\ell_1}^{I_{\beta}}(E_{\gamma_1}, \epsilon_{\gamma_1})}{\{\beta, \gamma\}}, \quad (55.I)$$

if  $E_{\gamma_1} < E_{\gamma}^0$ .

In expression (55.I), the symbol  $\{\beta, \gamma\}$  denotes the denominator of expression (54.I). The quantity  $A_{\ell_1}^{I_{\beta}}$  is a kind of "coefficient of adhesion" of the gamma photon to the nucleus [41]. The first of the sums in the denominator of expression (54.I) is a sum with respect to particles which takes into account the competition between particle and gamma photon emission; it also includes states with  $E_{\beta} \geq E_{\gamma}^0$ . It is obvious that this sum vanishes when  $E_{\beta} \leq Q_{\delta}$ .

The relations presented in this section are quite sufficient for us to proceed directly to calculations of the spectra of neutrons and gamma photons emitted in fission. It is best to simplify and modify these formulas as the need arises.

Chapter II. PROMPT FISSION NEUTRON SPECTRA  
INDUCED  $^{235}\text{U}$  FISSION

1. A short historical review of calculations of the spectra of prompt fission neutrons

All fission neutron spectrum calculations performed to date have relied in one way or another on the concepts contained in the evaporation theory first put forward by Frenkel and Weisskopf [42, 43].

According to Weisskopf, the spectrum of neutrons emitted by a nucleus with an excitation energy  $E$  has the form

$$Y(E, \epsilon) \sim \sigma_c(E, \epsilon) \epsilon \exp\{\sqrt{4a(E - Q_n - \epsilon)}\}, \quad (1.II)$$

where  $\epsilon$  is the kinetic energy of the emergent neutron,  $Q_n$  is its binding energy in the compound nucleus and  $\sigma_c(E, \epsilon)$  is the cross-section for the neutron re-radiation process.

Formula (1.II) has generally been used in the simplified form

$$Y \sim \sigma_c(\epsilon) \epsilon e^{-\frac{\epsilon}{T}}, \quad (2.II)$$

where  $T$  is the temperature of the nucleus after the emission of a neutron. This formula is a good approximation to expression (1.II) if the following conditions are satisfied:

1.  $\epsilon \ll E - Q_n$ ;
2.  $\sigma_c(E, \epsilon) = \sigma_c(\epsilon)$ , i.e. the cross-section for the formation of a compound nucleus by a neutron and an excited target nucleus does not depend on the excitation energy.

Strictly speaking, the first assumption does not hold, for according to the law of energy conservation the energy of the neutrons should vary within the range

$$0 \leq \epsilon \leq E - Q_n$$

Nevertheless, the approximation (1.II) does have meaning, for the main part of the neutron spectrum lies in the soft region, where  $\epsilon < 5-6$  MeV, if one considers the neutron spectrum in the centre of fragment mass system, to which only formula (2.II) relates, and the difference  $E - Q_n$  for fission fragments has an average value  $\sim 10-15$  MeV. Expansion of the exponent in formula (1.II)

and elimination of terms of the order  $\frac{a \epsilon^2}{(E - Q_n)}$  immediately gives the exponent standing in expression (2.II) [44].

As was shown in Ref. [45], the second assumption holds fairly well for the excitation energies possessed by fission fragments.

In the present paper, wherever the cross-section for the formation of a compound nucleus has been used it has been assumed that the second assumption is sufficiently accurate for neutron spectrum calculations.

Formula (2.II) describes the spectrum of neutrons emitted in the first cascade by the nucleus having a temperature  $T$ . It is obvious that the spectrum of the next neutrons to be emitted from the nucleus will no longer be described by formula (2.II), for after the emission of the first neutron there is a temperature distribution of the nuclei.

Neglecting this fact, Watt [46] - and subsequently Gurevich and Mukhin [47] - calculated the integral spectra of fission neutrons on the assumption that in the centre of fragment mass system the spectrum of neutrons emitted in a cascade has the form (2.II). Moreover, the cross-section for the formation of a compound nucleus was assumed by these authors to be proportional to  $\epsilon^{-\frac{1}{2}}$ , which contradicts data on inelastic neutron scattering according to which  $\sigma_c \cong \text{const}$  when  $\epsilon > 0.5$  MeV [49, 48]. Calculations based on the optical model [50] also point to the weak dependence of  $\sigma_c$  on neutron energy between 0.5 MeV and several MeV. Fortunately, these two errors cancel out, for according to Le Cauter [51] the spectrum of neutrons emitted in a cascade approximates roughly in the centre of fragment mass system to a Maxwellian distribution:

$$P(\epsilon) \sim \epsilon^{1/2} e^{-\frac{\epsilon}{T_{\text{eff}}}}, \quad (3.II)$$

where  $T_{\text{eff}}$  is the effective temperature, which is related in a fairly complex manner to the initial excitation energy of the nucleus. It is not surprising, therefore, that the authors of Refs [47, 46] succeeded in understanding correctly the energy dependence of the integral neutron spectrum in the laboratory system of co-ordinates. However, the parameters determining this spectrum contradict other data.

In fact, if one assumes that the neutron spectrum in the centre of fragment mass system has the form (3.II) and that the neutrons evaporate off the fully accelerated fission fragments, then, taking into account the



relationship between the energy of the neutron in the laboratory system of co-ordinates  $\epsilon_l$  and its energy in the centre of fragment mass system

$$\epsilon = \epsilon_l + \bar{W}_i - 2\sqrt{\epsilon_l \bar{W}_i} \cos \theta_l \quad (4.II)$$

and the corresponding transformation Jacobian

$$J = \frac{\sqrt{\epsilon_l}}{(\epsilon_l + \bar{W}_i - 2\sqrt{\epsilon_l \bar{W}_i} \cos \theta_l)^{1/2}}, \quad (5.II)$$

it is easy to find in the laboratory system of co-ordinates the neutron spectrum integrated over the neutron emergence angles  $\theta_l$  :

$$F_i(\epsilon_l) \sim e^{-\frac{\epsilon_l}{T_f^i}} \operatorname{sh} \frac{2\sqrt{\bar{W}_i \epsilon_l}}{T_f^i} \quad (6.II)$$

In relations (3.II)-(6.II)

$T_f^i$  is some effective temperature of the fission fragment nuclei,

$\bar{W}_i$  is the mean kinetic energy per nucleon of a fission fragment,

$\theta_l$  is the angle of emergence of the neutron in the laboratory system of co-ordinates relative to the direction of movement of the fission fragments.

The index  $i$  passes through two values:  $i = l, T$  (light or heavy fission fragments).

The total spectrum of light and heavy fission fragments is given by a linear combination of spectra, of the form (6.II):

$$F(\epsilon) = A_l F_l(\epsilon) + A_h F_h(\epsilon); \quad (7.II)$$

It is always possible to choose parameters in such a way as to achieve agreement between formula (7.II) and the data on integral fission neutron spectra. However, the parameters  $\bar{W}_i$ , for example, which give the best agreement

between formula (7.II) and the experimental data, contradict the direct fragment velocity measurements [53, 52].

Consequently, agreement between formula (7.II) and the experimental data on integral fission neutron spectra does not permit the conclusion that evaporation of fully accelerated fission fragments is the mechanism of prompt fission neutron formation.

After the calculations described above had been performed, it became clear that for a correct description of fission neutron spectra it was necessary to take into account fission fragment distributions by excitation energy, kinetic energy, mass, etc. As there are many factors influencing the spectrum of fission neutrons, one must obviously begin by considering the most important ones. The most important factor not taken into account in earlier calculations is the distribution of fission fragments by excitation energy and changes in this distribution as neutrons are emitted.

The most detailed calculations in this respect were those of Terrel [54]. He found the excitation spectra of fission fragments after the emission of one, two, etc. neutrons. His method for finding the excitation spectrum of fission fragments was as follows: if one assumes that up to the point of neutron evaporation the fission fragment nuclei have an excitation energy distribution of the form

$$X_0(E) = \frac{1}{s\sqrt{2\pi}} \exp\left[-\frac{(E-\bar{E})^2}{2s^2}\right], \quad (8.II)$$

then the excitation energy distribution of the fission fragments after the emission of one neutron is obtained from expression (8.II) by a simple shift to the left along the energy axis by an amount equal to the mean energy carried off by the neutron leaving the fission fragment. As will be shown later, this approximation works well at high excitation energies. However, at low excitation energies,  $E \sim 2Q_n$ , this method does not even qualitatively reproduce the excitation spectrum after the emission of the next neutron. In order to appreciate this, we shall consider the following example. Let the excitation energy distribution of fission fragment nuclei before neutron emission be represented by the rectangle shown in Fig. 5.

With the help of formula (1.II) it is easy to write an expression for the excitation spectrum of fission fragments after the emission of one neutron:

$$X_1(E_1) = \int_{Q_{n_1} + E_1}^{E_{\max}} N(E_0) \sigma_c (E_0 - Q_{n_1} - E_1) e^{\sqrt{4aE_1}} X_0(E_0) dE_0, \quad (9.II)$$

where  $X_0(E_0)$  is the rectangular excitation energy distribution of the fission fragment nuclei before neutron evaporation and the excitation energy of the final nucleus,  $E_1$  is found from the law of energy conservation:

$$E_0 = E_1 + Q_{n_1} + E_1 \quad (10.II)$$

The normalization factor  $N(E_0)$  is found from the condition

$$\int_0^{E_0 - Q_{n_1}} N(E_0) \sigma_c (E_0 - Q_{n_1} - E_1) e^{\sqrt{4aE_1}} dE_1 = \frac{\Gamma_n(E_0)}{\Gamma_n(E_0) + \Gamma_\gamma(E_0)}, \quad (11.II)$$

where  $\Gamma_n$  and  $\Gamma_\gamma$  are the neutron and radiation widths respectively.

The spectrum  $X_1(E_1)$  in Fig. 5 was found by assuming  $\sigma_c = \text{const}$ ,  $\Gamma_\gamma \sim 0.1$  MeV and  $a = 0.05$  A, where A is the fission fragment mass number (taken to be 100);  $\Gamma_n(E_0)$  was calculated in accordance with Ref. [44].

It can be seen from Fig. 5 that the excitation energy distribution of the fission fragments after the evaporation of one neutron has nothing in common with the rectangular distribution.

The same results can be reached on the basis of the following simple considerations. If  $\Gamma_\gamma \ll \Gamma_n$ , then the area under rectangular distribution  $X_0(E_0)$  for  $E_0 \gg Q_{n_1}$  must be equal to the area under the curve  $X_1(E_1)$ , for the number of nuclei before and after neutron emission must be the same. The distribution  $X_1(E_1)$  is shifted to the left along the energy axis relative to  $X_0(E_0)$  by an amount equal to the neutron binding energy  $Q_{n_1}$ . It is clear that the left-hand edge of the distribution  $X_1(E_1)$  will "rest against" the ordinate axis, which will raise  $X_1(E_1)$  at low values of  $E_1$  - and the lower the value of  $E_{\max}$ , the greater will be the distortion of the initial spectrum  $X_0(E_0)$  as it is transformed into  $X_1(E_1)$ .

In spite of what has just been said, Terrel obtained good agreement between the theoretical spectrum and the experimental data on integral neutron spectra for  $\sigma_c = \text{const}$  and  $\bar{W} = 0.76$  MeV (the value of  $\bar{W}$  chosen by Terrel coincides with the experimentally observed value [53, 52]).

Two conclusions can be drawn from this: either the integral neutron spectrum is very insensitive to the excitation energy distribution of the fission fragments or the agreement between Terrel's calculations and the experimental data is fortuitous. More exact calculations would clarify this point.

A further important step in the theoretical study of neutron spectra is the calculation of neutron angular distributions, which should certainly be more sensitive to the excitation energy distributions of fission fragments.

Calculations of the spectra of fission neutrons emitted at  $0^\circ$ ,  $45^\circ$  and  $90^\circ$  to the direction of fission fragment movement have been performed by Sirotinin [55], who used Terrel's method to find the temperature distribution of fission fragments. Instead of the kinetic energy distribution of fission fragments, only the mean kinetic energies of the light and heavy groups were used. Conversion to the laboratory system of co-ordinates and corrections for the experimental geometry gave neutron spectra in good agreement with the data presented in Refs [56-58].

This is very surprising. The calculations performed in Ref. [55] were repeated by the author of the present paper; Fig. 6 shows spectra calculated with the same initial data as in Ref. [55]. The experimental data from Refs [56-58] and the calculations of Sirotinin (continuous curves) are presented in Fig. 7. It can be seen that the relative positions of the curves depicting the spectra of neutrons emitted at  $0^\circ$ ,  $45^\circ$  and  $90^\circ$  to the direction of fission fragment movement in Fig. 6 do not reproduce the positions of the curves in Fig. 7 even qualitatively. On the other hand, one can readily establish that by multiplying each curve in Fig. 6 by its factor it is possible to achieve full agreement between the corresponding curves in Figs 6 and 7. However, this method of renormalizing spectra is not valid. It is possible to normalize a spectrum in the centre of fragment mass system. This means that, when a spectrum is renormalized in the laboratory system of co-ordinates, spectra calculated at different angles can be multiplied simultaneously by the same number.

From the calculations just described, the author has concluded that it is impossible to achieve agreement between spectra calculated at different angles and experimental spectra if one takes into account the excitation energy distribution of fission fragments by Terrel's method.

In this and the following chapters we describe calculations of the neutron spectra and the excitation energy distributions of residual fission fragment nuclei performed, where possible, on the basis of consistent use of the evaporation theory.

2. A method of neutron spectrum calculation in the centre of fragment mass system

The relations necessary for calculating a neutron spectrum in the centre of fragment mass system follow from the ideas set forth in Chapter I.

We shall here make the same assumptions 1 and 2 as in section 3 of Chapter I. With these assumptions, the probability of compound nucleus decay with the emission of a neutron assumes a form similar to expression (1.II).

In exactly the same way as when deriving cross-sections for cascade processes (Chapter I, section 4), one can easily write a formula giving the excitation energy distribution of fission fragments after the emission of  $\nu$  neutrons [59]:

$$X_{\nu}(E_{\nu}) = \int_{Q_{n\nu} + E_{\nu}}^{E_{\max} - \sum_{j=1}^{\nu-1} Q_{nj}} X_{\nu-1}(E_{\nu-1}) P_{\nu}(E_{\nu}, E_{\nu-1}) dE_{\nu-1}. \quad (12.II)$$

Here

$$P_{\nu}(E_{\nu}, E_{\nu-1}) = N_{\nu}(E_{\nu-1}) \sigma_c(E_{\nu-1} - Q_{n\nu} - E_{\nu}) \cdot \exp\{\sqrt{4aE_{\nu}}\} \quad (13.II)$$

is the probability of decay of a nucleus excited to an energy  $E_{\nu-1}$  with the emission of a neutron of energy  $\epsilon_{\nu}$  and the formation of a residual nucleus with an excitation energy  $E_{\nu}$ . The normalization factor  $N_{\nu}(E_{\nu-1})$  is found from condition (11.II).

If one assumes that  $\sigma_c = \text{const}$  and  $\Gamma_{\gamma} \approx 0.1$  eV (as will be done in all the neutron spectrum calculations performed below), then

$$N_{\nu}(E_{\nu-1}) = \frac{1}{10^{-9} \exp\{\sqrt{4aE_{\nu-1}}\} + \gamma_{\nu}(E_{\nu-1}, Q_{n\nu})}, \quad (14.II)$$

where

$$g_{\nu} = \frac{1}{8a^2} \left\{ 4a(E_{\nu-1} - Q_{n\nu}) - 6 + \exp \left\{ \sqrt{4a(E_{\nu-1} - Q_{n\nu})} \right\} \times \right. \\ \left. \times [8a(E_{\nu-1} - Q_{n\nu}) - 6\sqrt{4a(E_{\nu-1} - Q_{n\nu})} + 6] \right\}.$$

Here  $Q_{n\nu}$  is the binding energy of a neutron in a fission fragment which has already emitted  $\nu-1$  neutrons, and  $a$  is the level density parameter of the fission fragment nucleus.

The energy dependence of the level density was chosen in form

$$\rho = \text{const.} \cdot \exp \left\{ \sqrt{4aE} \right\}. \quad (15.II)$$

By analogy with expression (12.II) one can write the spectrum of neutrons emitted in groups of  $\nu$  in a cascade as follows:

$$\mathcal{P}_{\nu}(E_{\nu}, A) = \int_{Q_{n\nu} + E_{\nu}}^{E_{\text{max}}} \sum_{j=1}^{\nu-1} Q_{nj} X_{\nu-1}(E_{\nu-1}) Y_{\nu}(E_{\nu}, E_{\nu-1}) dE_{\nu-1}, \quad (16.II)$$

where

$$Y_{\nu}(E_{\nu}, E_{\nu-1}) = N_{\nu}(E_{\nu-1}) G_{\nu} E_{\nu} \exp \left\{ \sqrt{4a(E_{\nu-1} - Q_{n\nu} - E_{\nu})} \right\} \quad (17.II)$$

It should be noted that  $Y_{\nu}(E_{\nu}, E_{\nu-1})$  is obtained from expression (13.II) by replacing  $E_{\nu}$  in accordance with the relation

$$E_{\nu-1} = E_{\nu} + Q_{n\nu} + E_{\nu}.$$

The spectrum of all the neutrons in the centre of fragment mass system will be expressed by the sum

$$\mathcal{P}(E, A) = \sum_{j=1}^{\nu_{\text{max}}} \mathcal{P}_j(E, A). \quad (18.II)$$

The overall excitation energy distribution of the fission fragments after the emission of all neutrons will be

$$X(E) = \sum_{j=0}^{\nu_{\text{max}}} X_j(E). \quad (19.II)$$

The neutron spectrum  $P(\epsilon, A)$  and the fission fragment residual excitation spectrum  $X(E, A)$  are complex functions of the fission fragment mass number. The dependence on the fission fragment mass number results from factors to be explained below.

Above all, the level density of fission fragment nuclei (15.II) depends exponentially on  $A^{\frac{1}{2}}(a \approx 0.125 A)$ .

Moreover, all the formulas presented in this section contain the binding energy of a neutron  $Q_{n\nu}$  in a fission fragment of mass number  $A$  which has already emitted  $\nu-1$  neutrons; i.e.

$$Q_{n\nu} = Q_n(A - \nu + 1, Z_p^A). \quad (20.II)$$

Here  $Z_p^A$  denotes the most probable charge on a fission fragment of mass number  $A$  [60], calculated using the formula

$$Z_p^A = Z_A - \frac{1}{2} [Z_A + Z_{(A_f - \bar{\nu} - A)} - Z_f], \quad (21.II)$$

where

$$Z_A = \frac{A}{1,980670 + 0,0143524 A^{2/3}}$$

$Z_f$  is the charge on the fissioning isotope,  $A_f$  is its mass number and  $\bar{\nu}$  is the mean number of neutrons emitted in one fission event. The value of  $Z_p^A$  obtained with expression (21.II) was used for calculating  $Q_{n\nu}$  on the basis of Cameron's formula [61].

Lastly, there is a strong dependence on mass number in the excitation energy distribution of fission fragments up to the point of neutron emission.

The fission fragment excitation energy distribution function for a given mass ratio was derived from experimental data on the kinetic energies of fission fragments [53, 52] and the dependence of  $\bar{\nu}_{f.f.}^*$  on mass number and on the energy of the neutron causing fission [63, 62]. In the course of this operation it was found that the excitation energy distribution could be described adequately by a function of the form (8.II) if the mean fission fragment excitation energy  $\bar{E}$  and the curve width  $\delta$  were functions of mass number.

---

\* / f.f. = fission fragment.

However, the function (8.II) gives the distribution of the total excitation energy of two fission fragments. In neutron spectrum calculations it is necessary to know the excitation energy distribution for one fission fragment. According to Terrel [54], the distribution function for one fission fragment will also have a Gaussian form if the distribution by total excitation energy is Gaussian. Here

$$S_{\text{frag}} = \frac{\delta_{\text{total}}}{\sqrt{2}}, \quad \bar{E}_{\text{frag}} = \frac{\bar{E}_{\text{total}}}{2} \quad (22.II)$$

It is not difficult to show that the relations (22.II) are valid on the following assumptions:

1. The total excitation energy of two fission fragments is distributed in accordance with the law

$$X_0'(E) = \text{erf}\left(\frac{E}{\delta\sqrt{2}}\right) X_0(E). \quad (23.II)$$

The function  $\text{erf}\left(\frac{E}{\delta\sqrt{2}}\right)$  slightly distorts the form of  $X_0(E)$ : in the region  $E < \bar{E}$  the maximum deviations of the curve  $X_0'(E)$  from  $X_0(E)$  reach ~ 10-15%; at excitation energies  $E > \bar{E}$ ,

$$E > \bar{E}, \quad X_0'(E) \approx X_0(E)$$

2. The excitation energy is distributed between the fission fragments independently and solely in accordance with the law  $\varphi(E')$ .

The following equation is a consequence of these assumptions:

$$\text{erf}\left(\frac{E}{\delta\sqrt{2}}\right) X_0(E) = \int_0^E \varphi(E') \varphi(E-E') dE'. \quad (24.II)$$

Indeed, if a given fission fragment has an excitation energy  $E'$  with a probability  $\varphi(E')$ , while a second fission fragment has an energy  $E'' = E - E'$  with a probability  $\varphi(E - E')$ , then the probability of the two fission fragments having an energy  $E = E' + E''$  will be

$$\int_0^E \varphi(E') \varphi(E-E') dE'$$

On the other hand, according to assumption 1, the probability of two fission fragments having an excitation energy  $E$  is equal to  $\text{erf}\left(\frac{E}{\delta\sqrt{2}}\right) X_0$ . By direct



substitution one can see that the solution of equation (24.II) is the function

$$Y(E) = \frac{1}{\frac{s}{\sqrt{2}} \sqrt{2\pi}} e^{-\frac{(E - \bar{E})^2}{2(\frac{s}{\sqrt{2}})^2}}, \quad (25.II)$$

from the form of which the relations (22.II) follow.

The approximate nature of relation (25.II) is due not only to the replacement of  $X_0(E)$  by  $X'_0(E)$ ; assumption 2 is not strictly justified, for  $E'$  and  $E''$  are linked by the law of energy conservation. Moreover, there are also a number of factors which limit the independence of the excitation energy distribution between the fission fragments: these are attributable to the structure of the fissioning nucleus and the fission fragment nuclei. However, approximation (25.II) is used in the present paper.

3. Neutron spectrum conversion to the laboratory system of co-ordinates.  
A qualitative investigation of the spectrum of fission neutrons

If the direction of the fission fragment movement is fixed, then, as already indicated (see Chapter II, section 1), the neutron energy  $\epsilon$  in the centre of fragment mass system will be related to the neutron energy  $\epsilon_l$  in the laboratory system of co-ordinates by the expression

$$E = \epsilon_l + W(A) - 2\sqrt{\epsilon_l \cdot W(A)} \cos \theta_l, \quad (26.II)$$

where  $\theta_l$  is the angle at which the neutron emerges from the fission fragment in the laboratory system of co-ordinates relative to the direction of fission fragment movement and  $W(A)$  is the kinetic energy per nucleon of a fission fragment of mass  $A$ . The corresponding transformation Jacobian has the form

$$y = \frac{\sqrt{\epsilon_l}}{(\epsilon_l + W(A) - 2\sqrt{\epsilon_l W(A)} \cos \theta_l)^{1/2}} \quad (27.II)$$

Neutron spectra have been measured experimentally [56] at  $0^\circ$ ,  $45^\circ$  and  $90^\circ$  to the direction of fission fragment movement. The neutron detector established for each angle the sum of the spectra of the neutrons emitted by the light and the heavy fission fragments. The mass numbers of the fission fragments were not fixed.

If these peculiarities of the experiment described in Ref. [56] are taken into account, the neutron spectrum in the laboratory system of co-ordinates  $P_\ell(\varepsilon_\ell, \theta_\ell)$  is found from the relation

$$\mathcal{P}_\ell(\varepsilon_\ell, \theta_\ell) = \frac{1}{2\alpha} \int_{A_1}^{A_2} [\mathcal{P}_+(\varepsilon_\ell, \theta_\ell, A') J_+ + \mathcal{P}_-(\varepsilon_\ell, \theta_\ell, A) J_-] \times \Psi(A) dA, \quad A' = A_f - A \quad (28.II)$$

The function  $\Psi(A)$  gives the mass distribution of the fission fragments;  $\mathcal{P}_+$  and  $\mathcal{P}_-$  are obtained from expression (18.II) by replacing the variable

$$\varepsilon = \varepsilon_\ell + W(A) \mp 2\sqrt{\varepsilon_\ell W(A)} \cos \theta_\ell,$$

where the upper sign corresponds to fission fragments flying in the forward direction, i.e. towards the detector ( $\mathcal{P}_+$ ), and the lower sign corresponds to fission fragments flying in the reverse direction ( $\mathcal{P}_-$ );  $J_+$  and  $J_-$  are the corresponding transformation Jacobians. The quantity

$$\alpha = \int_{A_1}^{A_2} \Psi(A) dA,$$

where  $A_1$  and  $A_2$  are the mass numbers of the lightest and heaviest fission fragments respectively.

If the angular distribution of the fission fragments and the experimental geometry employed in Ref. [56] are taken into account, one can write the spectra of neutrons emitted at angles  $\theta_\ell$  of  $0^\circ$ ,  $45^\circ$  and  $90^\circ$  to the direction of fission fragment movement in the form

$$\Phi_{\theta_\ell}(\varepsilon_\ell) = \int_{\theta_{1i}}^{\theta_{2i}} \mathcal{P}_\ell(\varepsilon_\ell, \theta_\ell) Y_{\theta_\ell}(\theta_\ell) \sin \theta_\ell d\theta_\ell \quad (29.II)$$

The angular distribution functions  $Y_{\theta_\ell}(\theta) \sin \theta$  are found in Ref. [56] and have the form shown in Fig. 8.

In the formulas converting the fission neutron spectrum to the laboratory system of co-ordinates, it was tacitly assumed that the neutrons are emitted by the fission fragments when fully accelerated. Of course, before the experiment this is not at all obvious. As will be seen from the numerical spectrum calculations performed in the following sections, this assumption does not in general conflict with the experimental data. However, direct estimates making it possible to compare neutron emission and fission fragment acceleration times are also of interest.

The fission fragment acceleration time is easy to estimate if at the moment of fission the nucleus is represented in the form of two uniformly charged, osculating, unpolarized spheres. Naturally, the radii of the osculating spheres are chosen in such a way that the most probable fission fragment velocities are obtained correctly if the most probable charges on the fission fragments are given. This very simple model of a fissioning nucleus gives the time dependence of the relative fission fragment velocity shown in Fig. 9. As can be seen, the fission fragments accelerate to approximately 95% of their maximum velocity within a time  $t \sim 5 \times 10^{-21}$  s.

The time involved in neutron emission from a fission fragment can be estimated roughly by calculating the neutron width with the help of the statistical model, which gives the expression [44]

$$\Gamma_n = \frac{g M \sigma_c J(E, Q_n)}{\pi^2 \hbar^2 \exp\{\sqrt{4aE}\}}, \quad (30.II)$$

where  $J(E, Q_n)$  is given by formula (14.II),  $g = 2\sigma + 1$  ( $\sigma$  being the neutron spin),  $M$  is the neutron mass, and  $\sigma_c$  is the cross-section for neutron re-radiation from the fission fragment.

If one assumes that  $\sigma_c \approx 2$  barn and  $a = 0.1$  A then, at the excitation energies possessed by the fission fragments, the neutron emission time is found to be

$$\tau_n = \frac{\hbar}{\Gamma_n} \approx 10^{-19} \div 10^{-18} \text{ sec}$$

Thus, rough estimates show that the fission fragment acceleration time is much less than the neutron emission time. This also means, however, that neutrons are emitted from fission fragments which are more or less fully accelerated.

Let us now make a qualitative study of the neutron spectrum.

When written out in greater detail, formula (18.II), which gives the neutron spectrum in the centre of fragment mass system, has the form

$$\mathcal{P}(E, A) = \epsilon \sum_{\nu=1}^{\nu_{\max}} \int_{Q_{n\nu} + E}^{E_{\max} \sum_{j=1}^{\nu-1} Q_{nj}} \chi_{\nu,1}(E_{\nu,1}) \mathcal{J}_{\nu}(E, E_{\nu,1}) dE_{\nu,1}, \quad (31.II)$$

where

$$\mathcal{J}_{\nu}(E, E_{\nu,1}) = N_{\nu}(E_{\nu,1}, Q_{n\nu}) \exp\{\sqrt{4a(E_{\nu,1} - E - Q_{n\nu})}\}.$$

In each of the integrals of the sum in expression (31.II), the upper integration limit can be replaced by  $E_{\max}$  if it is assumed that  $X_{\nu-1}(E_{\nu-1})$  are zero in the region

$$E_{\max} - \sum_{j=1}^{\nu-1} Q_{nj} \leq E_{\nu-1} \leq E_{\max}$$

We shall assume that all  $Q_{n\nu} = \bar{Q}_n$ . Here, the line above  $Q_n$  denotes averaging over the mass numbers of the fission fragments appearing in the neutron cascade:

$$\bar{Q}_n = \frac{Q_n(A) + Q_n(A-1) + \dots + Q_n(A-\nu_{\max}+1)}{\nu_{\max}} \quad (32.II)$$

Replacing  $\varepsilon$  by  $\bar{\varepsilon}$  in the lower limit and expanding the exponent in  $\Phi_{\nu}$  for  $\varepsilon \ll E_{\nu-1} - \bar{Q}_n$ , we find

$$\mathcal{P}(\varepsilon, A) \approx \varepsilon \int_{\bar{E}_0}^{E_{\max}} \exp\left(-\frac{\varepsilon}{\sqrt{E-\bar{Q}_n}}\right) Z(E) dE, \quad (33.II)$$

where  $\bar{E}_0 = \bar{Q}_n + \bar{\varepsilon}$ , and

$$Z(E) = \sum_{\nu=1}^{\nu_{\max}} X_{\nu-1}(E) N_{\nu}(E, \bar{Q}_n)$$

On the basis of the mean value theorem, it is possible to write for each fixed value of  $\varepsilon$

$$\mathcal{P}(\varepsilon, A) \approx \varepsilon \exp\left(-\frac{\varepsilon}{\sqrt{\frac{\xi}{a} - \bar{Q}_n}}\right) \alpha(\xi), \quad (34.II)$$

where  $\alpha(\xi) = Z(\xi)(E_{\max} - \bar{E}_0)$ . It is obvious that when  $\varepsilon$  changes  $\xi$  will change and  $\alpha(\xi)$  will be some function of  $\varepsilon$ . For a qualitative study of the neutron spectrum in the laboratory system of co-ordinates it is sufficient to assume that the function  $\alpha(\xi)$ , which is weakly dependent on  $\varepsilon$ , is equal to some constant and that  $\xi = \xi_0$ .

Having assumed, for the sake of simplicity, that  $\sqrt{\frac{\xi_0 - \bar{Q}_n}{a}} = 1 \text{ MeV}$ , we find that in the laboratory system of co-ordinates the spectrum of neutrons emitted in the direction of fission fragment movement is

$$f_+(\epsilon_\ell, \theta_\ell) = (\epsilon_\ell + W - 2\sqrt{W\epsilon_\ell} \cos \theta_\ell)^{1/2} \sqrt{\epsilon_\ell} \times \\ \times \exp\{- (\epsilon_\ell + W - 2\sqrt{W\epsilon_\ell} \cos \theta_\ell)\}$$

Figs 10 and 10a depict qualitatively spectra for neutron emission at angles of  $0^\circ$  and  $90^\circ$  to the direction of fission fragment movement.

It is easy to show that the spectra of neutrons emitted at angles  $\theta_\ell \geq 90^\circ$  to the direction of fission fragment movement have the form  $f_+(\epsilon_\ell, 90^\circ)$ .

The authors of Refs [56-58] measured the total spectra of neutrons emitted from fission fragments flying in opposite directions. One would expect the experimental spectrum for neutron emission at an angle  $\theta_\ell = 0^\circ$  to have the form shown in Fig. 11. According to the data of the authors in question, however, this effect does not occur. The spectra of neutrons emitted in spontaneous  $^{252}\text{Cf}$  fission were measured in Ref. [64]. In the spectrum for neutron emission at an angle  $\theta_\ell = 11.25^\circ$  the effect occurs, but is rather weak. The spectra of neutrons emitted in  $^{235}\text{U}$  fission at various angles  $\theta_\ell$  were measured in Ref. [65]. The spectrum for  $\theta_\ell = 0^\circ$  clearly exhibits the effect shown in Fig. 11 (cf. Fig. 12).

#### 4. Discussion of calculations of the spectra of neutrons emitted in $^{235}\text{U}$ fission

Neutron spectrum calculations were performed for level density parameter values  $a = 0.05 \text{ A}$  and  $0.1 \text{ A}$  using the formulas presented above. As can readily be seen from Fig. 13, it is impossible to obtain good agreement with the data of Ref. [56] for any value of the level density parameter of the fission fragment nuclei, although the extent of agreement is much greater than that achieved by calculations based on Terrel's method.

For  $a = 0.05 \text{ A}$  the theoretical curves are in fairly good agreement with the hard part of the experimental spectrum ( $\epsilon_\ell > 2 \text{ MeV}$ ), but provide a poor description of the soft part.

If it is assumed that  $a = 0.1 \text{ A}$ , then the theory predicts too few hard neutrons. For  $a < 0.05 \text{ A}$  the theory leads to an excessively hard spectrum.

A common disadvantage of both computational variants is the fact that the relationship between the numbers of neutrons emitted at different angles for energies in the range 0.5-3 MeV is poorly reproduced. If the theoretical curves are arranged in such a way that the spectrum of neutrons emitted at an angle  $\theta_\ell = 0^\circ$  is described in the best possible manner, it is found that the theory predicts the emission of too few neutrons at an angle  $\theta_\ell = \frac{\pi}{2}$  and too many at an angle  $\theta_\ell = \frac{\pi}{4}$ .

These facts permit the following possible conclusions:

1. If the spectrum is isotropic in the centre of fragment mass system, then the evaporation theory predicts the spectrum incorrectly;
2. There is anisotropy of the spectrum in the centre of fragment mass system;
3. It is possible that a significant number of neutrons is emitted by the neck of the fissioning nucleus and that this makes a considerable contribution to the spectrum of neutrons emitted at an angle

$$\vartheta_{\ell} = \frac{\pi}{2} .$$

The first conclusion does not seem very convincing to the present author, for the evaporation theory was verified with ordinary nuclei and gave good results (see Chapter I). There are no serious grounds for assuming that, at the high excitation energies possessed by fission fragment nuclei ( $\sim 15-20$  MeV), when the levels overlap, the evaporation theory will fall down simply because the fission fragments are nuclei with a large neutron excess.

However, it will be possible to be more confident about this only after further calculations with other fissioning nuclei (including nuclei which undergo spontaneous fission), and there is consequently no need to consider the question of the separation from the general spectrum of those neutrons which are emitted before scission. Moreover, the spectra of neutrons emitted in spontaneous fission permit a more careful analysis of anisotropy in the centre of fragment mass system. Such an analysis is made in the following chapter.

### Chapter III. PROMPT FISSION NEUTRON SPECTRA

#### SPONTANEOUS $^{252}\text{Cf}$ FISSION

1. A kinematic analysis of the spectra of prompt neutrons emitted in spontaneous  $^{252}\text{Cf}$  fission

As was shown in section 4 of the preceding chapter, the use of the evaporation theory in describing fission neutron spectra is closely bound up with the existence of neutron spectrum anisotropy in the centre of fragment mass system and with the number of neutrons emitted from the neck of the fissioning nucleus.

Naturally, efforts have been made to separate the various aspects of this problem in some way and to analyse them individually.

In the present section an attempt is made to analyse from a purely kinematic point of view experimental data on the spectra of neutrons emitted in spontaneous  $^{252}\text{Cf}$  fission, without making any assumptions about the nature of the neutron spectrum [66].

In Ref. [64] measurements were made of the spectra of neutrons emitted in spontaneous  $^{252}\text{Cf}$  fission at various angles  $\vartheta_\ell$  to the direction of movement of the light fission fragment. Assuming that the evaporation theory is valid and applying it in an approximate manner, the authors analysed the spectra obtained and came to the conclusion that within 10-20% limits the spectra of the light and heavy fission fragments are isotropic in their centre of mass systems. Moreover, the analysis led to the conclusion that the light fission fragment emitted on an average 1.16 times as many neutrons as the heavy fission fragment.

In analysing the data from Ref. [64], we assume that the fission neutron spectrum is isotropic in the centre of fragment mass system and show that this assumption is sufficient for re-establishing the neutron spectrum in the centre of fragment mass system and for studying its properties.

Let us assume, therefore, that the isotropic spectra in the centre of mass systems of the light and heavy fission fragments are depicted by the functions  $P_\ell(\varepsilon, A_\ell)$  and  $P_h(\varepsilon, A_h)$  respectively, where  $A_\ell$  and  $A_h$  are the mass numbers of the light and heavy fission fragments.

Conversion to the laboratory system of co-ordinates by means of the formulas presented in the preceding chapter gives

$$\mathcal{P}(\varepsilon_\ell, \theta_\ell) = \frac{\sqrt{\varepsilon_\ell}}{d\varepsilon_\ell} \int_{A_{\ell 2}}^{A_{\ell 1}} \psi_\ell(A_\ell) \frac{\mathcal{P}_\ell(\varepsilon_\ell + W_\ell - 2\sqrt{\varepsilon_\ell W_\ell} \cos \theta_\ell, A_\ell) dA_\ell}{(\varepsilon_\ell + W_\ell - 2\sqrt{\varepsilon_\ell W_\ell} \cos \theta_\ell)^{1/2}} \quad (1.III)$$

$$+ \frac{\sqrt{\varepsilon_\ell}}{d\varepsilon_\ell} \int_{A_{h1}}^{A_{h2}} \psi_h(A_h) \frac{\mathcal{P}_h(\varepsilon_\ell + W_h + 2\sqrt{\varepsilon_\ell W_h} \cos \theta_\ell, A_h) dA_h}{(\varepsilon_\ell + W_h + 2\sqrt{\varepsilon_\ell W_h} \cos \theta_\ell)^{1/2}}$$

where  $\psi_\ell$  and  $\psi_h$  are the mass distributions of the light and heavy fission fragments,  $W_\ell$  and  $W_h$  are their kinetic energies per nucleon, and

$$\mathcal{L}_i = \int_{A_{i1}}^{A_{i2}} \psi_i(A_i) dA_i \quad (i = \ell, h)$$

The functions  $\frac{\psi_i}{a_i}$  are sharp peaks around the most probable values for the masses of the light and heavy fission fragments. Their replacement by  $\delta$ -functions leads to the approximate expression

$$\mathcal{P}(\epsilon_l, \vartheta_l) \approx \sqrt{\epsilon_l} \left[ \frac{\mathcal{P}_l(\epsilon_l + \bar{W}_l - 2\sqrt{\epsilon_l \bar{W}_l} \cos \vartheta_l, \bar{A}_l)}{(\epsilon_l + \bar{W}_l - 2\sqrt{\epsilon_l \bar{W}_l} \cos \vartheta_l)^{1/2}} + \right. \\ \left. + \frac{\mathcal{P}_h(\epsilon_l + \bar{W}_h + 2\sqrt{\epsilon_l \bar{W}_h} \cos \vartheta_l, \bar{A}_h)}{(\epsilon_l + \bar{W}_h + 2\sqrt{\epsilon_l \bar{W}_h} \cos \vartheta_l)^{1/2}} \right] \quad (2.III)$$

where  $\bar{W}_l = 1.02$  MeV and  $\bar{W}_h = 0.58$  MeV.

Comparison of expression (2.III) with the experimental data in Ref. [64] enables one to find the functions  $\mathcal{P}_l(\epsilon, \bar{A}_l)/\sqrt{\epsilon}$  and  $\mathcal{P}_h(\epsilon, \bar{A}_h)/\sqrt{\epsilon}$ , i.e. to re-establish the neutron spectra in the centre of mass system of each fission fragment.

Let us assume, in fact, that  $\vartheta_l = 0^\circ$  and  $\epsilon_l = 1$  MeV. Then the argument of the first term on the right-hand side of relation (2.III) is close to zero, while the argument of the second term is 3.2 MeV. If the estimates made in Ref. [64] are taken into account, this means that for  $\epsilon_l > 1$  MeV the contribution of the heavy fission fragment to the total spectrum is to within a few per cent negligible. For  $\epsilon_l > 1.5$  MeV, the same holds for angles in the range  $0 \leq \vartheta_l \leq 45^\circ$ .

In exactly the same way, when  $\epsilon_l > 1.5$  MeV and  $180^\circ \geq \vartheta_l \geq 135^\circ$  one can neglect the contribution of the light fission fragment to the total spectrum.

If we are justified in assuming that the neutron spectrum in the centre of fragment mass system is isotropic, then the functions  $R(\epsilon, \bar{A}_1)/\sqrt{\epsilon}$  ( $i$  being fixed) obtained from the data for different angles should agree.

The function  $\mathcal{P}_l(\epsilon, \bar{A}_l)/\sqrt{\epsilon}$  is obtained from neutron spectra measured for  $\vartheta_l = 11^\circ 15'$ ,  $22^\circ 30'$ ,  $33^\circ 45'$  and  $45^\circ$ . The corresponding curves in Fig. 17 agree within the limits of the experimental and computational errors.

The curves in Fig. 15 represent  $\mathcal{P}_h(\epsilon, \bar{A}_h)/\sqrt{\epsilon}$ ; they were obtained from data for  $\vartheta_l = 135^\circ$ ,  $146^\circ 15'$  and  $168^\circ 45'$ . They agree, except that the one obtained from the data for  $\vartheta_l = 168^\circ 45'$  lies above the others at  $\epsilon < 1$  MeV. However, the deviation of this curve from the others goes only slightly beyond the error limits of the experimental data and the calculations.

Converting the neutron spectra for the light and heavy fission fragments in Figs 14 and 15 from the centre of mass system to the laboratory system of co-ordinates and comparing the calculated spectra with the experimental ones



for  $\theta_2$  in the vicinity of  $90^\circ$ , one will readily see that for practical purposes the deviation of the calculated spectra from the experimental ones lies within the error limits of the experiment and the calculations (cf. Fig. 16). However, one cannot help noticing that the experimental points lie systematically higher than the calculated curves, especially in the soft part of the spectrum. This is probably due to those neutrons which are emitted from the neck of the fissioning nucleus before or at the very moment of scission. As can be seen from Fig. 16, however, such neutrons are rare.

Thus, it may be said that in the centre of mass systems of the light and heavy fission fragments the neutron spectra are isotropic to within 10-15%.

It is interesting to compare the re-established spectra of the neutrons emitted from the light and heavy fission fragments. Fig. 17 shows the spectra for a light (circles and dots) and a heavy (triangles and crosses) fission fragment. As can be seen from this figure, the spectra for the light and heavy fission fragments agree. Consequently, the light and heavy fragments emit on average the same number of neutrons. The continuous curve in Fig. 17 was used for converting the neutron spectrum to the laboratory system of co-ordinates.

From what has been said in this section it can be seen that, from the point of view of theoretical analysis, experimental data on the spectra of neutrons emitted in spontaneous  $^{252}\text{Cf}$  fission compare favourably with corresponding data on induced fission. In particular, the data on  $^{252}\text{Cf}$  neutron spectra obtained in Ref. [67] constitute good material for comparison with calculations on the basis of the evaporation theory and for obtaining, through such a comparison, information about the thermodynamic properties of fission fragments. The following sections deal with this question.

## 2. Calculations of the spectra of prompt neutrons emitted in spontaneous $^{252}\text{Cf}$ fission. Basic formulas and assumptions

All the basic expressions necessary for neutron spectrum calculations were presented in the preceding chapter. In this section, however, they will be modified somewhat [75] with a view to taking into account the energy gap in the excitation spectrum of fission fragment nuclei.

A definition of energy gap  $\Delta$  was given in Chapter I (see section 3). Here, the concept "energy gap" will be used in a somewhat different way - as a quantity which takes into account the relative "scarcity" of levels near the ground state of the nucleus. Everything that has just been said about the influence of the "energy gap" on the excitation spectrum of a nucleus can be expressed by writing the level density of the nucleus in, for example, the following form:

$$\rho_{\nu}(E) = m_{\nu} \delta(E) + \theta(E - \Delta_{\nu}) \bar{\rho}_{\nu}(E), \quad (3.III)$$

where  $\Delta_{\nu}$  is the pairing energy in a fission fragment which has emitted  $\nu$  neutrons;  $m_{\nu}$  is the effective number of discrete levels in the range from the ground state to an excitation energy equal to the "energy gap"  $\Delta_{\nu}$ ; the function  $\theta(X) = 0$  when  $X < 0$  and  $\theta(X) = 1$  when  $X \geq 0$ ; and  $\bar{\rho}_{\nu}(E)$  is a smooth energy function representing the level density of the nucleus when  $E \geq \Delta_{\nu}$ .

It is quite obvious that considerable account will have to be taken of the level density function in the form (3.III) for excitation energies  $E$  between the ground state and energies of the order of the neutron binding energy. This excitation energy range for residual fission fragment nuclei is particularly important for calculating gamma photon spectra and the total energy removed by the gamma photons emitted from fission fragments.

It was for the purpose of reconciling the calculated value of the total energy removed by the gamma photons emitted from fission fragments with the corresponding experimental value that V.P. Zommer proposed using the level density expression in the form (3.III).

It is also clear that at excitation energies corresponding to the inequality

$$\Delta \ll E - Q_n, \quad (4.III)$$

neutron emission by a fission fragment nucleus will proceed as if no gap existed. The region determined by the relation (4.III) is the main one for neutron emission. It is not surprising, therefore, that the neutron spectrum calculations performed with the "energy gap" taken into account showed that it could be neglected.

The situation changes radically when one considers the distribution of fission fragments by excitation energy from the ground state to the neutron binding energy after the emission of all neutrons. Here, the entire effect is due solely to the fact that there are no transitions to the residual nucleus excitation energy region

$$0 \leq E \leq \Delta$$

This causes a considerable redistribution of the level populations near the ground state.

As the excitation spectra of fission fragments will continue to be used in calculating gamma photon spectra, it is necessary to take into account the "gap" in the apparatus of the evaporation theory.

Here as in Chapter II, the angular momenta of the fission fragment nuclei will not be taken into account. Their influence on the emission of neutrons and gamma photons is discussed in Chapter IV.

Taking into account the energy gap, the probability of emission of a neutron with energy  $\epsilon_\nu$  by a nucleus having an excitation energy  $E_{\nu-1}$  is

$$Y(E_\nu, E_{\nu-1}) = N_\nu(E_{\nu-1}, Q_{n\nu}) E_\nu \left\{ m_\nu \delta(E_{\nu-1} - Q_{n\nu} - E_\nu) + n_\nu \theta(E_{\nu-1} - Q_{n\nu} - E_\nu - \Delta_\nu) \exp\left\{ \sqrt{4a_\nu(E_{\nu-1} - Q_{n\nu} - E_\nu - \Delta_\nu)} \right\} \right\} \quad (5.III)$$

The probability of fission fragment decay with neutron emission, expression (5.III), is obtained using the level density of the nucleus (3.III) where

$$\bar{\rho}_\nu(E) = n_\nu \exp\left\{ \sqrt{4a_\nu(E - \Delta_\nu)} \right\} \quad (6.III)$$

The excitation energy distribution of fission fragments after the emission of  $\nu$  neutrons now has the form

$$\chi_\nu(E_\nu) = m_\nu \delta(E_\nu) \beta_\nu + \theta(E_\nu - \Delta_\nu) R_\nu^\circ(E_\nu), \quad (7.III)$$

where

$$\beta_\nu = \int_{Q_{n\nu}}^{E_{\max} - \sum_{j=1}^{\nu-1} Q_{nj}} d_\nu R_{\nu-1}^\circ(E_{\nu-1}) dE_{\nu-1} \quad (8.III)$$

is the "population" of the ground state after the emission of  $\nu$  neutrons, while

$$R_\nu^\circ(E_\nu) = \theta(E_\nu - \Delta_\nu) \int_{Q_{n\nu} + E_\nu}^{E_{\max} - \sum_{j=1}^{\nu-1} Q_{nj}} R_{\nu-1}^\circ(E_{\nu-1}) P_\nu^\circ(E_\nu, E_{\nu-1}) dE_{\nu-1}, \quad (9.III)$$

$$d_\nu = m_\nu N_\nu(E_{\nu-1}, Q_{n\nu}) (E_{\nu-1} - Q_{n\nu}),$$

In expression (9.III)

$$P'_\nu(E_\nu, E_{\nu-1}) = N_\nu(E_{\nu-1}, Q_{n\nu})(E_{\nu-1} - Q_{n\nu} - E_\nu) \times \exp\{\sqrt{4a_\nu(E_\nu - \Delta_\nu)}\} \quad (10.III)$$

When the energy gap  $\Delta_\nu$  is taken into account, the normalization factor is given by the expression

$$N_\nu(E_{\nu-1}, Q_{n\nu}) = \frac{1}{\frac{\Gamma_\nu \hbar^2 n_\nu}{qM\sigma_c} \exp\{\sqrt{4a_\nu(E_\nu - \Delta_\nu)}\} + \mathcal{I}_\nu(E_{\nu-1}, Q_{n\nu})} \quad (11.III)$$

Here

$$\mathcal{I}_\nu(E_{\nu-1}, Q_{n\nu}) = m_\nu(E_{\nu-1} - Q_{n\nu}) + \frac{n_\nu}{8a_\nu^2} x^6 \times \theta(E_{\nu-1} - Q_{n\nu} - \Delta_\nu) [e^{x_\nu} (2x_\nu^2 - 6x_\nu + 6) + x_\nu^2 - 6], \quad (12.III)$$

and

$$x_\nu = [4a_\nu(E_{\nu-1} - Q_{n\nu} - \Delta_\nu)]^{1/2}$$

As usual, the factor (11.III) is found from the normalization condition

$$\int_0^{E_{\nu-1} - Q_{n\nu}} Y_\nu(E_\nu, E_{\nu-1}) dE_\nu = \frac{\Gamma_n^\nu(E_{\nu-1})}{\Gamma_n^\nu(E_{\nu-1}) + \Gamma_\nu} \quad (13.III)$$

In all the following calculations,  $\Gamma_\nu \approx 0.1$  eV and  $\sigma_c = \text{const.}$  On the assumption that  $\sigma_c = \text{const.}$ , the neutron width

$$\Gamma_n^\nu(E_{\nu-1}) = \frac{qM\sigma_c}{\hbar^2 n_\nu} \mathcal{I}_\nu(E_{\nu-1}, Q_{n\nu}) \exp\{-\sqrt{4a_\nu(E_{\nu-1} - \Delta_\nu)}\} \quad (14.III)$$

As in Chapter II, the problem reduces to that of calculating the sums

$$\mathcal{P}(E, A) = \sum_\nu \mathcal{P}'_\nu(E, A), \quad (15.III)$$

$$\chi(E, A) = \sum_{\nu} \chi_{\nu}(E, A), \quad (16.III)$$

which are respectively the neutron spectrum in the centre of fragment mass system and the excitation energy distribution after the emission of all neutrons.

When written out in greater detail, expression (15.III) has the form

$$\begin{aligned} \mathcal{P}(E, A) = & \sum_{\nu=1}^{\nu_{\max}} [R_{\nu-1}^{\circ}(Q_{n\nu} + E) N_{\nu}(Q_{n\nu} + E, Q_{n\nu}) E + \\ & + \int_{Q_{n\nu} + E}^{E_{\max} - \sum_{j=1}^{\nu-1} Q_{nj}} R_{\nu-1}^{\circ}(E_{\nu-1}) Y_{\nu}^{\circ}(\epsilon, E_{\nu-1}) dE_{\nu-1}], \end{aligned} \quad (17.III)$$

where

$$\begin{aligned} Y_{\nu}^{\circ}(\epsilon, E_{\nu-1}) = & N_{\nu}(E_{\nu-1}, Q_{n\nu}) \epsilon_{\nu} n_{\nu} \theta(E_{\nu-1} - Q_{n\nu} - \epsilon_{\nu} - \Delta_{\nu}) \times \\ & \times \exp \left\{ \sqrt{4a_{\nu}(E_{\nu-1} - Q_{n\nu} - \epsilon_{\nu} - \Delta_{\nu})} \right\}. \end{aligned} \quad (18.III)$$

The first term in the sum (17.III) describes transitions from the continuous spectrum of excited states to the ground state. As the calculations show, it is substantial only for low excitation energies (higher than but close to the neutron binding energy). In other words, the "gap" affects only the shape of the spectrum of those neutrons which are emitted last in the cascade.

For calculations using the formulas presented, we now need only the initial excitation energy distribution  $R_0^{\circ}$  of the fission fragments. We again assume that it has the form of a Gaussian curve  $X_0(E)$  with a mean excitation energy  $\bar{E}(A)$  and a distribution width  $\delta(A)$ . This curve was normalized to unity for each fission fragment in the excitation energy range from the ground state to  $E_{\max}(A)$ , which - for the sake of definiteness - is equal to  $\bar{E}(A) \times 20$  MeV.

The mean excitation energies were derived from experimental data [67] relating to the dependence of the number of neutrons emitted by a fission fragment on the mass number of the fission fragment, with allowance made for the energy removed by gamma photons [68, 69].

The distribution widths  $\delta(A)$  were determined from experimental data [67] relating to the dependence of the kinetic energy of a fission fragment on its mass number.

The values of these two parameters as functions of the mass number of the fission fragment nucleus are presented in Fig. 18.

The remaining parameters entering into the calculations were found in the same way as in Chapter II.

With a view to ascertaining the role of the energy gap in calculations of this quantity, two values (0 MeV and 1.5 MeV) were assigned for all fission fragments. Moreover, as the results of the calculations were found to depend only slightly on the number of discrete levels when it changed by less than a factor of ten, we assumed that  $m = 1$  in all calculations.

In concluding this section, we wish to say a few words about the algorithm for calculating the neutron spectra and the excitation energy distributions of fission fragments. S.V. Zhikhareva, who wrote the computer programme for the calculations in accordance with the formulas presented in this section, has shown that the problem of finding neutron spectra and excitation energy distributions can be reduced to a system of ordinary differential equations of first order, for the functions  $R_{\nu}^{\circ}$ ,  $P_{\nu}$  and  $\beta_{\nu}$  depend on the same parameters and are calculated within the same integration limits. If one assumes the upper limit of the integrals in terms of which these functions are expressed to be variable, then one can obtain the following system of equations after differentiation with respect to this limit:

$$\begin{aligned} \frac{dR_{\kappa}^{\circ}(E, x)}{dx^{\circ}} &= R_{\kappa-1}^{\circ}(x) \theta(E - \Delta_{\kappa}) P_{\kappa}^{\circ}(E, x), \\ \frac{dP_{\kappa}(E, x)}{dx} &= R_{\kappa-1}^{\circ}(x) \theta(x - Q_{n\kappa-1} - E - \Delta_{\kappa}) \mathcal{J}_{\kappa}(E, x), \\ \frac{d\beta_{\kappa}(E, x)}{dx} &= R_{\kappa-1}^{\circ}(x) \alpha_{\kappa}(E, x), \end{aligned} \quad (19. III)$$

The initial conditions of this system are as follows:

$$\begin{aligned} R_{\kappa}^{\circ}(E, Q_{n\kappa-1} + E) &= 0, \\ \beta_{\kappa}(E, Q_{n\kappa-1} + E) &= 0, \\ \mathcal{P}_{\kappa}(E, Q_{n\kappa-1} + E) &= m_{\kappa} R_{\kappa-1}^{\circ}(E, Q_{n\kappa-1} + E) \times \\ &\quad \times g_{\kappa}^{-1}(Q_{n\kappa-1} + E) \cdot E, \end{aligned} \quad (20. III)$$

where

$$g_{\nu}(x) = \frac{(x - Q_{n\nu-1})}{\alpha_{\nu}(x)}$$

The system (19.III) was solved by the Runge-Kutta method.

The spectra of  $^{252}\text{Cf}$  neutrons was calculated on a computer with a relative accuracy of  $10^{-3}$ , so that there were no approximations of a computational nature.

### 3. Calculations of $^{252}\text{Cf}$ neutron spectra and discussion of the results

One of the most interesting characteristics which can be determined from existing data on fission neutron spectra is the dependence of the level density parameter on the mass number of the fission fragment.

This characteristic of fission fragment nuclei is interesting for two reasons: firstly, it enables us to assess the properties of nuclei with a large neutron excess, on which there is virtually no experimental data; secondly, the level density of fission fragment nuclei is the decisive quantity in existing statistical theories relating to fission fragment mass and kinetic energy distributions [16-19].

Data on the level density of fission fragment nuclei derived from analyses of the prompt emission accompanying nuclear fission are considerably more reliable than data from statistical analyses of fission fragment mass and kinetic energy distributions. This is because the mechanism of neutron and gamma emission from fission fragments is essentially clear, whereas the mechanism of the fission process has not been thoroughly studied.

It would appear natural to change the statistical theory of fission in such a way that the data on the level density of fission fragments derived from analyses of the prompt emission accompanying fission completely explain the fission fragment mass and kinetic energy distributions. However, this lies outside the scope of the present article.

In order to derive as accurately as possible the level density parameter of fission fragments, it is necessary to derive all the other parameters entering into neutron spectrum calculations from the relevant experimental data or to calculate them more or less reliably. This was done above, to the extent that this is possible at the present time. Thus, the only parameter permitting the reconciliation of calculated and experimental neutron spectra is the level density parameter of fission fragment nuclei.

As direct calculations show, the quantity most sensitive to changes in the level density parameter is the mean neutron kinetic energy  $\bar{\epsilon}(A)$ .

The dependence of the fission fragment level density parameter on mass number was derived from a comparison of the calculated values of  $\bar{a}(A)$  with the corresponding experimental data [67]. Values of the level density parameter as functions of fission fragment mass number are presented in Table 5.

Of course, the values of the level density parameter depend on the shape of the level density function. As can be seen from the foregoing argument, we have neglected in the present article the energy dependence of the pre-exponential coefficient in the fission fragment level density function. For those excitation energies which are responsible for neutron emission, however, neglect of the weak energy dependence of the pre-exponential coefficient is unimportant.

The following form of the expression for the fission fragment level density was chosen as the main expression:

$$\bar{\rho}_\nu(E) = b \exp \left\{ \sqrt{4a_\nu(E - \Delta_\nu)} - \sqrt{4a_\nu(Q_{n\nu} - \Delta_\nu)} \right\} \quad (21. III)$$

where  $b$  determines the number of levels per unit energy interval near an excitation energy equal to the binding energy of a neutron in the nucleus under consideration. In all the calculations, the dependence of this parameter on the mass number of the fission fragment was assumed to be the same as for stable nuclei [70].

The uniqueness of the definition of the level density parameter can be seen from Fig. 19. The numbers alongside the curves indicate the mass numbers of the fission fragments. The horizontal lines indicate experimental values of the mean kinetic energies of neutrons emitted from a fission fragment of the mass in question.

It follows from Table 5 that for all fission fragment mass numbers from 85 to 121 good agreement is obtained if it is assumed that  $a(A) \approx 0.125 A$ . For fission fragment mass numbers from 151 to 161,  $a(A) = 0.1 A$ . In the region of the double-magic fission fragment with  $A = 132$ , the level density parameter reaches its minimum value:  $a \approx 1$  MeV. Thus, from the point of view of the shell structure of the nucleus, the behaviour of the level density parameter is reasonable.

This is an appropriate point to note that the level density parameter of fission fragments cannot be determined correctly from the dependence of the total number of prompt neutrons on the fission fragment mass (neutron spectrum zero moment). This quantity depends mainly on the excitation energy which the



fission fragment had before neutron emission, whereas the mean kinetic energy of a neutron (neutron spectrum first moment) is determined by the nature of the neutron emission - mainly by the hardness of the spectrum. The nature of the dependence of the total number of neutrons on the level density parameter can be seen from Fig. 20. The horizontal lines cutting the curves indicate experimental values of  $\nu(a)$  - for  $a = \xi A$ , the numbers alongside the curves are the mass numbers of the fission fragments.

Table 5 [76]

Dependence of the level density parameter of fission fragment nuclei produced in spontaneous  $^{252}\text{Cf}$  fission on the fission fragment mass number

A	$a(A), \text{MeV}^{-1}$	A	$a(A), \text{MeV}^{-1}$
89	11,1	127	3,8
91	11,4	129	2,2
93	11,6	131	2,45
95	11,9	133	1,7
97	12,1	135	1,3
99	12,4	137	5,1
101	12,6	139	5,5
103	12,9	141	8,5
105	13,1	143	10,0
107	13,4	145	11,6
109	13,6	147	11,8
111	13,9	149	11,9
113	14,1	151	15,1
115	14,3	153	15,3
117	14,6	155	15,5
119	14,9	157	15,7
121	15,1	159	15,9
123	15,4	161	16,1
125	6,6	163	20,4

Fig. 21 shows the dependence, obtained in the present article, of the level density parameter of a fission fragment on its mass number, together with the data of Lang [71], Ross [72] and Newton [73]. It can be seen that all the curves agree only qualitatively; the greatest divergences are observed in the region of symmetric fission.

Let us consider the data of Lang. His results were also obtained from experimental data [67], which he analysed on the basis of the approximate theory of cascade neutron evaporation developed in Refs [51, 74]. This theory is valid when the nuclear excitation energies are much greater than two binding energies. However, this condition does not hold in the case of fragments resulting from symmetric fission or of fragments with mass numbers from 80 to 100. As can be seen from Fig. 21, the divergence from Lang's data is great in these very mass number regions. Moreover, Lang's calculations were performed without detailed consideration being given to the excitation energy distributions of the fission fragments.

If the method of calculating spectra is a good one, then the reliability of the results will depend in effect on how well the theoretical neutron energy distributions, which determine the behaviour of  $\bar{\epsilon}(A)$ , agree with the experimental data. When comparing the results of neutron spectrum calculations with experimental data, a convenient starting point is the experimentally proved [67] existence of a "universal" spectrum form in the centre of fragment mass system.

The existence of a universal neutron spectrum form means that the shape of the energy distribution of neutrons from a fission fragment of any mass depends on two numbers - the number of prompt neutrons  $\nu(a)$  and the mean kinetic energy  $\bar{\epsilon}(A)$  of the neutrons emitted from a fission fragment of given mass - and on some universal function of a dimensionless parameter associated with the neutron energy, the shape of which is independent of the fission fragment mass number.

Calculations of neutron spectra having the "universal" form show that the theory also permits the conclusion that there is a universal fission neutron spectrum form despite the strong dependence of the average number of neutrons emitted on the fission fragment mass number.

The results of neutron spectrum calculations are presented in Fig. 22 for certain mass numbers. The dots indicate experimental data [67] in the "universal form". The pronounced divergence, going slightly beyond the error limits of the experimental data, is characteristic; for most mass numbers, the calculations yield less low-energy neutrons than are observed experimentally. This difference is due to the fact that the cross-section for the formation of a compound nucleus was assumed in the calculations to be independent of neutron energy, whereas at low neutron energies it varies with changing energy and considerably exceeds the value adopted in the calculations ( $\pi R^2$ ). Allowance for variations in  $\sigma_c$  with changing energy should lead to better agreement between theoretical and experimental spectra.

The neutron spectrum curve in Fig. 22, which corresponds to the mass number  $A = 133$ , shows how important it is to be consistent with regard to the fission fragment excitation energy distribution, especially when the excitation energy is low (as in the case when  $A = 133$ ).

Let us now consider in greater detail the residual excitation spectra of fission fragments after the emission of all neutrons.

Fig. 23 shows the residual excitation spectra of  $^{235}\text{U}$  fission fragments for the light ( $R_l^0$ ) and heavy ( $R_h^0$ ) groups. They were obtained without taking into account the pairing effect and indicate that, as a result of the cascade evaporation of neutrons, a significant fraction of the fragments is at low excitation energies: 1-2 MeV. This result, which is an exact one within the framework of the statistical theory, probably does not correspond to reality, for the fission fragments are nuclei for the most part with mass numbers close to those of magic nuclei, which exhibit a large energy gap in their excitation spectra.

When the energy gap is taken into account, the number of fission fragments having an excitation energy in the range from the ground state to the gap boundary will be zero; on the other hand, due to the condition that the number of particles be preserved, the number of fission fragments possessing higher excitation energies after the cascade evaporation of neutrons increases. This can be clearly seen if one compares the curves in Fig. 23 with the curve in Fig. 24 representing the residual excitation spectrum of a fission fragment of mass number  $A = 107$  produced in spontaneous  $^{252}\text{Cf}$  fission. An energy gap of 2 MeV was chosen.

Fig. 24b shows successive residual excitation energy spectra of a fission fragment with  $A = 107$  and the corresponding spectra of four neutrons emitted in a cascade. One cannot help noticing that after the emission of the first neutron the residual excitation energy curve virtually repeats the initial, pre-emission curve, there being only a slight reduction in its width. This means that at fission fragment excitation energies greater than  $\sim 15$  MeV (i.e. greater than two neutron binding energies) Terrel's approximation [54] still works well. At fission fragment excitation energies of the order of 15 MeV and less, however, it completely fails to reproduce the true excitation spectra and consequently cannot, generally speaking, lead to a correct neutron spectrum.

The spectra of the first three neutrons shown in Fig. 24b have the standard form, differing only in amplitude and in the mean kinetic energy removed by a neutron from the fission fragment. The spectrum of the fourth group of

neutrons to be emitted in the cascade differs from the others in that there is a characteristic break in the vicinity of neutron kinetic energies  $\epsilon \sim \Delta$ . This break in the curve is, of course, due to the existence of an energy gap in the fission fragment excitation energy spectrum. In the total spectrum of the neutrons shown in Fig. 24a, this break is hardly perceptible.

As can be seen, the energy gap has little influence on the total neutron spectrum; however, it may be expected to have a strong influence on gamma photon spectra, for the calculation of which one needs a thorough knowledge of the fission fragment distribution at low excitation energies. The influence of the energy gap on gamma spectra and on the total energy removed by gamma photons from fission fragments is studied in the following chapter.

#### 4. The hypothesis of "isothermal" neutron emission from fission fragments

At the Eighteenth Conference on Nuclear Spectroscopy, held in Riga in 1968, V.P. Zommer put forward the hypothesis of "isothermal" neutron emission from fission fragments [78].

The essence of this hypothesis is as follows. Let us assume that the fission fragments are virtually cold before scission. Immediately after scission, the fission fragment deformation energy will then become the excitation energy which makes neutron emission possible; in this connection, the relationship between the equilibrium deformation establishment time of a fission fragment  $t_\phi$  and the neutron emission time  $t_n$  is important. If  $t_\phi \ll t_n$ , then in the time it takes a fission fragment to reach equilibrium deformation there will be virtually no neutron emission. Then follows the neutron cascade, which removes most of the fission fragment excitation energy. This is the situation which has been considered so far in the theory of the emission accompanying nuclear fission.

As already mentioned (see Chapter II), at excitation energies corresponding to fission fragments the neutron emission time estimated on the basis of the statistical theory  $t_n \sim 10^{-18} - 10^{-19}$  s. The times corresponding to oscillatory motion of the fragments will have an order of magnitude  $\tilde{t}_\phi \sim 10^{-21} - 10^{-22}$  s (which corresponds to an oscillatory quantum  $\hbar\omega$  of 1-10 MeV). However, if the "viscosity" of the nuclear matter constituting the fission fragments is low and many oscillations can take place before their energy dissipates and "heats" the fission fragment matter, then the equilibrium deformation establishment time  $t_\phi$  may prove substantially greater than the characteristic oscillation time  $\tilde{t}_\phi$ . Let us assume that approximately  $10^3$  oscillations occur before their energy is converted to thermal energy. The equilibrium deformation establishment time  $t_\phi$  will then be comparable with the

neutron emission time  $t_n$ . If the number of oscillations necessary for dissipation is of the order of  $10^4-10^5$ , then  $t_\varphi \gg t_n$ .

The latter time relationship makes the neutron emission process qualitatively different from the one considered earlier. Indeed, if  $t_\varphi \gg t_n$ , then the fission fragment will heat up to an excitation energy exceeding the neutron binding energy by an amount equal to or somewhat greater than the mean neutron kinetic energy and a neutron will be emitted; having again become almost cold, the fission fragment will once more begin heating up and will reach a temperature at which a further neutron is emitted, etc. It is this process of neutron emission by a fission fragment that has been termed "isothermal" emission.

The satisfactory description of fission neutron spectra obtained earlier suggests that  $t_\varphi \ll t_n$ . Indeed, the level density parameters obtained in Chapter II agree qualitatively with Newton's data, which are probably equally applicable to normal nuclei and to those with a neutron excess. As has been shown by Le Couter and Lang [74], the cascade spectrum of neutrons in the centre of fragment mass system is approximated fairly well by the expression

$$\mathcal{P}(\varepsilon) = B \cdot \varepsilon^{1/2} e^{-\frac{\varepsilon}{T_{\text{eff}}}} \quad (22.\text{III})$$

As can be seen from Fig. 17, the continuous curve, plotted on the basis of expression (22.III) for appropriately selected values of B and  $T_{\text{eff}}$ , is a good approximation of the spectra of neutrons from the light and heavy fission fragments in their centre of mass systems. Expression (22.III) was obtained by Lang and Le Couter on the assumption that  $\sigma_c = \text{const}$ . This assumption is in good agreement with the predictions of the optical model and the corresponding experimental data for all neutron energies  $\varepsilon \gtrsim 1$  keV.

The one-time evaporation spectrum for  $\sigma_c = \text{const}$  is given by the expression

$$\mathcal{P}(\varepsilon) \sim \varepsilon e^{-\frac{\varepsilon}{T}} \quad (23.\text{III})$$

where  $aT^2 = E - Q_n$ , E being the excitation energy at which a neutron is emitted. The adduced facts indicate that the fission neutron spectra are most probably the result of cascade evaporation from the fission fragments. One other fact indicates the value of the cascade theory of neutron emission: the existing experimental data on neutron spectra [65] point to the presence

in the spectra, with an appreciable probability, of neutrons possessing an energy  $\sim 12$  MeV. Such neutron energies correspond to fission fragment excitation energies  $E \sim 22-24$  MeV. On the other hand, the fission fragment excitation energies corresponding to "isothermal" neutron emission  $E \approx Q_n + \bar{\epsilon} \cdot c$ , where  $c$  is close to or slightly greater than unity; i.e. in this case  $E \sim 7-8$  MeV ( $Q_n \sim 5-6$  MeV). It follows that the purely isothermal case, in which the relationship  $t_\phi \gg t_n$  really holds, conflicts with the experimental data, especially in that it corresponds to a very soft neutron spectrum.

On the other hand, if  $t_\phi \sim \bar{t}_n$ , where the line above  $t_n$  means that the neutron emission time is taken at the average excitation energy at which a neutron is emitted, then it is quite possible that  $c$  in the relation

$$E = Q_n + \bar{\epsilon} \cdot c \quad (24.III)$$

will be substantially greater than unity, and there will be some point in speaking of an "isothermal" mechanism if

$$Q_{n_1} + \bar{\epsilon}_1 \cdot c - \bar{\epsilon}_0 < Q_{n_2}, \quad (25.III)$$

where  $\bar{\epsilon}_0$  is the mean energy removed by a neutron from the fission fragment and the indices 1 and 2 refer to the first and second neutrons. The relation (25.III) corresponds to a fission fragment excitation energy  $E \lesssim 14-15$  MeV.

For  $E \sim 15$  MeV,  $c \sim 4-9$ . In the mass number regions  $A \leq 110$  and  $125 \lesssim A \lesssim 150$ , the mean excitation energy of  $^{252}\text{Cf}$  fission fragments does not in fact exceed  $\sim 15$  MeV. It is therefore difficult to distinguish between the "isothermal" process and the non-isothermal process in these fission fragment mass number regions.

Thus, for studying the nature of the process from the point of view under discussion, the most convenient fission fragment mass number regions are  $110 \leq A \leq 125$  and  $A \gtrsim 150$ .

Let us assume that the process proceeds isothermally, i.e. that neutron emission proceeds at excitation energies satisfying the requirement (25.III). The spectra of the successively emitted neutrons will then have the form (23.III), with approximately the same temperatures, while the mean neutron energy

$$\bar{\epsilon} = 2T \quad (26.III)$$

On the other hand,

$$E - Q_n = aT^2 = a \frac{\bar{\epsilon}^2}{4} \quad (27.III)$$

Combining expressions (27.III) and (24.III), we find

$$\bar{\epsilon} = \frac{4c}{a}. \quad (28.III)$$

Let us consider a fission fragment nucleus with  $A \approx 120$ . According to Newton, the level density parameter for this nucleus  $a \approx 17$  MeV. The mean neutron kinetic energy  $\epsilon \approx 1.7$  MeV (for  $^{252}\text{Cf}$ ,  $A = 120$ ). It then follows from expression (28.III) that  $c \approx 7.2$ , while  $E \approx 18$  according to expression (24.III). Taking into account the fact that the level density parameter theory developed by Newton [73] gives correct predictions only of the nature of the dependence of  $a$  on  $A$ , it may be assumed that the value obtained for the excitation energy at which neutron emission occurs does not conflict with requirement (25.III). In other words, by slightly reducing the level density parameter  $a$ , it is easy to satisfy requirement (25.III). Moreover, by selecting a value of  $c$  such that it does not conflict with expression (25.III) and using the experimental dependence  $\bar{\epsilon}(A)$ , it is easy to obtain values for the level density parameter from expression (28.III) and to establish that the resulting dependence  $a(A)$  agrees qualitatively with Newton's predictions (e.g. for  $4c = 13.68$ ). It can be seen, therefore, that the hypothesis of "isothermal" neutron emission does not in general conflict with experimental data on the mass number dependence of the mean neutron kinetic energy.

Relation (28.III) can also be obtained in a somewhat different way. It is obvious that the emission of a neutron occurs each time the neutron width reaches some critical value:

$$\Gamma_n [a(E - Q_n)] = \Gamma_n^{\text{cr}} \quad (29.III)$$

As the neutron width depends on the dimensionless quantity  $a(E - Q_n)$ , it always reaches its critical value at the same value of this quantity:

$$a(E - Q_n) = \text{const} \quad (30.III)$$

It follows from expressions (26.III), (27.III) and (30.III) that

$$\frac{a^2 \bar{E}^2}{4} = \text{const}, \quad \text{i.e.} \quad (31.III)$$

$$a \bar{E} = 2\sqrt{\text{const}}.$$

Assuming  $2\sqrt{\text{const}} = 4c$ , we obtain expression (28.III).

There is a further effect which may be a consequence of "isothermal" neutron emission from fission fragments: an increase in the number of neutrons emitted at  $90^\circ$  to the direction of fission fragment movement compared with the number corresponding to isotropic neutron emission in the centre of fragment mass system. This effect was encountered in section 1 of the present chapter, where the neutron excess was attributed to emission from the neck of the fissioning nucleus before or at the moment of scission. However, the situation may be somewhat different. Let us assume that the fission fragments are so cold before scission that neutron emission is impossible. Anisotropy of neutron emission in the centre of fragment mass system may then occur for two reasons. As has been shown by Strutinsky [79], anisotropy of neutron emission in the centre of mass system of an emitting nucleus may result from its inherent high angular momentum. However, as was shown in section 1 of the present chapter, the neutron excess resulting from the high momentum of a fission fragment and manifesting itself at small angles to the direction of fission fragment movement is small and virtually imperceptible within the limits of experimental and computational errors. Another possible reason for the anisotropy of neutron emission is the "shadow effect" associated with fission fragment deformation. The essence of this effect is as follows: if one assumes, for the sake of simplicity, that neutrons are emitted in equal numbers from any unit of fission fragment area, then the ratio of the numbers of neutrons emitted at  $90^\circ$  to the major axis of the fission fragment and in the direction of this axis will be approximately equal to the ratio of the areas of the corresponding spheroid sections:

$$d = \frac{J_{ab}}{J_{a^2}} = \frac{b}{a} \quad (32.III)$$

where  $a$  and  $b$  are the minor and major semi-axes of the spheroid. If we now assume that after scission the major semi-axis of the fission fragment lies on average in the plane of fission fragment movement, a neutron excess is to be expected at  $90^\circ$  to the direction of fission fragment movement. This effect



is obviously least pronounced when equilibrium fission fragment deformation has been achieved. In isothermal neutron emission, the emitting fission fragments are in states with high deformations, which must lead to an increase in the number of neutrons at  $90^\circ$  to the direction of fission fragment movement. In the picture we are considering, the greatest deformations are those of fission fragments which emit the largest number of neutrons. It is in this fission fragment mass number range that experimentalists should look for the greatest anisotropy of the spectrum in the centre of fragment mass system.

It will be possible to say whether or not "isothermal" neutron emission occurs in reality only after further - primarily experimental - study of the properties of the emission accompanying nuclear fission. More detailed calculations in relation to the consequences of "isothermal" neutron emission are also necessary.

This section is based on extensive discussions with V.P. Zommer, so that it may be considered the fruit of our common labours.

#### Chapter IV. PROMPT GAMMA PHOTONS EMITTED IN NUCLEAR FISSION

While fission neutrons carry information about the properties of fission fragment nuclei with high excitation energies, the prompt gamma photons accompanying fission carry information about their low excited states. Unfortunately, the experimental data on gamma spectra are not as detailed and accurate as the corresponding data on neutron spectra.

In this chapter, we describe calculations of the spectra of gamma photons accompanying  $^{235}\text{U}$  and  $^{252}\text{Cf}$  fission. We also consider the question of the total energy removed by gamma photons from fission fragments [75, 77], and that of the competition between neutron and gamma emission from fission fragments.

##### 1. Method and results of calculating the spectra of gamma photons accompanying $^{235}\text{U}$ and $^{252}\text{Cf}$ fission

A method for calculating the spectra of gamma photons accompanying nuclear reactions was developed by Strutinsky and co-workers [80] and by Troubetzkoy [81]. Here, as in the case of neutron emission, a decisive part is played by statistical concepts.

The probability of the emission of a gamma photon with energy  $E_\gamma$  by a nucleus having an excitation energy  $E$  is given by the expression

$$W_\gamma = N_\gamma(E) \cdot E_\gamma^3 \rho(E - E_\gamma), \quad (1. IV)$$

where  $N_Y(E)$  is a normalization factor computed from the condition

$$\int_0^E W_Y(E, E_Y) dE_Y = 1. \quad (2.IV)$$

The probability (1.IV) is obtained from relation (54.I) on the following assumptions:

1. The excitation energy of the nucleus emitting the gamma photon is less than the neutron binding energy;
2. The discrete spectrum of the nuclear states is not considered;
3. The probability of gamma emission does not depend on the spins of the initial and final states of the fission fragment nucleus;
4. Only electric dipole photons ( $l_1 = 1$ ) are emitted;
5. The matrix elements of the electromagnetic transitions do not depend on the initial and final states of the nucleus.

The probability of finding a nucleus with an excitation energy  $E$  after the emission of a gamma photon of energy  $E_Y$  is

$$W_Y(E, E - E_Y) = P_Y(E, E_Y). \quad (3.IV)$$

In exactly the same way as for neutrons (formally at  $Q_n = 0$ ), it is possible to write

$$R_k(E_k) = \int_{E_k}^{Q_n} P_Y^k(E_{k-1}, E_k) \cdot R_{k-1}(E_{k-1}) dE_{k-1} \quad (4.IV)$$

where  $R_k(E_k)$  is the level population after the emission of the  $k$ -th gamma photon. If we designate the "level population after the emission of all gamma photons" by

$$R(E) = \sum_{k=1}^M R_k(E_k), \quad (5.IV)$$

then by a simple summation of expression (4.IV) over the index  $k$  it is possible to find

$$R(E) = R_0(E) + \int_E^{Q_n} P_Y(E', E) R(E') dE' \quad (6.IV)$$

Thus, in order to find the level population after the emission of all gamma photons it is sufficient to know the initial level population  $R_0(E)$ .

The gamma spectrum is now defined as

$$\mathcal{P}(E_\gamma) = \int_{E_\gamma}^{Q_n} W_\gamma(E, E_\gamma) \cdot R(E) dE \quad (7.IV)$$

Here, as in Chapter III, the level density is chosen in the form (3.III). Accordingly,

$$\mathcal{P}(E_\gamma) = m f^{-1}(E_\gamma) E_\gamma^3 R(E_\gamma) + \int_{E_\gamma + \Delta}^{Q_n} R(E) \bar{W}_\gamma(E, E_\gamma) dE, \quad (8.IV)$$

where

$$\bar{W}_\gamma = f^{-1}(E) \cdot (E - E')^3 \theta(E - \Delta) \rho(E),$$

and

$$f(E) = m E^3 + \int_{\Delta}^E (E - y)^3 \bar{\rho}(y) dy.$$

The initial level population  $R_0(E)$  is determined by the preceding emission of neutrons by fission fragments excited to an energy  $E \geq Q_n$  and is given by the expression

$$R_0 = \sum_{k=0}^{\nu_{max}} R_k^0(E), \quad (9.IV)$$

where  $R_k^0(E)$  is the excitation energy distribution after the emission of the  $\nu$ -th neutron.

If  $R_0(E)$  is determined by relation (9.IV), then  $Q_n$  in expression (6.IV) has to be replaced by some "effective binding energy"  $\epsilon$ , which can be determined on the basis of the expression

$$\sum_{\nu=0}^{\nu_{max}} (\beta_\nu + \int_{\Delta}^{\epsilon} R_\nu^0(E) dE) = 1 \quad (10.IV)$$

the meaning of which is that, after the emission of all neutrons, the fission fragment will - with a probability equal to unity - be either in the ground state or in states with an excitation energy between  $\Delta$  and  $\epsilon$ . The population of the ground state after emission of the  $\nu$ -th neutron is  $\beta_\nu$ .

$R_v^0$  and  $\beta_v$  are calculated using the formulas given in Chapter III.

For ordinary nuclei, the energy gap fluctuates between zero and  $\sim 1.5$  MeV on average. In the gamma spectrum calculations it was assumed that it fluctuated within the same limits for fission fragments.

As can be seen from the formulas presented in this section, the gamma spectrum calculations were performed without taking into account competition between neutron and gamma emission, which is obviously important only near the neutron binding energy.

If one assumes that  $\Gamma_\gamma \ll \Gamma_n$  and neglects the influence of the angular momenta of the fission fragments, the total energy removed by gamma photons from the fission fragments will be

$$\tilde{E}_\gamma \cong \int_{\Delta}^{\epsilon(A)} E R_\nu(E, A) dE \quad (11.IV)$$

The approximate equality sign in expression (11.IV) means that a more exact value of the total gamma energy emitted is given by the formula

$$\tilde{E}_\gamma = \sum_{\nu=0}^{\nu_{max}} \int_{\Delta_\nu}^{Q_{n\nu}} E R_\nu^\nu(E) dE \quad (12.IV)$$

If all  $Q_{n\nu}$  are replaced by  $\epsilon(A)$  and definition (9.IV) is used, we then obtain expression (11.IV).

The results of gamma spectrum calculations for light and heavy fragments in the case of  $^{235}\text{U}$  fission by thermal neutrons are presented in Fig. 25. The broken lines represent the spectra of the light and heavy fission fragments ( $P_\ell(E_\gamma)$  and  $P_h(E_\gamma)$ ) and their sum. The continuous curve represents experimental data from Ref. [82]. The calculations were performed for  $\Delta = 0$  and using the spectra in Fig. 23 of the residual excitation energies after the emission of all neutrons from the light and heavy fission fragments.

It can be seen that the total calculated gamma photon yield per fission event corresponds approximately to the experimentally observed yield. However, the experimental spectrum is harder than the theoretical one. This is probably due to the influence of the angular momenta of the fission fragment nuclei. The existence of high momentum at excitation energies  $Q_n \leq E \leq 2Q_n$  leads to strong suppression of the neutron width, so that gamma photons can with an appreciable probability be emitted from the excitation energy range indicated. These questions are discussed in greater detail in the following section. As can be seen from what follows, the gap in the fission fragment excitation

spectrum has a strong influence on the gamma photon spectrum.

The total energy removed by gamma photons from  $^{235}\text{U}$  fission fragments is

$$\tilde{E}_\gamma = \tilde{E}_{\gamma l} + \tilde{E}_{\gamma h} = \int_0^{\bar{Q}_l} E R_l^o(E) dE + \int_0^{\bar{Q}_h} E R_h^o(E) dE, \quad (13.IV)$$

where the indices  $l$  and  $h$  relate to the light and the heavy fission fragment respectively. In this case the following results were obtained:

$$\begin{aligned} \tilde{E}_{\gamma l} &= 2.83 \text{ MeV}, \\ \tilde{E}_{\gamma h} &= 3.07 \text{ MeV}, \end{aligned}$$

i.e. the total gamma energy per fission event was found to be 5.9 MeV, which is considerably lower than the experimental value ( $\sim 7.2$  MeV).

One possible reason for such a low calculated value of the total gamma energy emitted is that the emission of gamma photons when  $E > Q_n$  was ignored. In fact,

$$\tilde{E}_\gamma \cong \int_{\Delta}^{E_{max}} E R^o(E, A) \frac{\Gamma_\gamma(E)}{\Gamma_n(E) + \Gamma_\gamma(E)} dE, \quad (14.IV)$$

where  $\Gamma_\gamma$  and  $\Gamma_n$  - the radiation and neutron widths - are assumed to be still independent of the fission fragment momenta. In the higher estimate made on the basis of expression (14.IV) for  $\Delta = 0$ , the total gamma energy per fission event was about 0.3 MeV higher. This again is insufficient for reconciling the theoretical and experimental values.

One can easily see that, if the pairing energy is taken into account, the agreement between calculation and experiment will improve substantially. Let us, for example, assume that  $R^o(E) \approx \frac{1}{\varepsilon(A) - \Delta}$  (see Fig. 24a); with the help of expression (11.IV), we then obtain per fission fragment

$$\tilde{E}_\gamma \approx \frac{E + \Delta}{2}. \quad (15.IV)$$

Relation (15.IV) shows that by choosing a pairing energy for fission fragments within reasonable limits it is possible to achieve agreement between the calculated and experimental values of the total gamma energy emitted. Exact calculations for spontaneous  $^{252}\text{Cf}$  fission confirm this. Indeed, if one assumes that  $\Delta = 1.5$  MeV for all fission fragments, then the value - averaged over the mass distribution - of the total energy removed from the fission fragments

by gamma photons is found to be 8.6 MeV. The corresponding experimental value is 8.2 MeV. If one takes into account the fact that about 25% of fission fragments are odd-odd nuclei for which pairing does not occur, the calculated value of the total energy of the gamma photons accompanying fission is found to be 8 MeV, which is very close to the experimental value. Of course, this result does not exhaust the question of the total gamma energy emitted; it is possible that the value assigned to the pairing energy is much too high because the momenta of the fission fragment nuclei are not taken into account.

Calculations have shown that the form of the spectrum of prompt gamma photons emitted from fission fragments depends both on the fission fragment mass ratio and on the pairing energy  $\Delta$ . For the range of mass numbers corresponding to symmetric fission, gamma spectra were found to be softer than for asymmetric fission.

In Fig. 26, the results of calculations of the hard part of the spectrum of gamma photons accompanying  $^{252}\text{Cf}$  fission ( $E_\gamma \geq 1.5$  MeV) are presented for several fission fragment mass ratios ( $R = M_h/M_l$ ) together with an experimental curve obtained by averaging over the mass distribution [69].

It can be seen from Fig. 26 that the gamma spectrum for  $\Delta = 0$  is considerably softer than when  $\Delta = 1.5$  MeV for the same fission fragment mass ratio.

## 2. Influence of the angular momenta of fission fragments on gamma photon spectra

Throughout the preceding section it was assumed that, when calculating the spectra of neutrons and gamma photons, one can neglect effects associated with the angular momenta of the excited fission fragments. In the present section, we discuss the influence of the momenta of fission fragments on the gamma spectra and estimate the neutron width when its momentum dependence is taken into account at fission fragment excitation energies exceeding the neutron binding energy by 1-2 MeV.

With regard to the neutron spectrum calculations, it has been shown that agreement with the experimental data can be achieved even without taking angular momenta into account. With the calculation of gamma spectra the situation is more complex.

The spectra of gamma photons emitted from fission fragments are peculiar in that they are characterized by a large (compared, for example, with the case of radiative neutron capture) number of gamma photons in the cascade (7-10) and a high value of the total energy removed by the gamma photons in the cascade (7-9 MeV). As has been shown, the latter peculiarity can be attributed

to the existence of a gap in the fragment excitation energy spectrum. However, the value assigned to the gap may have been too high, for the increase in the total gamma energy emitted may also have been due partly to the fact that the fission fragment momentum was high ( $J \sim 10\hbar$ ) [83]; a large number of gamma photons in the cascade is evidently due solely to the large fission fragment momentum [83]. Indeed, if it is assumed that on the whole only gamma photons of low multipole orders are emitted and that they have to remove a large momentum in the cascade, it becomes clear why the number of gamma photons must be of the same order as the fission fragment momentum itself. Consequently, as noted in Ref. [83], fission gamma photons must possess angular anisotropy relative to the line of fission fragment movement; this has been confirmed experimentally [84].

Of course, the questions connected with the influence of angular momenta on the spectrum of gamma photons (spectrum shape, angular distribution, etc.) can be answered only after appropriate exact calculations have been performed. However, the question of the total gamma energy emitted can be resolved even on the basis of the estimates which follow.

To answer the question regarding the influence of fission fragment angular momenta on the total gamma energy emitted, one must understand the nature of the competition between neutron and gamma emission at excitation energies  $Q_n \leq E < 2Q_n$ .

Competition between neutron and gamma emission is to be expected in those cases where the neutron has to remove a large angular momentum  $J_n = \vec{l}_n + \vec{\sigma}_n$  and consequently overcome a high centrifugal barrier. This situation cannot arise at excitation energies  $E > 2Q_n$ , for at such energies the neutron has every possibility of removing a small angular momentum. The neutrons corresponding to the fission spectrum are emitted mainly with small orbital momenta and at excitation energies  $E > 2Q_n$ , with random magnetic quantum number values. This means that fission fragments which at the beginning of neutron emission have a mean angular momentum  $\bar{J}$  must in effect conserve it right up to excitation energies  $Q_n \leq E < 2Q_n$ . The last neutron emitted by a fission fragment which is at excitation energies  $Q_n \leq E \leq 2Q_n$  must leave the fission fragment nucleus at excitation energies  $0 < E \leq Q_n$ , where  $\Gamma_n(E) \equiv 0$ . Let us consider what requirements must be met by the angular momentum removed by the neutron. We shall assume that the emitting fission fragment has an excitation energy  $E \approx 2Q_n$ . The residual nucleus will then have an excitation energy  $E \sim 4-5$  MeV, for the mean binding energy of a neutron in <sup>252</sup>Cf fission fragments  $\bar{Q}_n = 6$  MeV, while the mean kinetic energy  $\bar{\epsilon} = 1-2$  MeV.

Using the level density expression with allowance for momenta - for example, in accordance with Ref. [85] - it is easily estimated that when a fission fragment nucleus has an excitation energy  $\sim 5-4$  MeV and a mass number  $A \sim 100$ , it will have an average momentum  $\bar{J}' \approx (4-5)\hbar$ . Consequently, when a neutron is emitted by a fission fragment at  $E \sim 2Q_n$ , it will remove on average an orbital moment  $l_n \sim 5\hbar$ . According to the data in Ref. [50], the neutron penetrability of the nuclear surface  $T_e(\epsilon)$  for nuclei with  $A \sim 100$  and for neutron kinetic energies up to  $\epsilon \sim 4$  MeV becomes less than  $10^{-2}-10^{-3}$  if  $l \sim 5\hbar$ . We make a neutron width estimate below using these facts.

Let us assume that the initial nucleus, having an excitation energy  $E$  and angular momentum  $\vec{J}$ , emits a neutron with kinetic energy  $\epsilon$  and momentum  $\vec{J}_n = \vec{l}_n + \vec{\sigma}_n$ , being left with an excitation energy  $E - Q_n - \epsilon$  and momentum  $\vec{J}'$ , so that

$$\vec{J} = \vec{J}' + \vec{J}_n$$

Then, in the spirit of Chapter I, one can write for the probability of neutron emission

$$W_{n\gamma\ell_n}^{\gamma\gamma_n}(\epsilon)d\epsilon = \frac{\rho_{A-1}(E-Q_n-\epsilon, \gamma')}{\rho_{(A)}(E, \gamma)} \sigma_{c\gamma_n}(E, \epsilon) \times (16.IV)$$

$$\times (2\sigma_n + 1) \cdot \frac{M\epsilon d\epsilon}{g^2 \hbar^3},$$

where  $\rho_{(A)}(E, J)$  - the nuclear level density with allowance for the angular momenta - is determined by the relation (49.I) and

$$\sigma_{c\gamma_n} = \frac{\pi}{k^2} \frac{2J'+1}{(2I_0+1)(2\sigma_n+1)} T_{\ell_n\gamma_n}(\epsilon),$$

where  $I_0$  is the spin of the ground state of a fission fragment of mass number  $A-1$ .

When expression (16.IV) is used, the total neutron width will have the form

$$\frac{\Gamma_n^{\gamma}}{\hbar} = \int_0^{E-Q_n} d\epsilon \int dJ' \sum_{\gamma_n=|\gamma-\gamma'|}^{\gamma+\gamma'} \sum_{\ell_n=|\gamma_n-\sigma_n|}^{\gamma_n+\sigma_n} W_{n\gamma'\ell_n}^{\gamma\gamma_n}, \quad (17.IV)$$

where integration over  $dJ'$  has to be performed from zero to some possible mean value at excitation energies  $0 \leq E < Q_n - \bar{\epsilon}$ .

Estimates performed on the basis of formula (17.IV) for excitation energies  $E = (Q_n + 1)$  MeV and  $E = (Q_n + 2)$  MeV give  $\Gamma_n^{\bar{J}} \approx 0.1$  eV and  $\Gamma_n^{\bar{J}} \approx 1$  eV respectively if  $\bar{J} \sim 10\hbar$ .



It is now possible to estimate the energy removed by gamma photons from fission fragments possessing an excitation energy  $E \geq Q_n$ .

Let us assume that the excitation energy distribution of the fission fragment nuclei after the emission of all neutrons is given by the function  $X(E, J)$  for the region  $E \geq Q_n$ . The energy removed by the gamma photons from the fission fragments for  $E \geq Q_n$  is then

$$\Delta \tilde{E}_\gamma = \int_{Q_n}^{E_{max}} X(E, J) E \frac{\Gamma_\gamma^J(E)}{\Gamma_\gamma^J(E) + \Gamma_n^J(E)} dE dJ \quad (18.IV)$$

To evaluate expression (18.IV), we approximate the energy dependence  $X$  by a constant equal to  $\frac{1}{Q_n}$ . At the same time, it is natural to assume that the dependence on the momentum  $J$  coincides with the dependence of the fission fragment level density on this quantity (see expression (43.I)). Taking into account what has just been said and the estimates of  $\Gamma_n^J$  presented above, we find

$$\Delta \tilde{E}_\gamma \approx 1 \text{ MeV}$$

It is interesting to note that, if one assumes  $\Delta = 0$ , then for the total gamma energy emitted from  $^{252}\text{Cf}$  fission fragments one obtains  $\tilde{E}_\gamma \approx 8 \text{ MeV}$ , i.e. a value close to the experimental value. For  $^{235}\text{U}$  fission fragments, the estimate obtained leads to  $\tilde{E}_\gamma \approx 7.5 \text{ MeV}$ , as  $Q_n = 5.5 \text{ MeV}$  in this case. Here again,  $\tilde{E}_\gamma$  virtually coincides with the experimental value. However, the zero pairing energy is unreasonable and the resulting estimate is probably somewhat too high.

It can be seen from what has been said in the present section that it is necessary to calculate more accurately the spectra of gamma photons occurring in fission and the level populations of fission fragment nuclei with allowance for the influence of angular momenta.

#### CONCLUSIONS

As noted in Chapter I, it is simple to generalize the Hauser-Feshbach statistical method to cover multi-particle nuclear reactions while retaining the main advantages of the method - automatic allowance for the discreteness of the excitation energy spectrum of the final nuclei and the fact that the

cross-sections are expressed in terms of quantities that have been thoroughly studied (the "penetrability of the nuclear surface"). It is interesting to note that allowance for correlations between cascades, even when they are weak, leads to a form of the dependence of the cross-section on the penetrability coefficients which is qualitatively different from the normal Hauser-Feshbach expression. The discussion in Chapter I shows that cross-section expressions in terms of penetrability coefficients can also be obtained without recourse to detailed balance relations, and it is therefore not necessary to consider the corresponding penetrability coefficients in the sense of an inverse reaction. All the computational formulas for the cascade emission of neutrons and gamma photons employed in Chapters II-IV are a direct consequence of the expressions in Chapter I.

The statistical method of Hauser and Feshbach in conjunction with the optical model is highly suitable for describing the elastic and inelastic scattering of neutrons by medium and heavy nuclei in the incident neutron energy range between  $\sim 0.3$  MeV and  $\sim 6$  MeV.

It is also suitable for describing total cross-sections for  $(n,p)$  and  $(n,\alpha)$  reactions in some light and intermediate nuclei at incident neutron energies between the reaction threshold and  $\sim 14$  MeV. It is interesting to note in this connection that, in spite of the use of the nuclear level density function in the calculations, it is possible to speak of quantitative agreement between the theory and the experimental data.

This justifies the use of the statistical method in describing the spectra of neutrons and gamma photons emitted in fission. Of course, this application of the statistical theory to fission fragment nuclei is an extrapolation to the region of nuclei with a large neutron excess. However, the calculations which have been performed show that such extrapolation is fully justified. The same calculations indicate that the emission of neutrons and gamma photons from fission fragments is a statistical process.

Comparison of calculated and experimental spectra made it possible to obtain values of the level density parameter of fission fragment nuclei as a function of their mass number. This is the most important and valuable information which can be derived from existing experimental data on neutron and gamma photon spectra. The nature of the fission fragment mass number dependence of the level density parameter is essentially the same as that predicted by the statistical theory which takes into account shell effects

[73], etc. Generally speaking, the dependence obtained agrees in form with the data of Ross [72] and Lang [71]; however, the parameter values obtained in the present article are anomalously low ( $a \sim 1 \text{ MeV}^{-1}$ ) in the region of the double-magic fission fragment with  $A \approx 132$ .

It should be borne in mind that, if "isothermal" neutron emission is significant, the resulting data will contain errors, for this form of neutron emission was not taken into account in the calculations.

The level density parameter is interesting not only in that it determines the thermodynamic properties of the fission fragment. The level density parameters of fission fragments are the most important quantities when one is analysing statistically the distributions of fission fragments by mass and kinetic energy (this question is discussed in greater detail below).

If the level density parameters are known and there is information available on the excitation energy distribution of the fragments before neutron emission (e.g. from data on the kinetic energies of the fission fragments, etc.), then it is possible to predict with confidence the spectra of the fission neutrons.

It is important to take into account pairing in calculations of neutron spectra if the emitting fission fragment is weakly excited ( $E \lesssim Q_n$ ). For the majority of fission fragments, however, this is not the case and nucleon pairing can be neglected.

Nucleon pairing in a fission fragment nucleus must be taken into account in the calculation of fission fragment residual excitation spectra when  $E \leq Q_n$ . Information on the excitation energy distribution of fission fragments is decisive for calculating the total gamma energy emitted.

Neutron spectrum calculations were performed on the assumption that the neutron emission occurs when the fission fragments are fully accelerated. Both the calculations themselves and special estimates of the fission fragment acceleration and neutron emission times confirm this assumption.

Kinematic analysis of the spectra of prompt fission neutrons showed that in the centre of fragment mass system the neutron spectrum can be considered isotropic to within 10-15%. For a more exact analysis of neutron spectrum anisotropy in the centre of fragment mass system we need detailed experimental data on the spectra of neutrons emitted at small angles to the direction of fission fragment movement.

Throughout the calculations of neutron spectra and residual excitations use was made of a cross-section for the formation of a compound nucleus by a neutron and an excited fission fragment nucleus which is dependent neither on neutron energy nor on fission fragment excitation energy. This approximation is fully justified, except for neutron energies  $\epsilon$  of the order of a few keV. It is clear that in this energy region the cross-section must increase with decreasing  $\epsilon$ . This is probably the reason for the slight discrepancies between the calculated and experimental data on neutron spectra at low neutron energies.

Calculations have confirmed the experimental fact that there is a "universal form" of neutron spectrum in cases of asymmetric fission. When the fission fragments are only slightly excited, the theory which takes into account nucleon pairing in fission fragments predicts a spectrum which differs substantially from the "universal form". In this connection, a more exact experimental investigation of the spectra of prompt neutrons corresponding to weakly excited fission fragments would be useful.

It is to be expected that there is a "universal spectrum form" associated with the asymmetric fission of all transuranic elements. If this is so, then the problem of finding the neutron spectrum of a given fissioning isotope reduces to finding the dependence of the number of neutrons and the mean neutron kinetic energy on the fission fragment mass number.

Qualitative investigations and numerical calculations have pointed to the existence of a dip in the neutron spectrum in the laboratory system of co-ordinates at angles  $\vartheta_{\ell} \approx 0^{\circ}$  or  $180^{\circ}$  relative to the direction of fission fragment movement and at a neutron energy equal to the fission fragment kinetic energy per nucleon. As we saw, this fact has been confirmed experimentally. It is worthy of note that the dip occurs only if one assumes that the cross-section for the formation of a compound nucleus  $\sigma_c = \text{const.}$

The gamma spectrum calculations which have been performed give a satisfactory description of the form of spectra at gamma energies  $E_{\gamma} > 1.5$  MeV. In this respect, therefore, one need not take into account the influence of the angular momenta of the fission fragments. However, the number of gamma photons emitted per fission event (8-10) is not reproduced at all - and it is evidently impossible to reconcile the theory with the experimental data without taking into account the angular momenta of the fission fragments.

The total gamma energy emitted can be explained without recourse to the spins of the fission fragment nuclei if nucleon pairing is taken into account; however, there is no guarantee that the extent of pairing (the gap) will not be too great. Neutron width estimates which take into account the angular momenta of the fission fragments show that the increases in the total gamma energy emitted due to the influence of the large angular momentum of the fission fragment and due to the pairing energy are comparable. This calls for exact calculations of gamma spectra, fission fragment level "populations" and neutron widths taking into account fission fragment spins and the pairing energy.

Let us consider once more the value of the fission fragment level density parameter. As already noted, the level density is the most important quantity in the statistical analysis of fission fragment mass and kinetic energy distributions. However, in this area the position cannot be regarded as satisfactory: in spite of the fact that different authors use, generally speaking, different level density parameter values, there is so far no satisfactory description of - for example - the mass distributions of fission fragments. Nevertheless, in the present author's opinion there is no reason for pessimism. The crux of the matter is that two major causes of divergence between theory and experimental data have still to be eliminated. One of these lies in the use of fission fragment level density parameters which are not connected with any experimental data relating to fission, and as the level density is a strong function of the level density parameter, all analyses necessarily involve considerable arbitrariness in introducing other factors designed to ensure agreement between theory and experiment. The second cause lies in the uncertainty regarding the fission fragment excitation energy which should be used when one is considering, say, mass distributions. This uncertainty is closely bound up with the question of the "heated condition" of fission fragments immediately before scission of the fissioning nucleus. It is obvious that the mass and charge distribution is fully determined at the moment of time immediately preceding scission, and possibly even earlier - at the saddle point, where the future fission fragments can already be regarded as more or less formed. If this is so, however, then the excitation energy to be used in finding the fission fragment level density involved in describing the mass distribution should be taken at the moment before scission or even earlier. Special studies will have to be performed in order to remove this uncertainty.

To remove the uncertainties due to the first of the above-mentioned causes, it is reasonable in the statistical theory of fission fragment mass and kinetic energy distributions to use level density parameters obtained from

analyses of data on prompt fission radiation. More precisely, these parameters should be the initial material for extrapolating into the region where the fission fragments are strongly deformed - as they are before scission.

Removal of the second of the above-mentioned causes would appear to be more difficult. The associated uncertainties decrease as the excitation energy of the fissioning nucleus increases. This is evidently one of the reasons for the greater success in applying the statistical theory to mass distributions at high excitation energies. At low excitation energies of the fissioning nucleus and in the case of spontaneous fission, the question of the "heated condition" of the fission fragments before scission is still open. With regard to spontaneous  $^{252}\text{Cf}$  fission, it may be said that the excitation energies of the fission fragments before scission are low if the excess of neutrons at  $\vartheta_{\ell} = 90^{\circ}$  to the direction of fission fragment movement is related to evaporation from the excited fission fragments before scission. However, this same neutron excess can be ascribed to evaporation from the moving, but strongly deformed, fission fragments if "isothermal" neutron emission occurs. This calls for a detailed theoretical analysis of the "isothermal neutron emission" hypothesis.

Thus, there arises a whole group of problems which need to be solved, on the basis of level density data obtained from the analysis of prompt radiation. The final objective of such studies would be to obtain a description of mass, kinetic energy, etc. distributions and data on the prompt radiation accompanying fission from a single statistical point of view and with a single system of level density parameters, structural (shell) and dynamic factors being considered only where necessary.

REFERENCES

- [1] HAUSER, W., FESHBACH, H., Phys. Rev. 87 (1952) 366.
- [2] STRUTINSKY, V.M., TYAPIN, A.S., Zh. eksp. teor. Fiz. 45 (1963) 960.
- [3] MYERS, W.D., SWIATECKI, W.J., Nucl. Phys. 81 (1966) 1.
- [4] STRUTINSKY, V.M., Nucl. Phys. A 95 (1967) 420; A122 (1963) 1.
- [5] TYAPIN, A.S., Yadernaya Fizika 11 (1970) 98.
- [6] SEEGER, P.A., PERISHO, R.C., Proc. 3rd Int. Conf. Atomic Masses, Winnipeg (1967) 85.
- [7] STRUTINSKY, V.M., Nucl. Phys. A 95 (1968) 420; STRUTINSKY, V.M., BJORNHOLM, S., Int. Symp. Nucl. Structure, Dubna (1968); ZYNN, J.E., Int. Symp. Nucl. Structure, Dubna (1968).
- [8] RAINWATER, J., Phys. Rev. 79 (1950) 432.
- [9] BOHR, A.N., in Problemy sovremennoj fiziki (Problems of contemporary physics), No. 9, Izd-vo inostr. lit., Moscow (1955).
- [10] HILL, J., et al., Usp. fiz. Nauk 52 (1954) 2.
- [11] NILSSON, S., in Deformacija atomnyh jader (Deformation of atomic nuclei), Izd-vo inostr. lit., Moscow (1958).
- [12] IGNATYUK, A.V., Yadernaya Fizika 7 (1968) 1043.
- [13] NEWTON, T.D., Can. J. Phys. 34 (1956) 804.
- [14] CAMERON, A.G.W., Can. J. Phys. 36 (1958) 1040.
- [15] MALYSHEV, A., Plotnost urovnej i struktura atomnyh jader (Level density and structure of atomic nuclei), Atomizdat (1969).
- [16] FONG, P., Phys. Rev. 89 (1953) 332.
- [17] FONG, P., Phys. Rev. 102 (1956) 434.
- [18] NEWTON, T.D., Proc. of the Symposium on the Physics of Fission, CRP - 642 A (1956).

- [19] CAMERON, A.G.W., Can. J. Phys. 35 (1957) 1021.
- [20] HUIZENGA, J.R., VANDENBOSCH, R., in Jadernye reakcii (Nuclear reactions), Vol. III, chapter entitled "Delenie jader" (Nuclear fission), Moscow (1964).
- [21] WHEELER, J.A., Verojatnost delenija (Fission probability), in Uspehi fiziki delenija (Advances in fission physics), Moscow (1965).
- [22] AUERBACH, E.H., MOORE, S.O., Phys. Rev. 163 (1967) 1124.
- [23] LANE, A., THOMAS, R., Teorija jadernyh reakcij pri nizkih energijah (Theory of nuclear reactions at low energies), Moscow (1960).
- [24] LAZAREV, L.M., Yadernaya Fizika 5 (1967) 101.
- [25] MOLDAUER, P.A., Phys. Rev. 136 (1964) 947.
- [26] SAVELIEV, A.E., Obobščenie metoda Hausera-Feshbacha na slučaj mnogočastotnyh jadernyh reakcij (Generalization of the Hauser-Feshbach method to cover multi-particle nuclear reactions), paper presented at 20th All-Union Conference on Nuclear Spectroscopy, Leningrad (1970).
- [27] AUERBACH, E.H., MOORE, S.O., Phys. Rev. 135 (1964) B895.
- [28] AVERYANOV, I.K., SAVELIEV, A.E., DZYUBA, B.M., Byulleten Informacionnogo Centra po Jadernym Dannym (Bulletin of the Information Centre for Nuclear Data), 1969 issue.
- [29] AVERYANOV, I.K., SAVELIEV, A.E., DZYUBA, B.M., Byulleten Informacionnogo Centra po Jadernym Dannym (Bulletin of the Information Centre for Nuclear Data), 1970 issue.
- [30] BJORKLUND, F.J., FERNBACH, S., Phys. Rev. 109 (1958) 1295.
- [31] DZHELEPOV, B.S., PEKER, L.K., SERGEEV, V.O., Shemy raspada radioaktivnyh jader (Radioactive decay schemes), Izd-vo Akad. Nauk SSSR, Moscow-Leningrad (1963); DZHELEPOV, B.S., PEKER, L.K., Shemy raspada radioaktivnyh jader (Radioactive decay schemes), Izd-vo Akad. Nauk SSSR, Moscow-Leningrad (1966).



- [32] SHUBIN, Yu.N., MALYSHEV, A.V., STAVINSKY, V.S., paper CN-23/106 presented at IAEA Conference on Nuclear Data for Reactors, Paris (1966).
- [33] NEMIROVSKY, P.E., ADAMCHUK, Yu.V., Nucl. Phys. 39 (1962) 553.
- [34] SAVELIEV, A.E., AVERYANOV, I.K., DZYUBA, B.M., Rasčety sečenij neuprugogo vzaimodejstvija nejtronov s jadrami, soprovoždajuščegosja vyletom protonov i alfa častic (Calculated cross-sections for inelastic neutron-nuclear interaction accompanied by proton and alpha particle emission), paper presented at 20th All-Union Conference on Nuclear Spectroscopy, Leningrad (1970); also submitted to Yadernaya Fizika.
- [35] SHUBIN, Yu.N., Plotnost urovney atomnyh jader (Level density of atomic nuclei), preprint FEI-102 (1967).
- [36] PEREY, F.G., Phys. Rev. 131 (1963) 745.
- [37] HODGSON, P.E., The optical model of elastic scattering, Oxford Univ. Press, London (1963).
- [38] BNL-325.
- [39] ALIEV, A.I., DRYNKIN, V.I., LEIPUNSKAYA, D.I., KASATKIN, V.A., Jadernofizičeskie konstanty dlja nejtronogo i aktivacionogo analiza (Nuclear physics constants for neutron and activation analysis), Handbook (1969).
- [40] CINDRO, N., Rev. Mod. Phys. 38 (1966) 391.
- [41] BLATT, J.M., WEISSKOPF, V.F., Theoretical nuclear physics, Wiley, New York (1952).
- [42] FRENKEL, Ya.I., Sov. Phys. 9 (1936) 533.
- [43] WEISSKOPF, V.F., Phys. Rev. 52 (1937) 295.
- [44] DAVYDOV, A.S., Teorija atomnogo jadra (Theory of the atomic nucleus), Fizmatgiz (1958) 123.
- [45] ZHMAILO, V.A., Zh. eksp. teor. Fiz. 43 (1962) 473.
- [46] WATT, B.E., Phys. Rev. 87 (1952) 1037.

- [47] GUREVICH, I.I., MUKHIN, K.N., review by Erozolimsky, B.G., in supplement No. 1 to *Atomn. Energ.* (1957) 74.
- [48] ZAMYATNIN, Yu.S., GUTNIKOVA, E.K., IVANOVA, N.I., SAFINA, I.N., *Atomn. Energ.* 3 (1957) 540.
- [49] NEILL, G.K.O., *Phys. Rev.* 95 (1954) 1235.
- [50] AVERYANOV, I.K., PURTSELADZE, Z.Z., *Yadernaya Fizika* 6 (1966) 293.
- [51] LE CAUTER, K., *Proc. Phys. Soc. A* 65 (1952) 718.
- [52] WAHL, J.S., *Phys. Rev.* 95 (1954) 126.
- [53] STEIN, W.E., *Phys. Rev.* 108 (1957) 94.
- [54] TERREL, J., *Phys. Rev.* 113 (1959) 527.
- [55] SIROTININ, E.I., *Atomn. Energ.* 13 (1962) 530.
- [56] VASILIEV, Yu.A., et al., *Atomn. Energ.* 9 (1960) 449.
- [57] NEFEDOV, V.N., *Zh. eksp. teor. Fiz.* 38 (1960) 1657.
- [58] BLINOV, M.B., KAZARINOV, N.M., PROTOPOPOV, A.N., paper presented at All-Union Conference on the Physics of Nuclear Fission, Leningrad (1961).
- [59] SIROTININ, E.I., SAVELIEV, A.E., paper presented at All-Union Conference on the Physics of Nuclear Fission, Leningrad (1961).
- [60] *Canad. J. Chem.* 36 (1958) 1711.
- [61] CAMERON, A.G.W., *Can. J. Phys.* 35 (1957) 1021.
- [62] TERREL, J., *Phys. Rev.* 127 (1962) 880.
- [63] SMIRENKIN, G.N., et al., *Atomn. Energ.* 4 (1958) 188.
- [64] BOWMAN, H.R., THOMPSON, S.G., MILTON, J.C.D., SWIATECKI, W.J., *Phys. Rev.* 126 (1962) 2120.
- [65] SKARSVAG, K., BERGHEIM, K., *Nucl. Phys.* 45 (1963) 72.
- [66] SAVELIEV, A.E., *Atomn. Energ.* 19 (1965) 59.
- [67] BOWMAN, H.R., MILTON, J.C.D., THOMPSON, S.G., SWIATECKI, W.J., *Phys. Rev.* 129 (1963) 2133.
- [68] BOWMAN, H.R., THOMPSON, S.G., *Proc. of the Second UN Intern. Conf. on the Peaceful Uses of Atomic Energy, Geneva Vol. 15* (1958) 212.

- [69] SMITH, A.B., FIELDS, P.R., FRIEDMAN, A.M., Phys. Rev. 104 (1956) 699.
- [70] KOSORUKOV, A.L., STRUTINSKY, V.M. Yadernaya Fizika 2 (1965) 657.
- [71] LANG, D., Nucl. Phys. 53 (1964) 113.
- [72] ROSS, A., Phys. Rev. 108 (1957) 720.
- [73] NEWTON, T., Can. J. Phys. 34 (1956) 804.
- [74] LE COUTER, K., LANG, D., Nucl. Phys. 13 (1959) 32.
- [75] ZOMMER, V.P., SAVELIEV, A.E., ZHIKHAREVA, S.V., Atomn. Energ. 23 (1967) 327; ZOMMER, V.P., SAVELIEV, A.E., ZHIKHAREVA, S.V., Byulleten Informacionnogo Centra po Jadernym Dannym (Bulletin of the Information Centre for Nuclear Data), issue 3, Atomizdat (1966) 34.
- [76] ZOMMER, V.P., SAVELIEV, A.E., Yadernaya Fizika 4 (1966) 1255.
- [77] ZOMMER, V.P., SAVELIEV, A.E., PROKOFIEV, A.I., Atomn. Energ. 19 (1965) 116.
- [78] ZOMMER, V.P., Mgnovennoe izlučenie iz jader-oskolokov delenija (Prompt radiation from fission fragment nuclei), Programma i tezisy dokladov XVIII ežegodnogo soveščanija po jadernoj spektroskopii i strukture atomnogo jadra (Programme and summary papers of 18th Annual Conference on Nuclear Spectroscopy and Nuclear Structure), Riga, 25 January-2 February 1968, Izd-vo "Nauka", page 259.
- [79] STRUTINSKY, V.M., Nucl. Phys. 8 (1958) 284.
- [80] STRUTINSKY, V.M., GROSHEV, A.V., AKIMOVA, M.A., Zh. eksp. teor. Fiz. 38 (1960) 598.
- [81] TROUBETZKOY, E.S., Phys. Rev. 122 (1961) 212.
- [82] SMITH, A., et al., Proc. of the Second UN Intern. Conf. on the Peaceful Uses of Atomic Energy, Geneva Vol. 15 (1958) 392.
- [83] STRUTINSKY, V.M., Zh. eksp. teor. Fiz. 37 (1959) 861.
- [84] PETROV, G.A., Yadernaya Fizika 1 (1965) 476.
- [85] GORDEEV, I.V., KARDASHEV, D.A., MALYSHEV, A.V., Jaderno-fizičeskie konstanty (Nuclear physics constants), Gosatomizdat (1963).

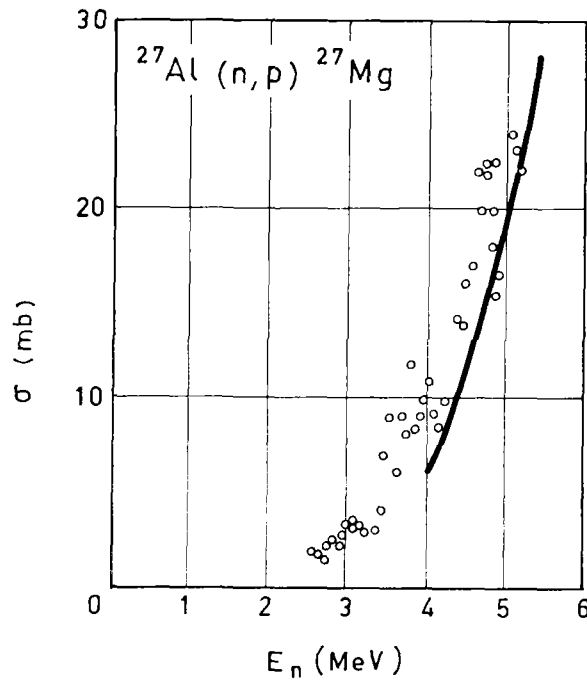


Fig. 1a. Total cross-section for the reaction  $^{27}\text{Al}(n,p)^{27}\text{Mg}$ . Comparison of calculations (continuous line) with experimental data.

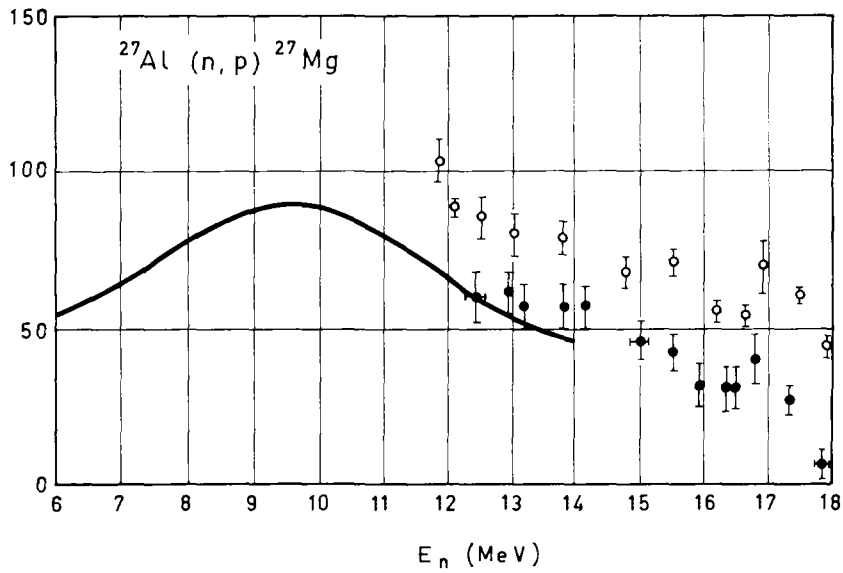


Fig. 1b. The same as Fig. 1a, but for higher incident neutron energies.

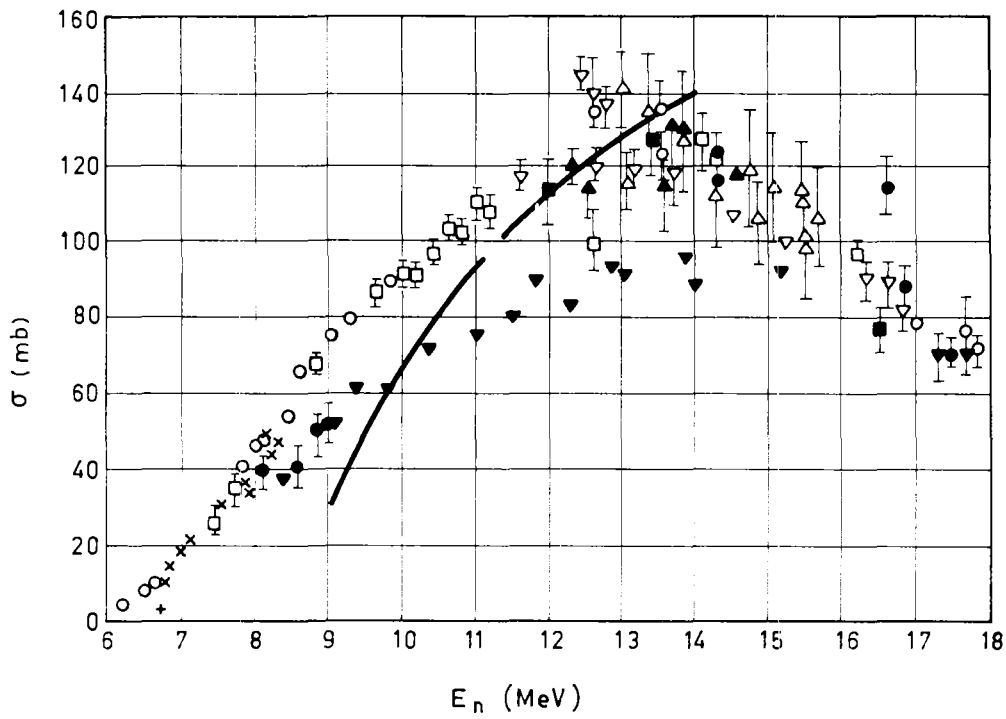


Fig. 2. Total cross-section for the reaction  ${}^{27}_{13}\text{Al}(n, \alpha)$ . Comparison of calculations (continuous line) with experimental data.

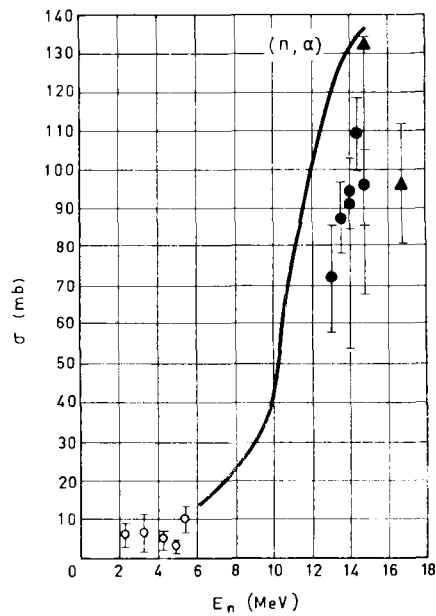


Fig. 3. The same as Fig. 2, but for the reaction  ${}^{54}_{26}\text{Fe}(n, \alpha)$ .

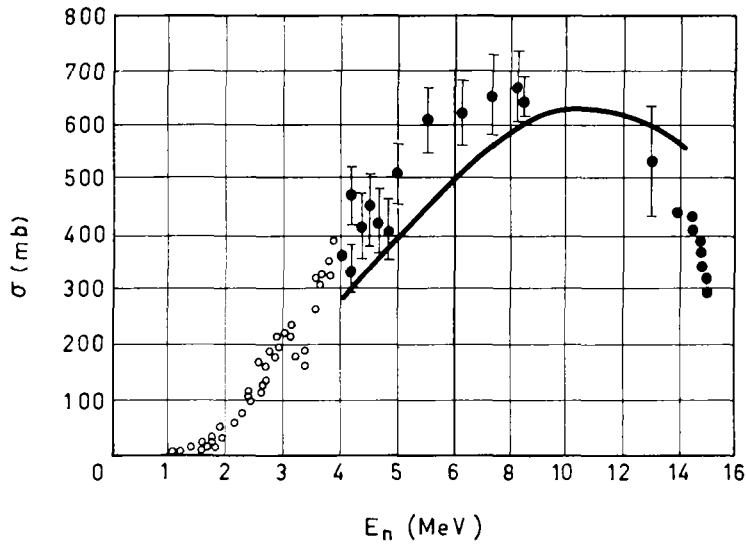


Fig. 4. Total cross-section for the reaction  $^{58}_{28}\text{Ni}(n,p)$ . Comparison of calculations (continuous line) with experimental data.

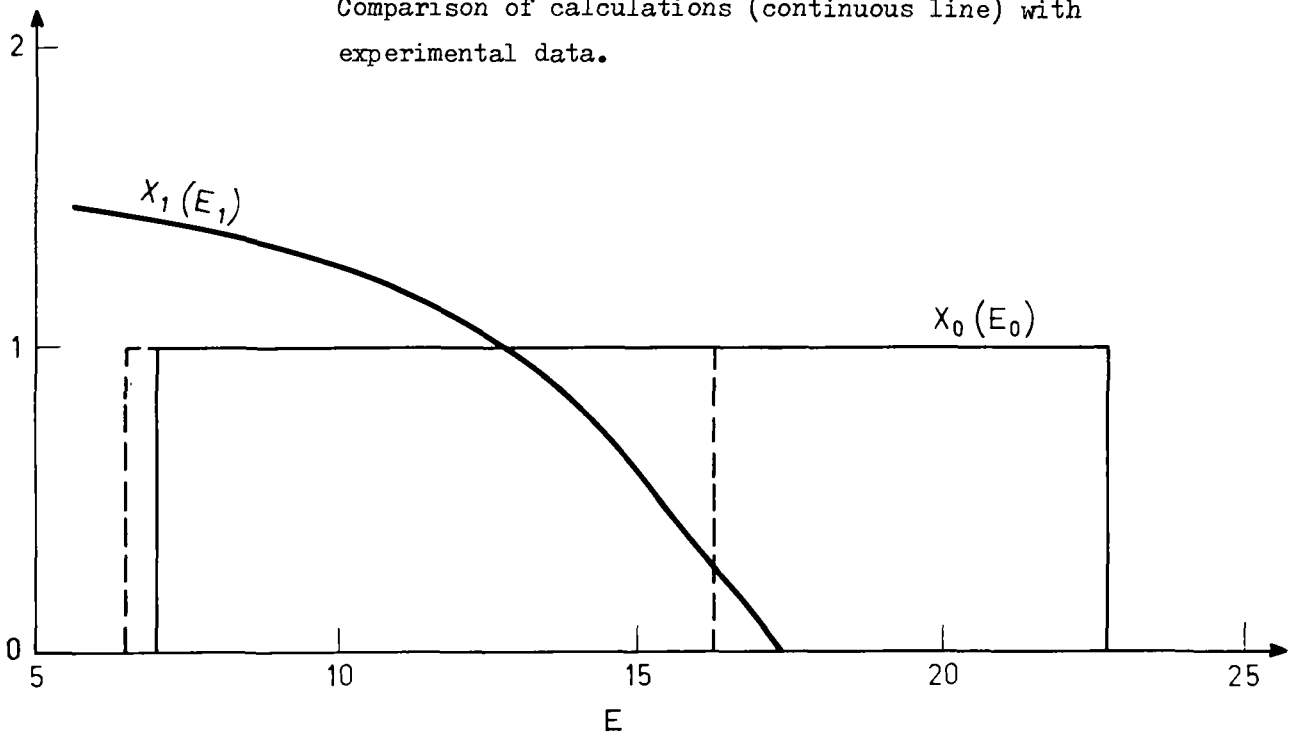


Fig. 5. Illustration of the change in the shape of the excitation energy distribution of fission fragment nuclei after the emission of one neutron.

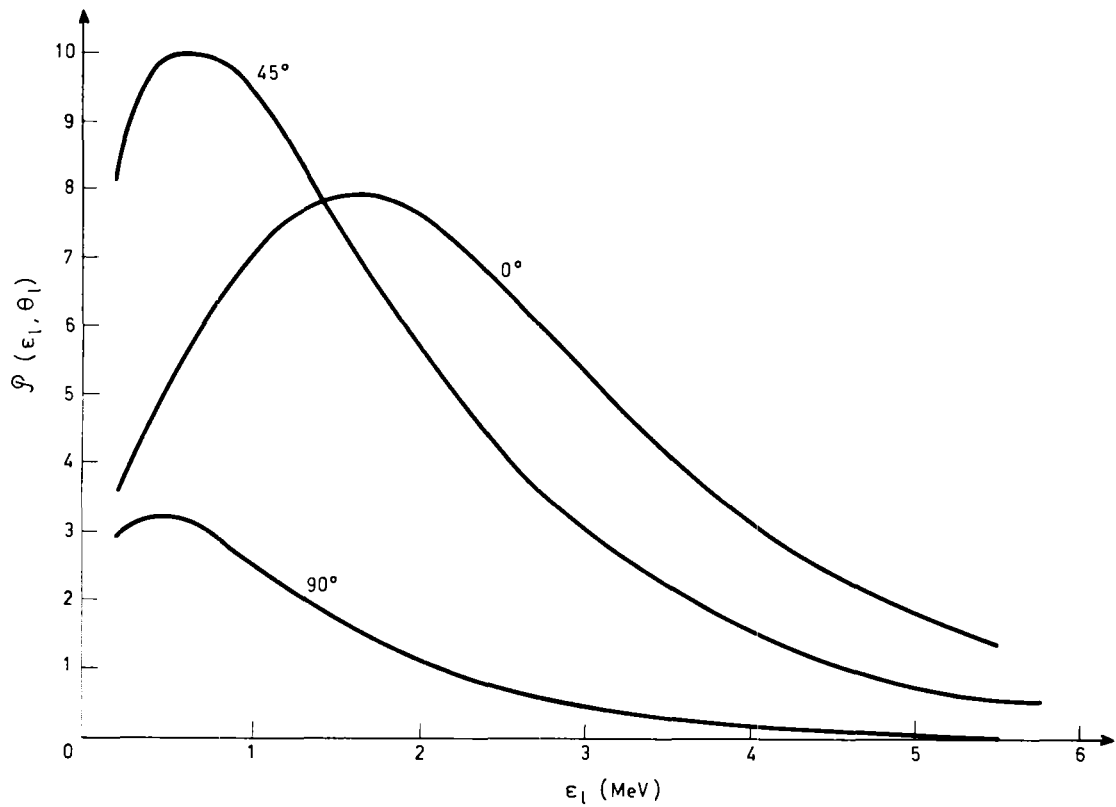


Fig. 6. Calculated spectra of  $^{235}\text{U}$  fission neutrons emitted at  $0^\circ$ ,  $45^\circ$  and  $90^\circ$  to the direction of fission fragment movement. The excitation energy distribution of the fission fragments after the emission of all neutrons was found using Terrel's method.

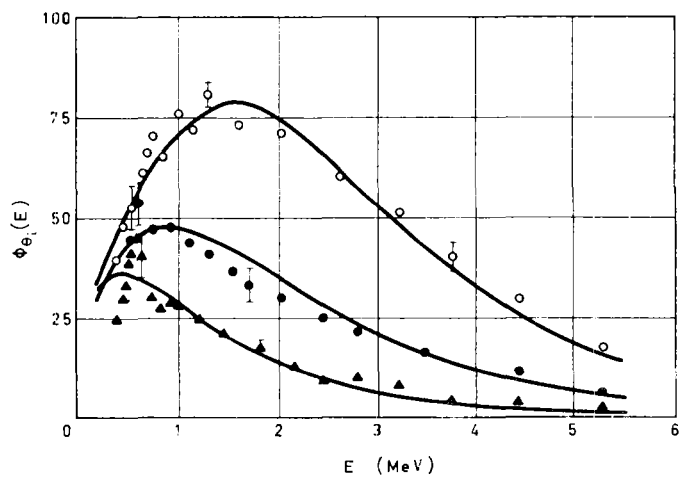


Fig. 7. Comparison of calculations by E.I. Sirotinin (continuous curves) with experimental data on  $^{235}\text{U}$  fission neutron spectra.

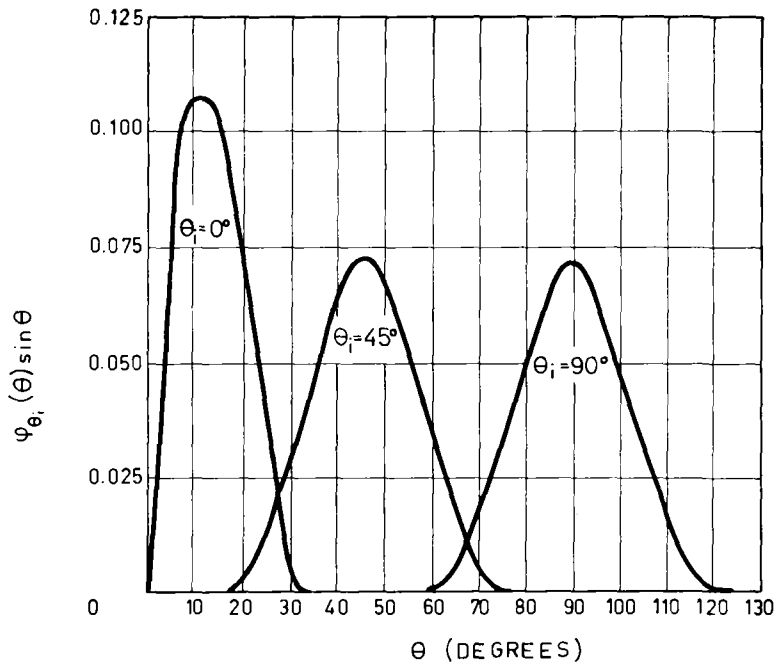


Fig. 8. Angular resolution functions found in Ref. [56].

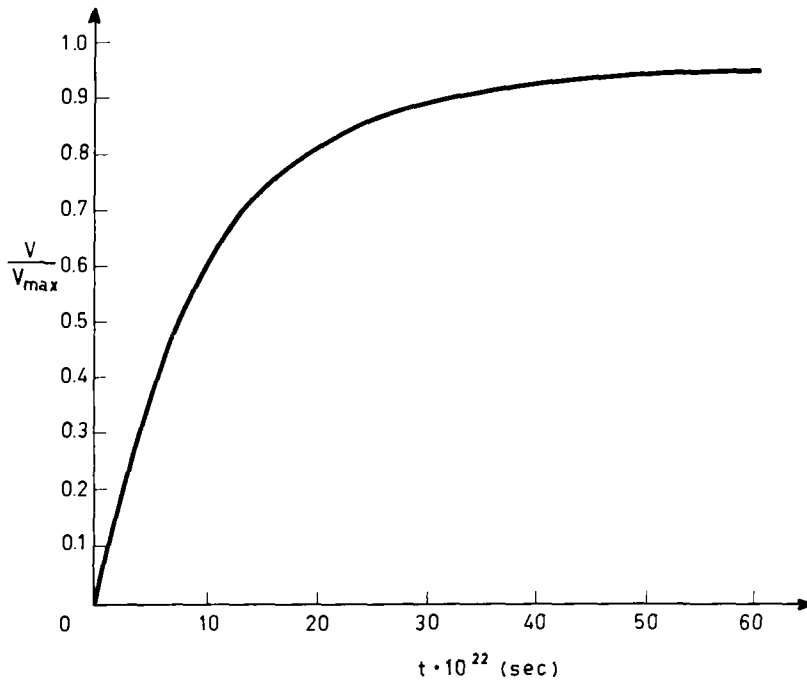


Fig. 9. Time dependence of relative fission fragment velocity.



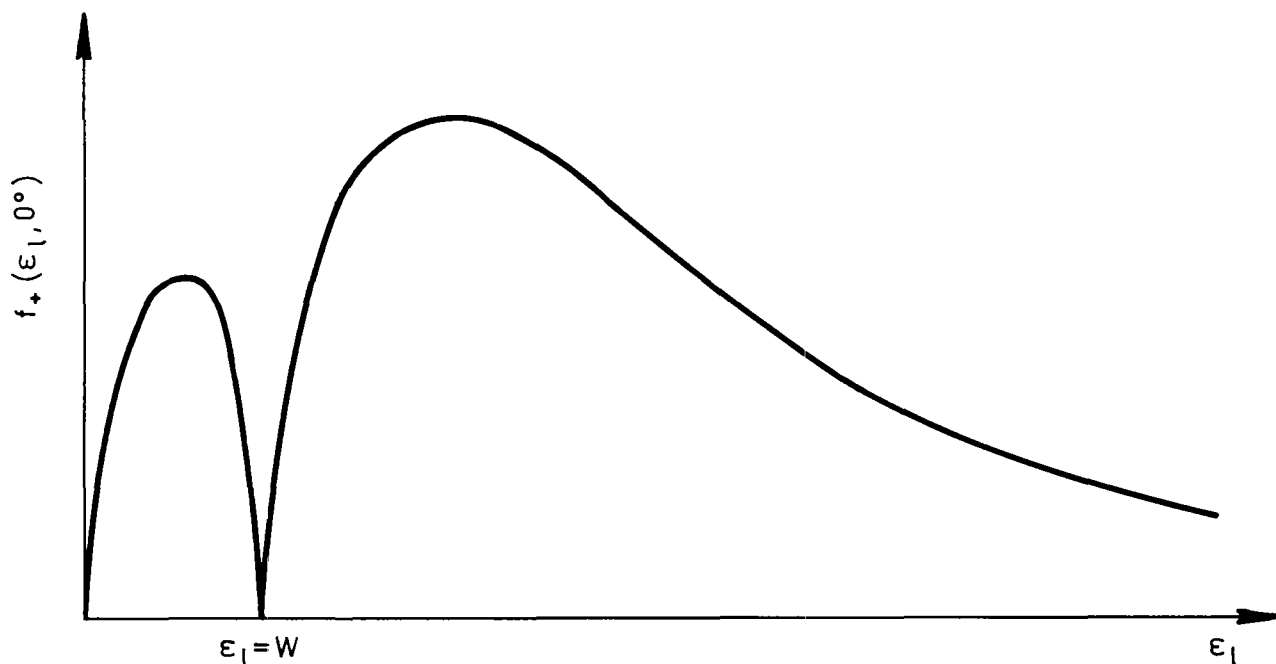


Fig. 10. Spectrum of neutrons emitted from fission fragments moving towards neutron detector in the laboratory system of co-ordinate.

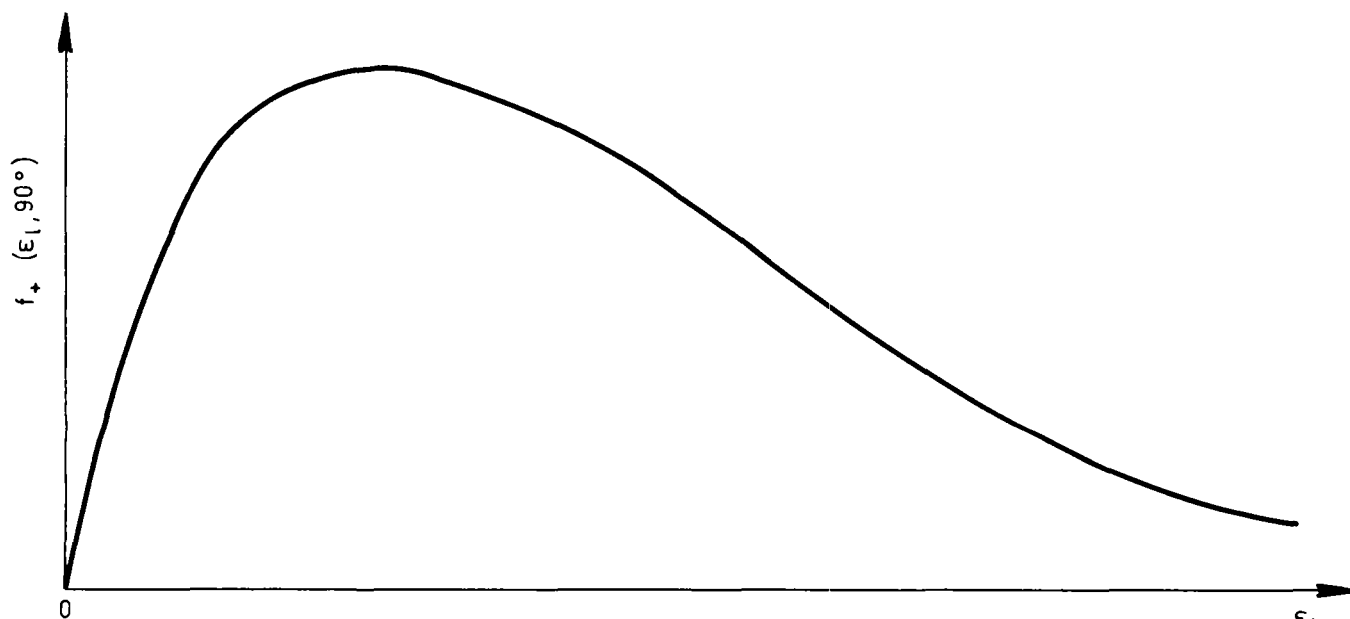


Fig. 10a. Spectrum of neutrons emitted from fission fragment at  $90^\circ$  to direction of fission fragment movement in the laboratory system of co-ordinates.

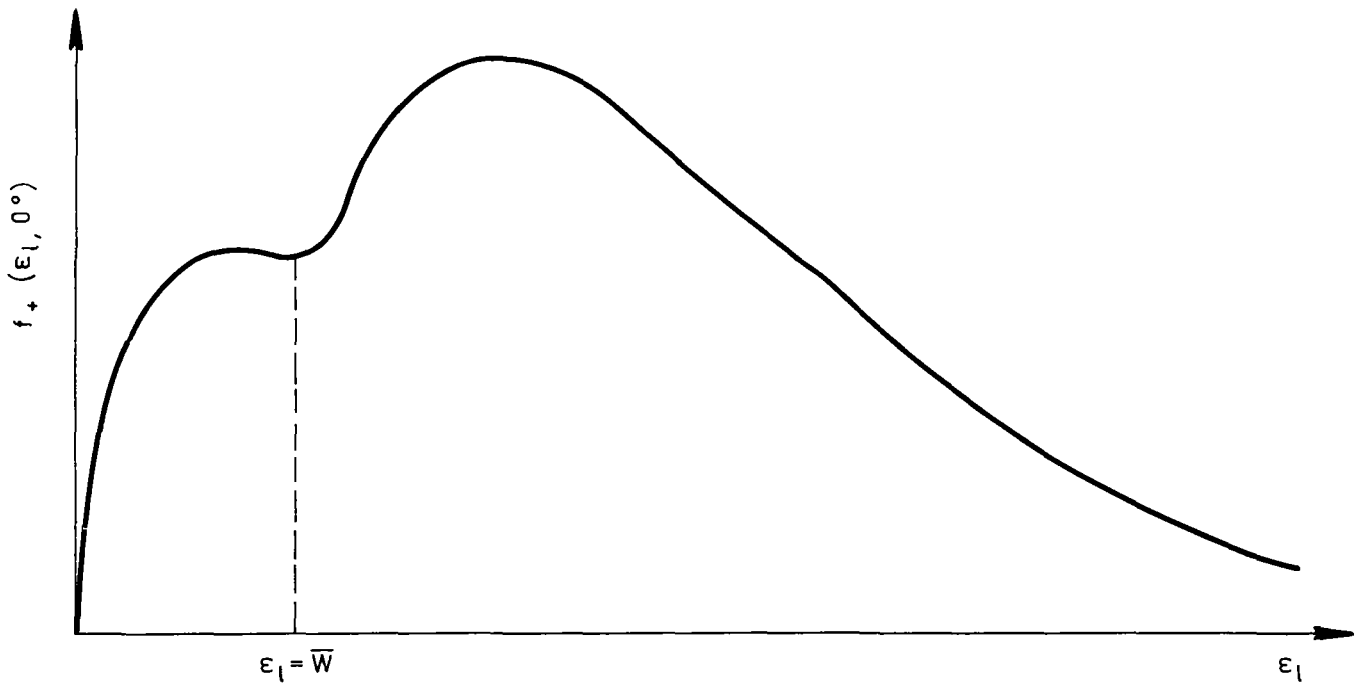


Fig. 11. Total spectrum of neutrons emitted from two fission fragments at  $0^\circ$  to the direction of fission fragment movement.

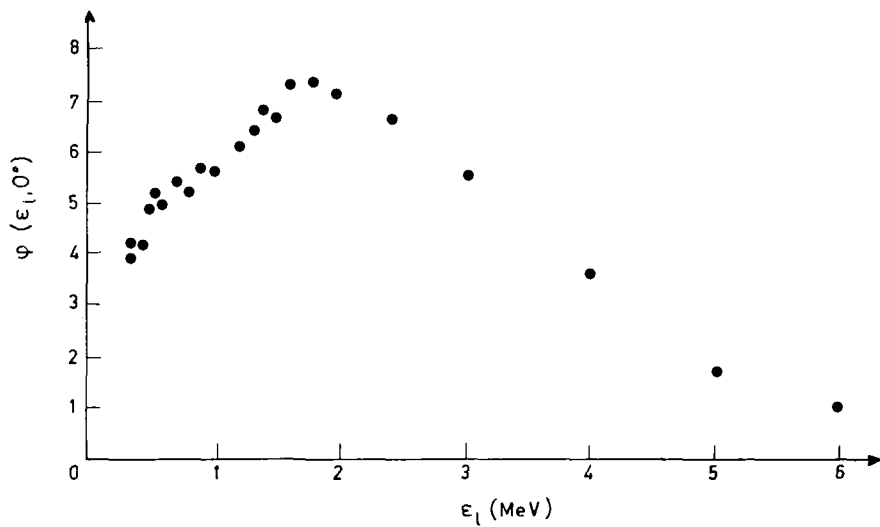


Fig. 12. Experimentally observed spectrum of neutrons emitted at  $0^\circ$  to the direction of fission fragment movement in  $^{235}\text{U}$  fission induced by thermal neutrons [65].

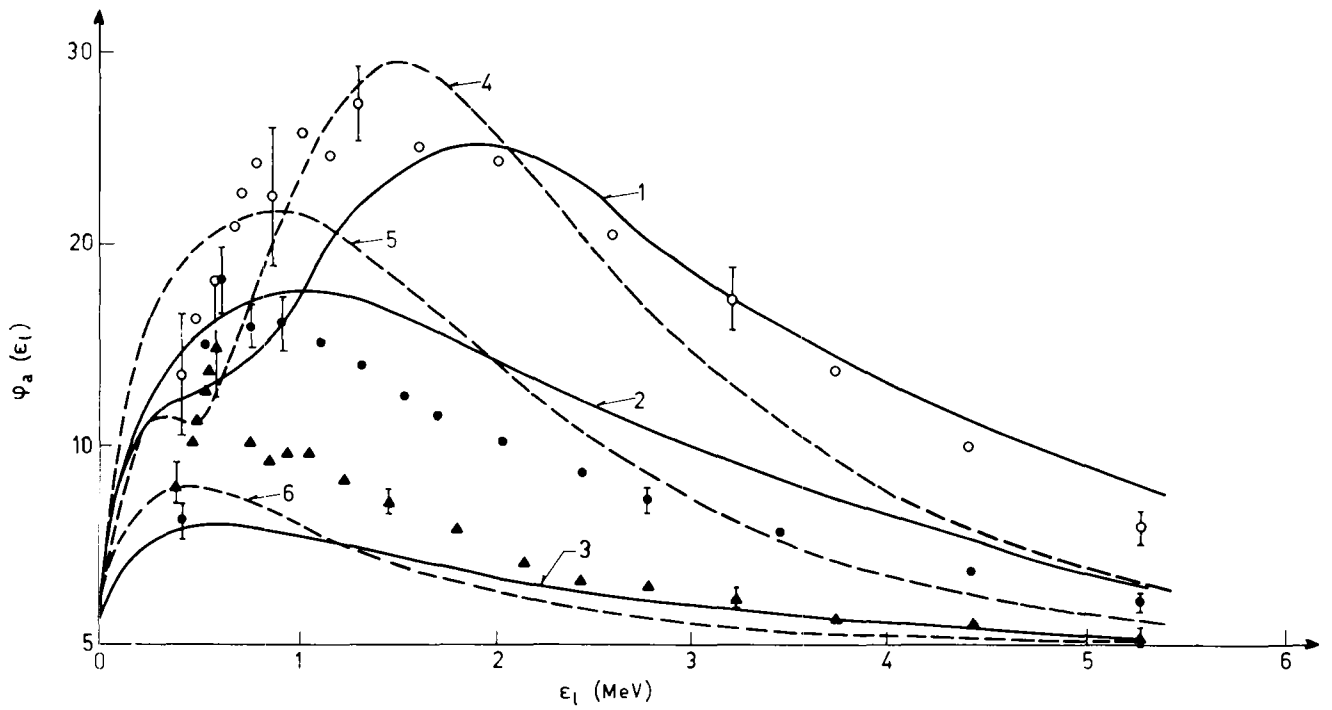


Fig. 13. Comparison of calculated neutron spectra (continuous and broken curves) with experimental data [56] (---  $a = 0.05 \text{ \AA}$ , —  $a = 0.1 \text{ \AA}$ ).

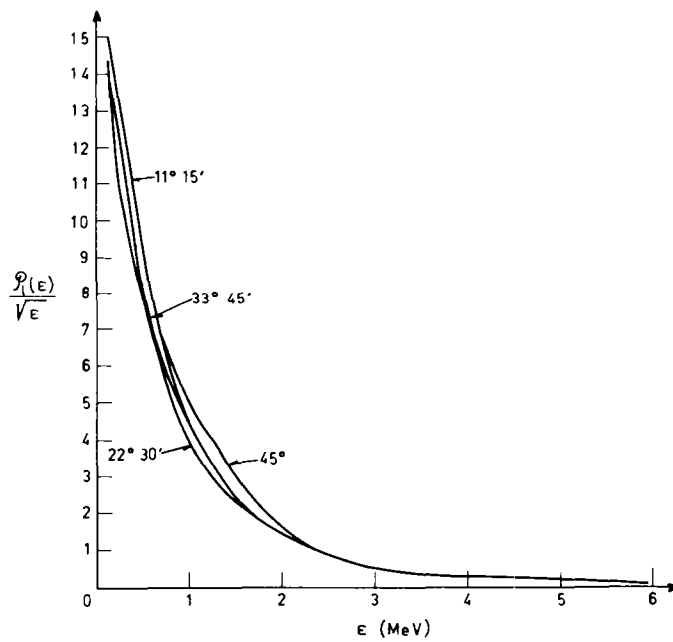


Fig. 14. Spectrum of neutrons from a light fission fragment at its centre of mass, obtained from experimental data for  $\theta_g = 11^\circ 15'$ ,  $22^\circ 30'$ ,  $33^\circ 45'$ ,  $45^\circ$  [64].

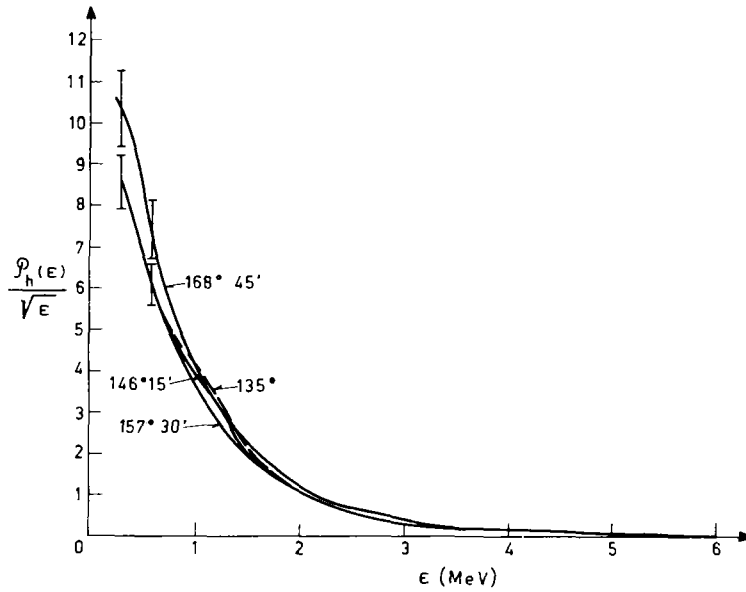


Fig. 15. Spectrum of neutrons from a heavy fission fragment at its centre of mass, obtained from experimental data for  $\vartheta_L = 135^\circ, 146^\circ 15', 157^\circ 30', 168^\circ 45'$  [64].

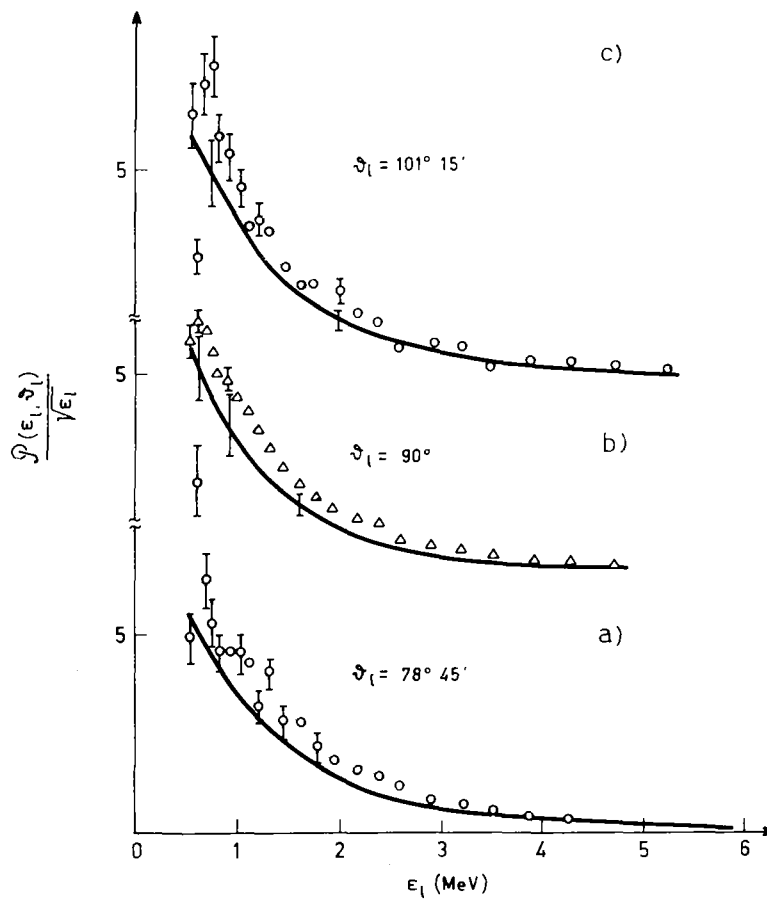


Fig. 16. Comparison of experimental neutron spectra for  $\vartheta_L = 78^\circ 45', 90^\circ$  and  $101^\circ 15'$  with calculated spectra corresponding to isotropic neutron evaporation at the centres of fragment mass.

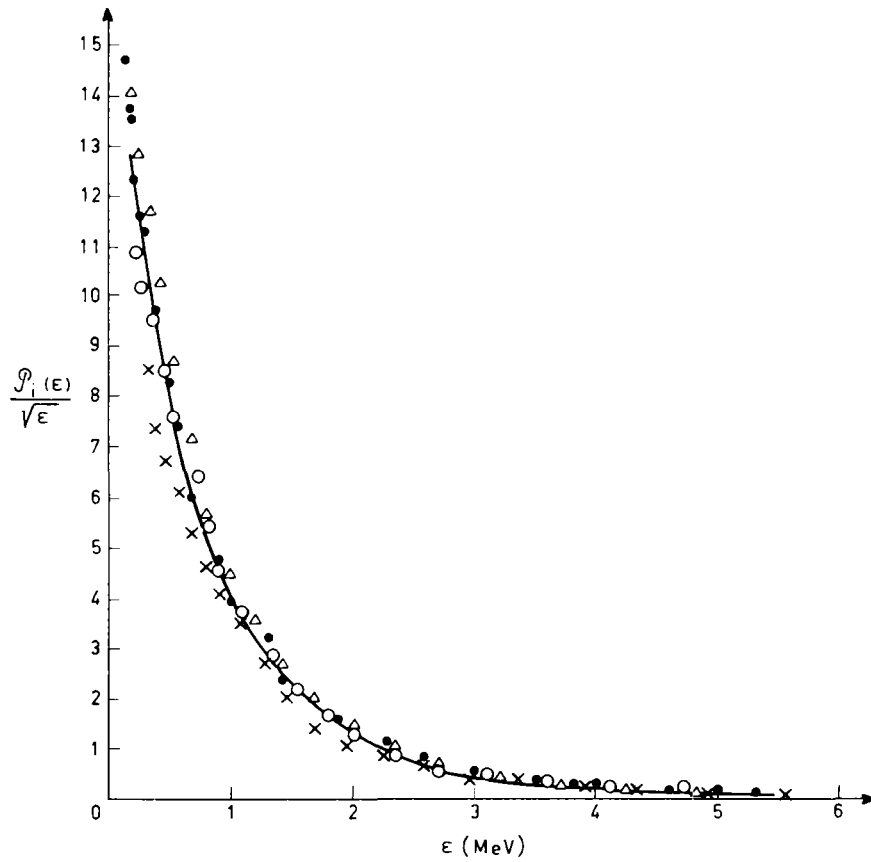


Fig. 17. Comparison of the neutron spectra of light and heavy fission fragments at their centres of mass (o - light fission fragment,  $\Delta, X$  - heavy fission fragment).

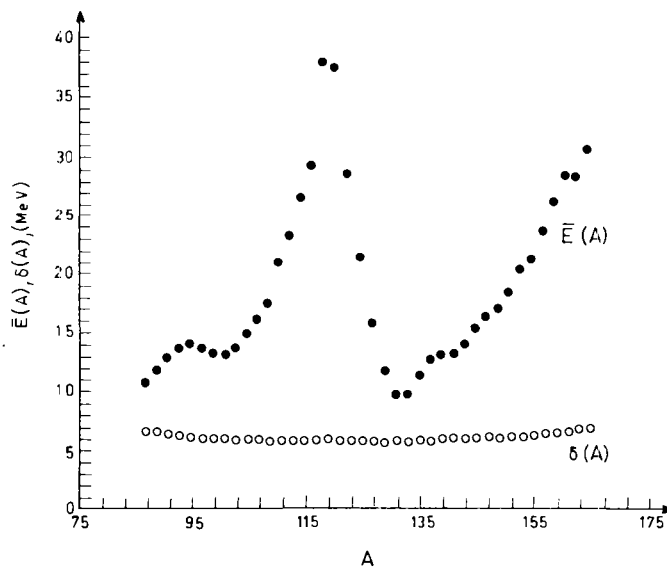


Fig. 18. Fission fragment mass number dependence of mean excitation energy  $\bar{E}$  and excitation energy distribution width  $\delta$  for  $^{252}\text{Cf}$  [67].

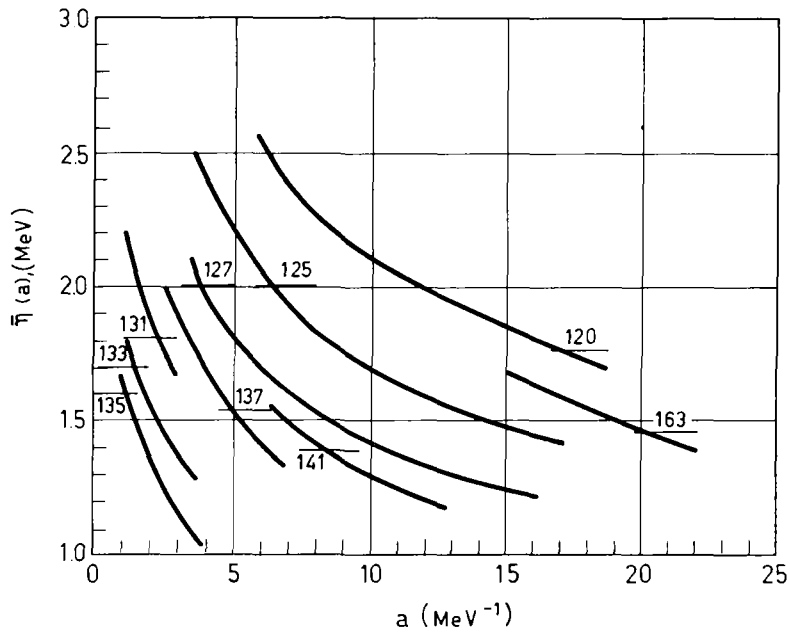


Fig. 19. Dependence of mean neutron kinetic energy on fission fragment level density parameter  $a$  (see text).

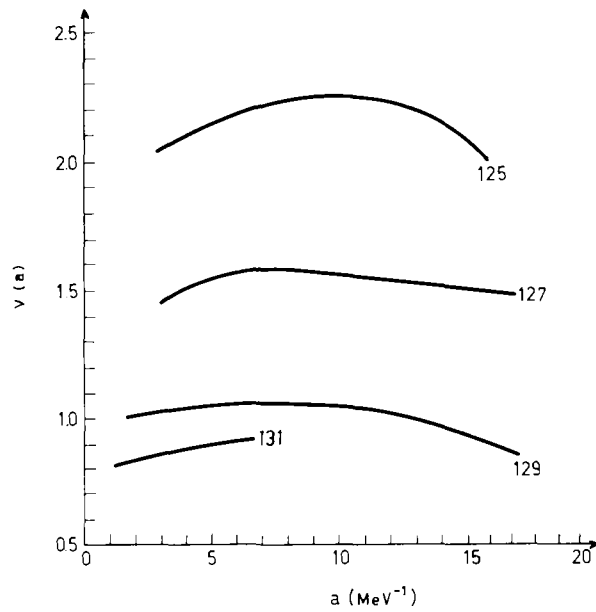


Fig. 20. Total number of neutrons emitted from a fission fragment as a function of the level density parameter  $a$  (see text).

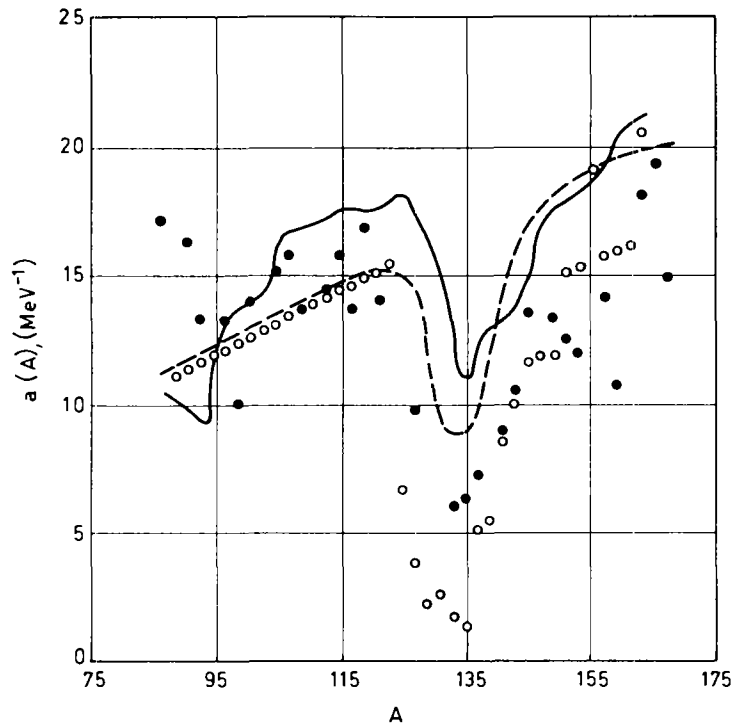


Fig. 21. The level density parameter as a function of the mass number of a  $^{252}\text{Cf}$  fission fragment ( o present article; ● Lang; — Ross; - - - Newton).

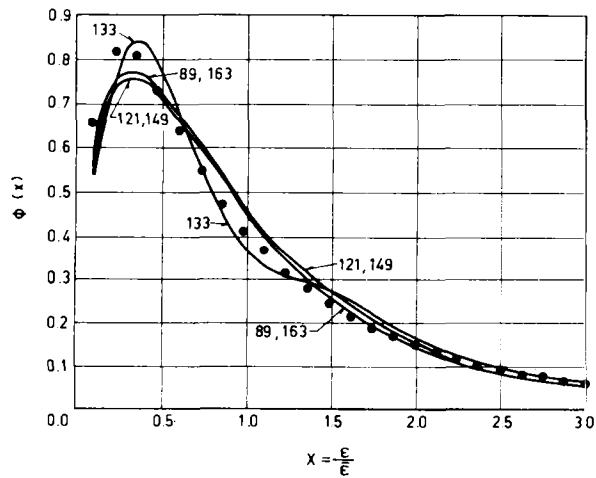


Fig. 22. Calculated neutron spectra (continuous curves) for various fission fragments in the "universal" form compared with the experimentally observed "universal" neutron spectrum form (dots).

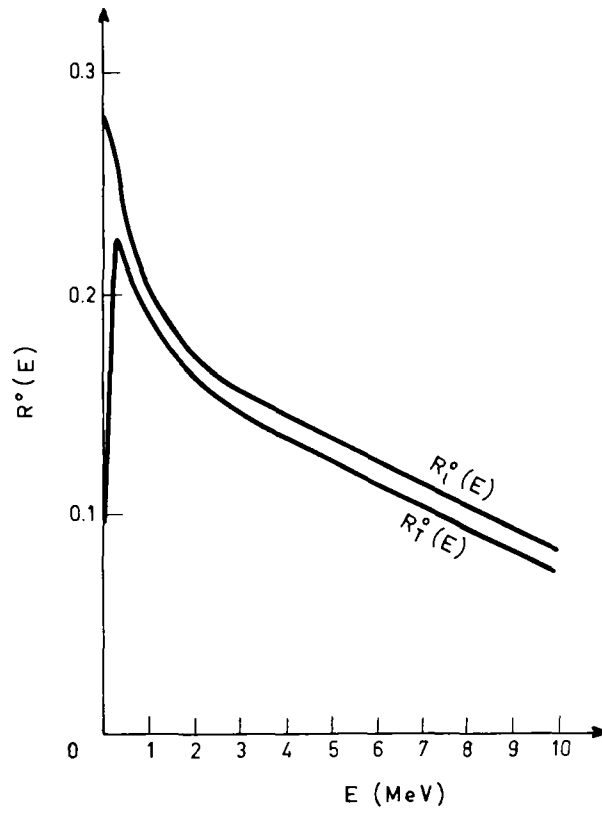


Fig. 23. Excitation energy distributions of light and heavy  $^{235}\text{U}$  fission fragments after the emission of all neutrons (calculated).



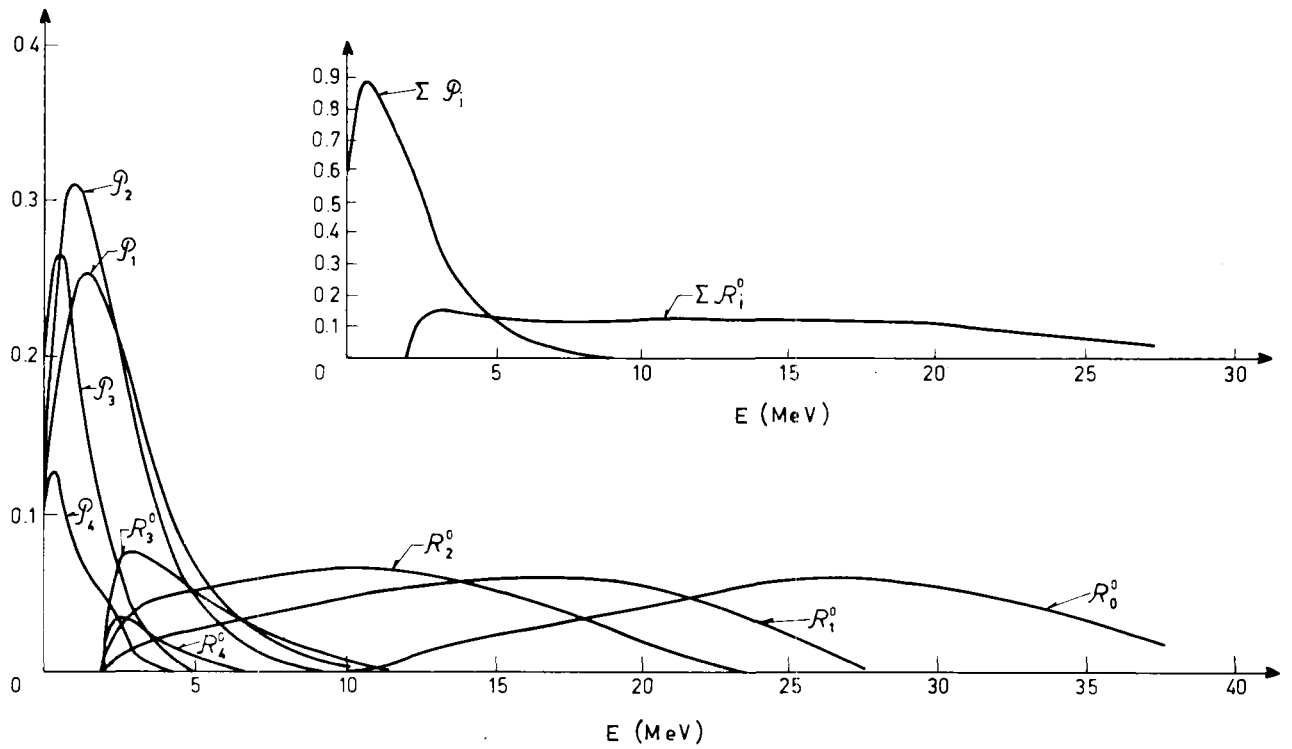


Fig. 24a. Excitation energy distributions of  $^{252}\text{Cf}$  fission fragments with mass number  $A = 107$  after the emission of all neutrons ( $\Sigma R_i^0$ ) and the spectrum of all the neutrons ( $\Sigma P_i$ ).

Fig. 24b. Successive residual excitation energy spectra of a fission fragment with  $A = 107$  and the corresponding spectra of four neutrons emitted in a cascade.

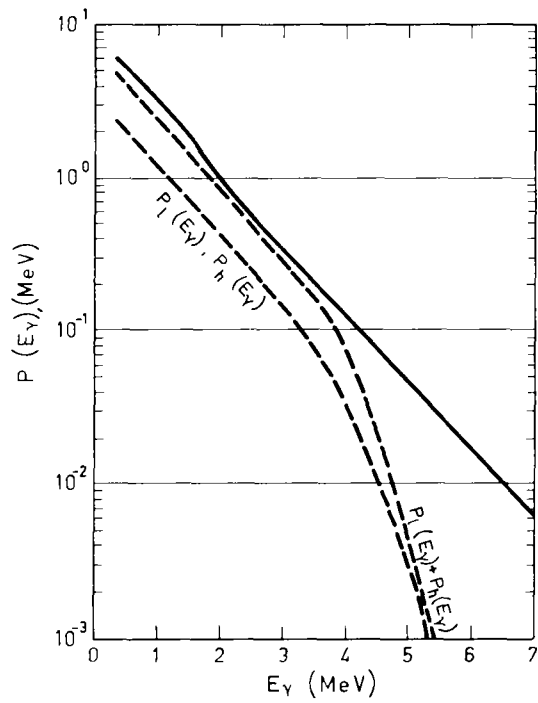


Fig. 25. Spectra of gamma photons emitted in  $^{235}\text{U}$  fission induced by thermal neutrons (--- theory, — experiment).

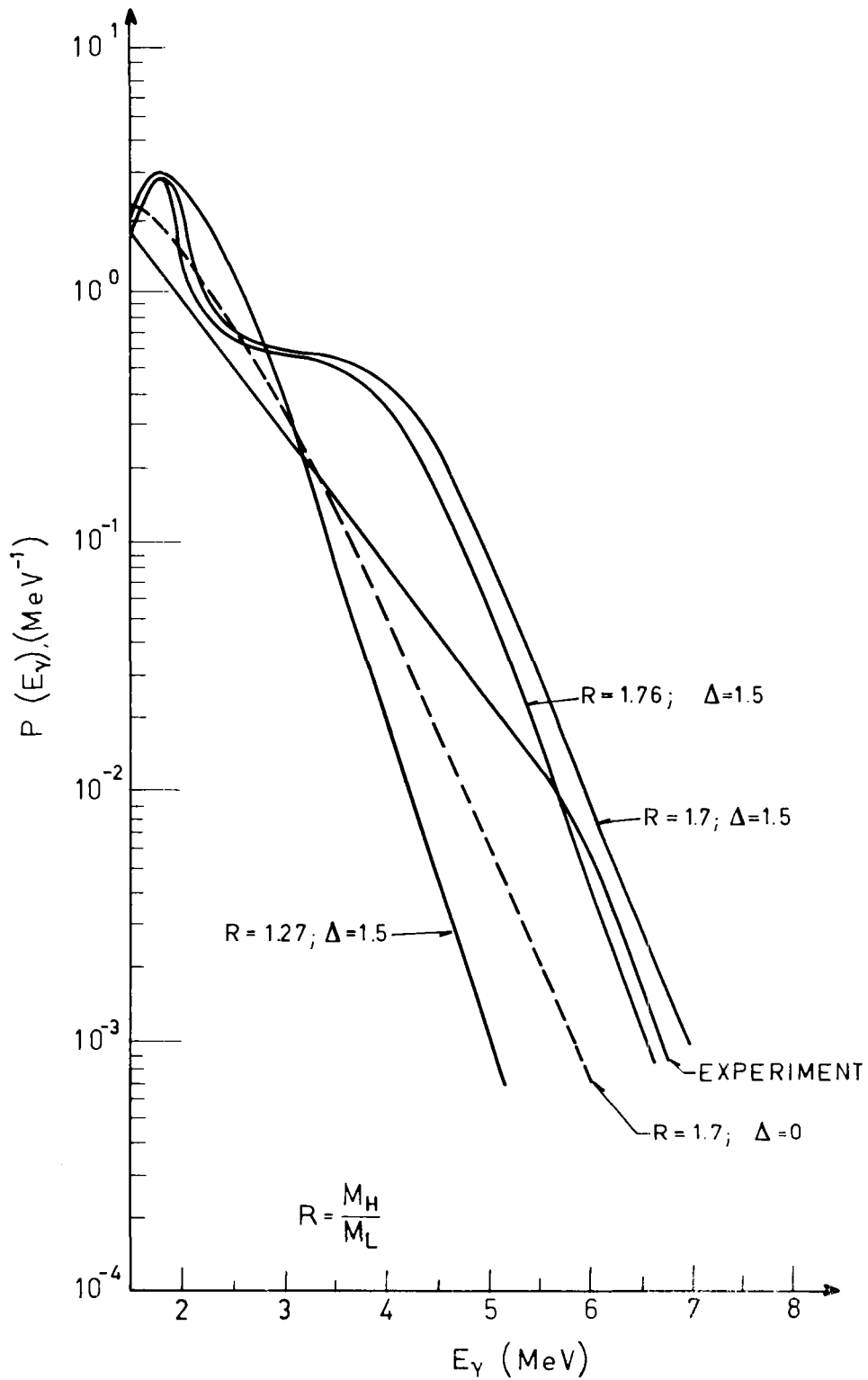


Fig. 26. Calculated spectra of gamma photons emitted in  $^{252}\text{Cf}$  fission for various fission fragment mass ratios  $R$  and various values of the energy gap  $\Delta$ ; experimental gamma spectrum.